

A verification study and trend analysis of simulated boundary layer wind fields over Europe

(Vom Department Geowissenschaften der Universität Hamburg im Jahr 2010 als Dissertation angenommene Arbeit)

J. Lindenberg

A verification study and trend analysis of simulated boundary layer wind fields over Europe

(Vom Department Geowissenschaften der Universität Hamburg im Jahr 2010 als Dissertation angenommene Arbeit)

Janna Lindenberg

Die HZG Reporte werden kostenlos abgegeben.
HZG Reports are available free of charge.

Anforderungen/Requests:

Helmholtz-Zentrum Geesthacht
Zentrum für Material- und Küstenforschung GmbH
Bibliothek/Library
Max-Planck-Straße 1
21502 Geesthacht
Germany
Fax.: +49 4152 87-1717

Druck: HZG-Hausdruckerei

Als Manuskript vervielfältigt.
Für diesen Bericht behalten wir uns alle Rechte vor.

ISSN 2191-7833

Helmholtz-Zentrum Geesthacht
Zentrum für Material- und Küstenforschung GmbH
Max-Planck-Straße 1
21502 Geesthacht
www.hzg.de

A verification study and trend analysis of simulated boundary layer wind fields over Europe

(Vom Department Geowissenschaften der Universität Hamburg im Jahr 2010 als Dissertation angenommene Arbeit)

Janna Lindenberg

122 pages with 32 figures and 10 tables

Abstract

Simulated wind fields from regional climate models (RCMs) are increasingly used as a surrogate for observations which are costly and prone to homogeneity deficiencies. Compounding the problem, a lack of reliable observations makes the validation of the simulated wind fields a non trivial exercise. Whilst the literature shows that RCMs tend to underestimate strong winds over land these investigations mainly relied on comparisons with near surface measurements and extrapolated model wind fields.

In this study a new approach is proposed using measurements from high towers and a robust validation process. Tower height wind data are smoother and thus more representative of regional winds. As benefit this approach circumvents the need to extrapolate simulated wind fields.

The performance of two models using different downscaling techniques is evaluated. The influence of the boundary conditions on the simulation of wind statistics is investigated. Both models demonstrate a reasonable performance over flat homogeneous terrain and deficiencies over complex terrain, such as the Upper Rhine Valley, due to a too coarse spatial resolution (~50 km). When the spatial resolution is increased to 10 and 20 km respectively a benefit is found for the simulation of the wind direction only. A sensitivity analysis shows major deviations of international land cover data. A time series analysis of dynamically downscaled simulations is conducted. While the annual cycle and the interannual variability are well simulated, the models are less effective at simulating small scale fluctuations and the diurnal cycle.

The hypothesis that strong winds are underestimated by RCMs is supported by means of a storm analysis. Only two-thirds of the observed storms are simulated by the model using a spectral nudging approach. In addition "False Alarms" are simulated, which are not detected in the observations.

A trend analysis over the period 1961 - 2000 is conducted for two RCM simulations and their driving reanalysis. The RCMs generally reproduce the trend pattern of the driving fields. On regional scales, deviations occur due to their higher resolution and the expected added value for complex terrain. A piecewise trend analysis reveals two dominant trend patterns. These can be linked to a positive NAO index and a northward shift of the North Atlantic storm track until 1990 and a southward shift afterwards.

Verifizierung und Trendanalyse simulierter Windfelder der Grenzschicht über Europa

Zusammenfassung

Als Alternative zu Windmessungen, die für ihre Inhomogenität bekannt sind, finden immer häufiger simulierte Windfelder von Regionalen Klimamodellen Anwendung. Ihre Validierung gestaltet sich wegen des Mangels an zuverlässigen Daten schwierig. Bisherige Analysen lassen vermuten, dass regionale Modelle die hohen Windgeschwindigkeiten über Land unterschätzen. Diese Analysen basieren allerdings hauptsächlich auf Vergleichen mit bodennahen Daten und extrapolierten Modellwinden.

In dieser Studie wird ein neuer Ansatz gewählt, in dem simulierte Windfelder anhand von Messdaten hoher Messtürme validiert werden. Die höhere Messhöhe sorgt für eine deutlich höhere Repräsentativität der Daten und umgeht zu dem ein Extrapolieren des Modellwindes. Die Umgebung der Messtürme variiert in der Komplexität des Geländes und der Landnutzung. Dies eröffnet die Möglichkeit, die Güte der Simulationen für verschiedene räumliche Bedingungen zu prüfen.

Zunächst wird die Güte zweier regionaler Klimamodelle (RCM) mit verschiedenen Downscaling-Verfahren verglichen und der Einfluss der Randbedingungen auf die Simulation von mittleren Windstatistiken untersucht. Beide Modelle zeigen eine vernünftige Simulation von Windstatistiken über relativ ebenem bzw. homogenem Terrain. Für komplexeres Gelände wie dem Oberrheingraben oder für Waldstationen ergeben sich große Defizite in der Modellierung, da die geringe Gitterauflösung von ca. 50 km die Komplexität nicht erfassen kann. Eine Erhöhung der Gitterauflösung auf 20 und 10 km bringt, entgegen der Erwartung, nur Verbesserungen für die Windrichtungsverteilung. Eine Sensitivitätsanalyse zeigt nicht zu vernachlässigende Unterschiede zwischen internationalen Landnutzungsdaten. Eine vernünftige Simulation des Jahresganges und der natürlichen jährlichen Variabilität wird insbesondere über ebenem Gelände erreicht. Aufgrund einer bekannten Unterschätzung der Strahlung treten Defizite bei der Simulation des Tagesganges auf.

Eine Sturmanalyse bestätigt die Hypothese, dass Starkwinde über Land unterschätzt werden. So werden auch mit Anwendung eines „Spectral Nudging“-Verfahrens nur zwei Drittel der Stürme vom Modell wiedergegeben. Des Weiteren simuliert das Modell zum Teil Sturmereignisse, die nicht in der Stärke in den Beobachtungen zu finden sind.

Auf Basis der guten Simulation der jährlichen Variabilität wird eine Trendanalyse bodennaher Winde zweier RCM-Simulationen und der jeweiligen Antriebs-Reanalyse-Daten für die Periode 1961 - 2000 durchgeführt. Die RCM reproduzieren die Trendmuster der Reanalysen bis auf geringe regionale Unterschiede, die mit ihrer deutlich höheren Auflösung und dem damit verbundenen erwarteten Mehrwert in komplexeren Gebieten in Verbindung gebracht werden. Ebenfalls treten in einigen Regionen Unterschiede in den Trendmustern der Reanalysen auf. Ein „Piecewise-Trend“-Verfahren erkennt zwei dominante Muster in allen Datensätzen, die mit einer nördlichen Verlagerung des North Atlantic Storm Tracks und einem positiven NAO-Index bis etwa 1990 in Verbindung gebracht werden können.

Contents

1	Introduction	1
1.1	Motivation and background	1
1.2	Quality of near surface measurements	3
2	Data sets	11
2.1	Tower measurements	11
2.2	Model data	13
2.2.1	Reanalysis data	13
2.2.2	Regional Climate Model data	14
3	Verification of simulated wind statistics	17
3.1	Methods	19
3.2	Results and Discussion	21
3.2.1	Comparison CCLM-SNN50 and WEST	21
3.2.2	Influence of the roughness field	28
3.2.3	Influence of the spatial resolution	35
3.2.4	Influence of the external forcing	41
3.3	Conclusions	44

4	Verification of simulated wind time series	49
4.1	General time series analysis.....	50
4.1.1	Methods	50
4.1.2	Results and Discussion	52
4.1.2.1	Annual cycle.....	58
4.1.2.2	Diurnal Cycle.....	60
4.1.2.3	Interannual variability.....	62
4.2	Storm detection.....	65
4.2.1	Methods	65
4.2.2	Results.....	66
4.3	Summary and conclusions	74
5	Trend analysis of simulated wind fields	77
5.1	Methods	79
5.2	Results for Europe 1961 - 2000	80
5.3	Summary and conclusions	86
6	Summary and outlook	89
	List of Abbreviations	93
	List of Figures	95
	List of Tables	99
	References	101
	Appendix	113
	Acknowledgements	113

1 Introduction

1.1 Motivation and background

It has become common practise to use regional climate models (RCMs) to simulate regional wind conditions when no measurements are available. Furthermore, RCMs are used in order to predict possible changes and effects on the regional wind climate and as such contribute to community understanding of the impacts of climate change. Hindcast simulations - presenting the climate of the past - are investigated for the existence of trends in the mean or extreme wind climate. These Hindcasts are simulations with regional climate models driven by global reanalysis products. They downscale the climate forcing to serve as input for further geo scientific applications and impact studies for instance for storm surge models or in ecological studies (Weisse et al. 2009).

The wind energy sector is becoming increasingly dependent on detailed knowledge about the wind climate for the operation, design, sales and marketing of wind turbines. Mesoscale simulations are increasingly been used for resource assessment and considered to provide reasonable understanding of regional wind conditions (e.g. Frank and Landberg 1997; Benoit et al. 2004).

Due to the limited number of reliable observations the verification of simulated wind fields is a difficult task. So far the model skill regarding the reasonable simulation of boundary layer wind fields is primarily investigated by means of marine wind fields and/or near-surface observations. Smooth water surfaces

provide a relatively good condition for the comparison with model grid boxes. The verification of simulated wind fields over land, the main scope of this study, bears a larger challenge. Previous comparisons are mainly based on near surface measurements from meteorological stations, which are subjected to homogenisation algorithms to derive local wind climate estimate.

The homogenisation of near surface observations is a very complex process. One should always consider the station location and surrounding environment. The influence of the nearest surrounding on wind speed measurements is demonstrated for the station Helgoland in Chapter 1.2.

The extrapolation of modeled wind speeds from the lowest model level to 10 m height as typical height of near surface measurements is also fraught with issues. This study proposes a new approach to solving this problem. This approach reduces the disturbances due to the surface in the observations by using data from higher measurement sources (towers). Simply put, such data are less affected by surface roughness and obstacles and are more representative of a larger area. In addition, no extrapolation of modeled wind data is required. The occurrence of the extrapolation error is avoided by comparing measurements with simulated values, which were either interpolated between two model level heights or which were extracted directly at the given model level heights.

Data sets from tall measurement towers are rare and therefore of significant scientific value. Towers of this height are often privately owned and operated by wind companies. For this study a data base of five anemometer towers could be established. Together they offer insight into regional conditions for different terrain complexity. This database, the towers and their geographical context and mesoscale models used in this thesis are discussed in Chapter 2.

In Chapter 3 two fundamentally different modeling approaches to downscale mean wind, wind speed distribution and wind direction distribution profiles are

compared. COSMO-CLM is a regional climate model using a dynamical downscaling technique while the Wind Energy Simulation Toolkit (WEST) uses a statistical-dynamical downscaling approach. The more computationally efficient model, WEST, allows a detailed investigation of the influence of boundary conditions like the roughness field and the forcing data. Furthermore, WEST's computational efficiency allows the modeler to increase the spatial resolution of the modeling domain in this study up to 1 km. On the other hand WEST is not able to simulate time series. Therefore, only time series from two COSMO-CLM simulations are used to determine the temporal simulation skill in Chapter 4. Wind speed variations as well as extreme values are analyzed.

After evaluating the performance of COSMO-CLM on temporal scales, a trend analysis is conducted in Chapter 5. Trends of annual mean wind speed and 99th percentiles are compared for two RCM simulations and their forcing reanalyses. The scope is to see, if both reanalyses show similar trend patterns of the mean and extreme wind speed and to what extent these patterns are reproduced in the RCMs. A piecewise trend analysis for wind speed over Europe over the period 1961 - 2000 is conducted, considering possible changes in the wind climate related to atmospheric large scale conditions.

1.2 Quality of near surface measurements

Near surface wind measurements are a common source of information for studies in the wind energy sector and also in ecological, actuarial and meteorological related studies. Despite known problems with the homogeneity and the representativity of measured wind data series (Wieringa 1996; WMO 2008), wind measurements from near surface weather stations are used in several studies (for example for wind farm sitings based on wind atlases (Troen and Petersen 1989) or for verifications of simulated marine wind fields). The main focus of this chapter is to background on the impact of the land surface on observed wind speed data.

For this purpose, information about the former and present status of a number of stations, shown in Figure 1.1, is used as an example and to highlight the influence of sites location on its wind observations. Wind speed time series from five stations are considered. These stations are part of the synoptic measuring net (SYNOP) of the German Meteorological Service (DWD).

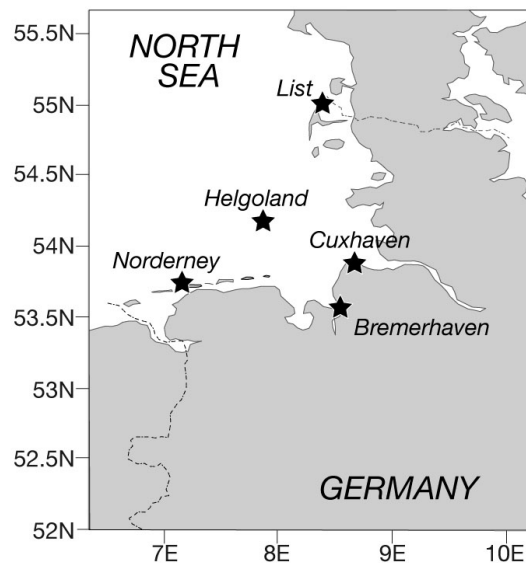


Figure 1.1: Positions of the chosen stations along the coasts of the German Bight.

Selection criteria for these sites are (a) similar temporal availability and (b) the short distance to the North Sea coast and (c) close proximity to each other. Accordingly, the stations should more or less exhibit the same regional wind climate and similar relationships as to temporal variation can be expected for the stations.

Meteorological data for forecast purposes are called SYNOP, as they are observed synchronous. The data are observed hourly, resp. three- or six-hourly. The data of wind speed are averages over ten minutes. A common observation period of 53 years (from 1953 to 2005) is covered with data for all five stations. The measuring frequency of the SYNOP net changed from three-hourly to hourly records in 1978 (Behrendt et al. 2006). However, a continuous hourly sampling frequency since

1979 was only found for the stations Helgoland and Bremerhaven. The other stations show gaps especially at night or at particular hours (e.g. at 7 and 8 pm). Consistent hourly records started in Cuxhaven in 1987 and in Norderney and List since 1989. Before the temporal adjustment the sampling frequency varied from 3 to 8 times a day, often only covering day time. The unit of the wind speed and the accuracy changed from knots to m/s in October 1998 and to 0.1 m/s in April 2001 (Behrendt et al. 2006).

The yearly means and 99th percentiles of the wind speed of the five stations from the SYNOP records show a low similarity (Figure 1.2 and Figure 1.3).

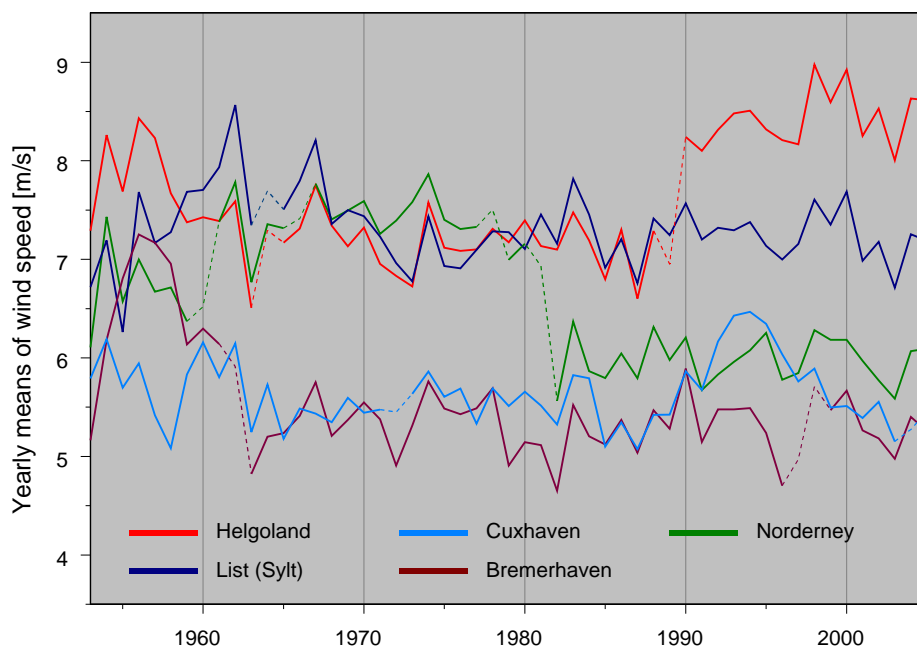


Figure 1.2: Yearly means of wind speed measurements from five synoptic near coastal stations: Helgoland (red), List (blue), Norderney (green), Cuxhaven (light blue), Bremerhaven (purple). Shaded lines label years with known station relocations.

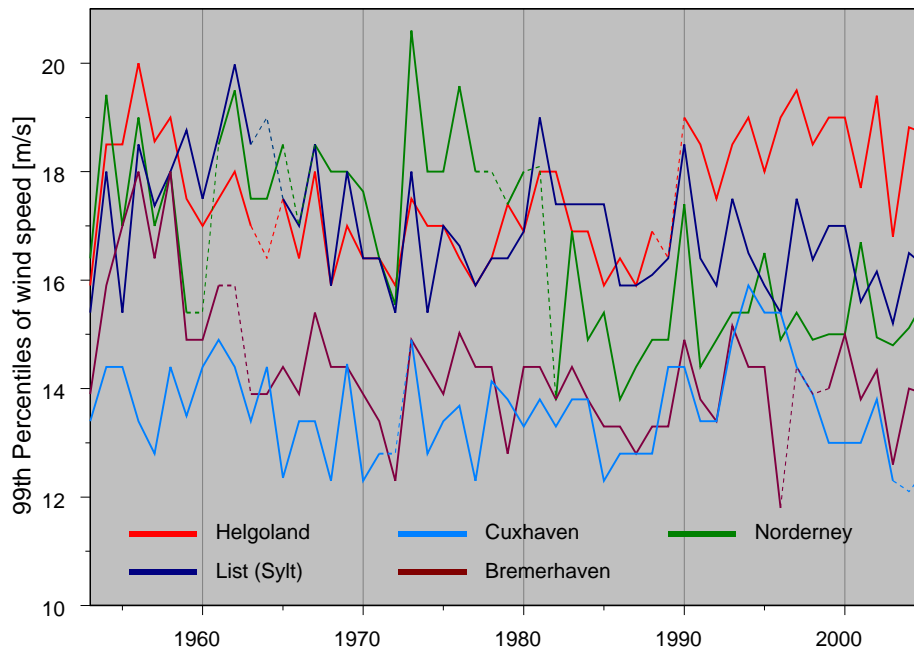


Figure 1.3: Yearly 99th percentiles of wind speed measurements from five synoptic near coastal stations. Helgoland (red), List (blue), Norderney (green), Cuxhaven (light blue), Bremerhaven (purple). Shaded lines label years with known station relocations.

Except of similar small scale variations between the time series of some stations no common general large scale tendency can be identified, although the wind conditions should be dominated by similar regional wind regimes and are expected to reflect the same regional wind climate.

Comparisons with yearly means and 99th percentiles of the FF net, which is homogeneous in sampling time and unit, show that changes in sampling frequency and unit have a negligible effect and do not explain the large variations in the time series.

The similar small scale behaviour between some stations at least indicates consistent short term trends. E.g. at Helgoland and List a quite similar curve shape can be observed in the yearly means neglecting the abrupt increase in 1990 in the Helgoland data. This increase in wind speed is caused by a station relocation.

The station histories (Appendix A1) reveal that each of the stations was relocated at least once during the considered time period. These relocations are not only restricted to changes in location and therewith the environment. Changes of the anemometer height, which varies between 10 and up to 28 m above ground level (AGL) for the five stations, also play a decisive role.

The years with relocations or changes of the anemometer height are marked with dashed lines in Figure 1.2 and Figure 1.3. Not surprisingly, they often result in abrupt increases or decreases of the yearly mean and of the 99th percentiles. E.g., the abrupt decrease in the yearly means and in the yearly 99th percentiles of Norderney from 1981 to 1982 occurs directly after a station relocation including a change in the measuring height from 21 to 12 m AGL in September 1981.

At the station Helgoland an increase of 1.25 m/s is seen in the means of the 10 years before and after the year with the relocation (1989), even though the measuring height changed from 15 to 10 m above ground level and from 19 to 15 m above mean sea level.

To illustrate the strong influence of the environment on wind measurements and therewith the possible magnitude of the effect of a station relocation on the measurements, a detailed investigation for the station Helgoland is conducted.

Helgoland consists of the “Unterland”, the flat area around the port, the “Oberland”, elevated with a mean height of 50 m, and the Dune. Figure 1.4 shows a map of Helgoland and the last three positions of the wind measurement station at the southern port, the airport on the dune and the mole.

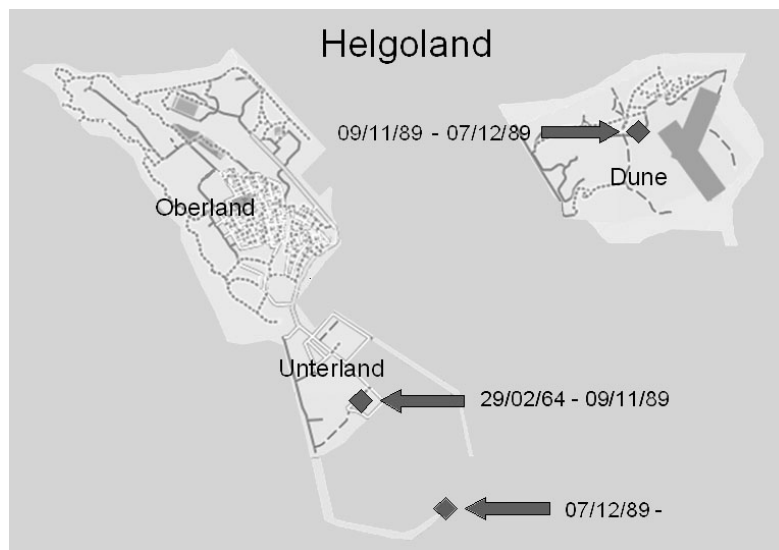


Figure 1.4: Position of the wind masts on the island of Helgoland since 1964¹

From February 1964 to November 1989 the wind speed was recorded from a tower in the South of the port close to the meteorological station building in a distance of approx. 375 m to the edge of the “Oberland” (Schmidt et al. 1993). In the opposite direction the building of the station influenced the data until this tower was damaged in November 1989. Therefore, data from the tower close to the airport, on the dune, have been used as substitute for almost one month. Afterwards, data from the tower at the end of the southern mole are used. The distance of this new position to the edge of the “Oberland” is now larger than 1 km. The measurements are obviously much less disturbed than the measurements located in the port, where the “Oberland”, the observatory and the other buildings and facilities strongly influenced the observations. This resulted in reduced wind speeds indicated by the lower yearly means and the lower 99th percentiles before 1989, even though the height of the anemometer was 5 m higher above ground level at the Tonnenhof station. Thus, higher wind speeds would be expected for the first period. Especially the north westerly winds must have been strongly disturbed by the shape of the “Oberland”. The measurements from the dune, usually taken for quality controls of the main measurements (port

¹ Map based on: www.openstreetmap.org, License: Creative Commons Attribution-Share Alike 2.0 Openstreetmap

and mole), are affected by a higher roughness because of the drag of the airport facilities and the surface of the island. Assuming instrumental effects are negligibly small, the differences between the wind records at the positions can be attributed to the different environments.

The influences of the station relocations show the high sensitivity of the wind measurements to changes in the environment. By using near surface wind measurements as representatives for wind fields for any purpose, a valuation of the homogeneity of these data should be conducted, as Wieringa has already noted in his golden rule “never to use wind data from unspecific locations” (Wieringa 1996). Requesting the station’s metadata from the provider of the data is compulsory. The occurrence of differences between measuring nets must be considered. The metadata give a first impression of the homogeneity of the time series. In cases of relocations these changes should be reported and can be found in the station history. However, slowly developing changes in the environments like vegetation growth or building of facilities close to the wind measurement stations are usually not reported and hard to detect in most cases. Therefore, more detailed information about the environment of former and present locations is necessary. Approaches to achieve homogenization of wind data by means of such information about station environment and more precisely the roughness length and fetch (e.g. Wieringa 1976; Wieringa 1996; van der Meulen 2000) can help to increase the reliability of the measurements. Such homogenization approaches were applied for the stations Helgoland (Niemeier and Schlünzen 1993) and Norderney (Schmidt and Pätsch 1992). The application of such is unavoidable before using near surface wind measurements. Homogenization processes may become quite complex and require detailed information about the anemometer locations and meteorological expertise.

The existence of errors in wind statistics due to the inhomogeneity of the input data can not be ruled out. They are indeed most likely.

Comparisons with yearly means and 99th percentiles from four other near coastal stations show that this is not a single and a “worst” case scenario. All stations were affected by at least one station relocation during a period of 44 years. In most of the cases these station relocations led to a detectable sudden increase or decrease in the yearly means and yearly 99th percentiles.

There are reasonable alternatives to the direct use of measured wind data. One is the use of wind proxies derived from pressure measurements, which are not sensitive to influences of the environment (e.g. Schmidt and von Storch 1993). Another possibility is the use of data from tall measurement towers. These measurements are not affected by station relocations and they are much more homogenous also due to the strongly decreased influence of the environment.

2 Data sets

2.1 Tower measurements

Analysis of measurements from synoptic stations (with measuring heights around 10 m) show that they are often not representative over large areas and for comparisons with simulated winds in grid boxes of low spatial resolution without homogenization (Chapter 1.2; Wieringa 1976; Wieringa 1983). To reduce the influence of the disturbances due to the environment, measurements from five tall meteorological towers are used in this study. The data sets were provided by different research institutions.

A brief description of the towers and their surroundings is given in Table 2.1. The environments of these towers and therefore the simulated areas vary in complexity of terrain structure and land use. Cabauw is located in a homogenous flat area and Lindenberg is surrounded by agricultural fields and small forests. The Hamburg tower is located in an industrial area of the city. Cabauw, Lindenberg and Hamburg have comparably simple conditions for the simulation of mean wind fields. In contrast, the conditions at the sites Juelich and Karlsruhe are quite different as both towers are located in forests. Juelich in a broad leaf forest and the site Karlsruhe features predominately coniferous species and a more complex terrain structure. At both of these sites land use parameterisation and orography play an important role on the simulations.

Table 2.1: Description Tower Measurements

Station	ASL:	Owner:	Environment	Starting time
Hamburg	0.3 m	University of Hamburg	Land cover: Suburban, flat industrial area; rather homogeneous orography	01.2001 (UltraSonic)
Cabauw	-0.3 m	Koninklijk Nederlands Meteorologisch Instituut (KNMI)	Grasslands, agricultural and small villages; open and flat terrain	05.2000
Lindenberg	73 m	Richard-Aßmann-Observatory, German Meteorological Service	Mixed land cover: arable fields and small forests	06.1998
Juelich	91 m	Research Center Juelich	Located in a small clearing in a broad leaf forest, surrounded by research Center facilities	01.1995
Karlsruhe	110 m	Research Center Karlsruhe	Needle-leaf forest, surrounded by research Center facilities Located in the Upper Rhine valley	01.1974

For a better illustration the towers are separated into two groups according to the complexity of terrain and land use:

- *Northern stations:*
Flat/homogenous terrain: Cabauw and Lindenberg and urban: Hamburg
- *Southern stations:*
Complex terrain/forests: Juelich and Karlsruhe

Outliers are removed from the observations and data adjusted to remove the influence of the tower ensuring error as small as possible. Either the tower has more than one measuring arm or the data are removed in cases in which the wind comes from the mast direction.

To reduce the influence of the immediate surroundings the main focus of this analysis is on results at and above 50 m heights.

Table 2.1 shows that data from all towers are available for the period 2001 - 2005. No major gaps are found for this period. Therefore, representative measurements over the period (2001 - 2005) can be ensured for the chosen stations and heights. This period serves as reference period for the verification of mean wind statistics and the sensitivity analysis presented in Chapter 3. Due to a deviating simulation period of one of the RCM simulations, covering 1991 - 2000, also a second period is chosen for the time series analysis in Chapter 4. The second period differs for the towers depending on the availability of the measuring data after 1991 and before 2001 (Table 2.1). E.g. for Karlsruhe, the whole 10 years are covered, while the data from Cabauw are starting in May 2000. Furthermore, some longer gaps are found in this period.

2.2 Model data

2.2.1 Reanalysis data

Reanalysis data are a combination of different kinds of observations e.g. data from weather stations, buoys, radiosondes and satellite images assimilated into modern prediction models. The assimilation scheme provides for a uniform spatial and temporal coverage and a gridded dataset. Because reanalysis data are based on observations they are subject to changes in time and space and should not be seen as absolute reliable representatives of the true climate (Kistler et al. 2001; Reichler and Kim 2008).

NCEP/NCAR Reanalysis 1 (NCEP)

The 10 m wind speed derived from wind components in zonal and meridional direction of the NCEP/NCAR Reanalysis 1 is used for the trend detection analysis. The data are provided by NOAA/OAR/ESRL PSD, Boulder, Colorado, USA². Starting 1948 it contains 6 hourly model output. The 10 m wind speed

² <http://www.esrl.noaa.gov/psd>

components are available on a global T62 Gaussian ($\sim 1.875^\circ$) grid. A detailed description of the NCEP/NCAR Reanalysis 1 is given in Kalnay et al. (1996).

ERA40 Reanalysis (ERA)

In addition ERA40-Reanalysis data are investigated within the trend detection process. 10 m wind components of the reanalysis data of the European Centre for Medium-range Weather Forecasts (ECMWF) are available on a 1.125° grid for the period 1958 - 2002 with an output interval of 6 h. A detailed description can be found in Uppala et al. (2005).

Japanese 25-year Reanalysis (JRA)

The JRA reanalysis was conducted by the Japan Meteorological Agency (JMA) in collaboration with the Central Research Institute of Electric Power Industry (CRIEPI). The data set has a spatial resolution of ~ 120 km (T106 grid) covering the period 1979 up to the present (Onogi et al. 2007). Data over the period 2001 - 2005 are used for the sensitivity analysis in Chapter 3.

2.2.2 Regional Climate Model data

SN-REMO

In this study data of a simulation with the hydrostatic regional climate model REMO (REgional MOdel, Jacob and Podzun 1997) by Feser et al. (2001) is used for the trend detection. REMO is based on the Europa-Modell (EM) from the German Weather Service. 10 m wind speeds are taken from a Hindcast simulation, covering the period 1948 - 2006. The simulation was done on a rotated grid that covers Europe with a spatial resolution of $0.5^\circ \times 0.5^\circ$ and 20 vertical levels.

For this Hindcast simulation REMO 5.0 was forced by the NCEP/NCAR-Reanalysis 1 and NCEP/NCAR-Reanalysis 2 after 03/1997 at the lateral boundaries and within the domain by a spectral nudging approach influencing the

wind components of the upper layers (von Storch et al. 2000). The spectral nudging approach includes an assimilation of large scales from the reanalysis, spectrally composed, to the wind components of REMO (Feser and von Storch 2005). Therefore it forces the RCM closer to the large scale behaviour of the reanalysis. The nudging starts at the top of the model and the coefficient decreases with height to 850 hPa. This gives the RCM more freedom for lower heights, where regional features have higher influence and an added value due to the higher resolution of the RCM is expected.

COSMO-CLM

The regional climate model COSMO-CLM (Böhm et al. 2006) is the climate version developed from the non-hydrostatic Local Model (COSMO) of the German Weather Service (DWD) by the CLM community³. Details about the physical parameterizations, dynamics and numerics of the model can be found in Doms et al. (2005), Doms and Schättler (2002) and Schulz (2009). Within this study three different simulations are used:

CCLM-SNN50

For this study data of version 3.21 from a simulation by the GKSS Research Center Geesthacht is taken for the verification of simulated mean wind statistics and the sensitivity analysis in Chapter 3 as well as for the verification of time series in Chapter 4. The simulation area covers Europe and uses a rotated grid with a spatial resolution of $0.44^\circ \times 0.44^\circ$ (~50 km), 32 vertical levels, and an output interval of 3 hours, covering 2001 - 2005. The simulation is spectrally nudged with the NCEP/NCAR-reanalysis 1.

CCLM-SNE50

For the trend analysis 10 m wind speed from a simulation of Version 3 (2.4.6) from the ENSEMBLES project is used (Hewitt and Griggs 2004). This simulation

³ www.clm-community.eu

has the identical spatial resolution of $0.44^\circ \times 0.44^\circ$ (~ 50 km) and 32 vertical levels, but it has the higher output interval of 1 h. The simulation is spectrally nudged by ERA 40.

CCLM-LC20

Within the LandCare 2020 project (Köstner et al. 2009) a simulation of COSMO-CLM 2.4.11 with a spatial grid resolution of $0.165^\circ \times 0.165^\circ$ (~ 20 km) was conducted, forced at the boundaries by NCEP/NCAR Reanalysis 1 but not spectrally nudged. It has 32 vertical levels and an output interval of 3 hours over the period 1991 - 2000. This simulation is used for the time series analysis in Chapter 4.

Wind Energy Simulation Toolkit (WEST)

The Wind Energy Simulation Toolkit uses a statistical-dynamical downscaling approach described in Frey-Buness et al. (1995) and Mengelkamp (1999). A classification of geostrophic wind data from a forcing data set is conducted. Mean geostrophic wind and temperature profiles for each class are used as initial conditions at the center of the chosen domain (Yu et al. 2006). A mesoscale model simulation with the Canadian Mesoscale Compressible Community Model MC2 (Tanguay et al. 1990 and Thomas et al. 1998) is conducted for each class. The results are weighted by the frequency of the occurrence of the class in the forcing period. A statistical module calculates mean fields which can be seen as representatives for the mean wind fields over the whole forcing period (Pinard et al. 2005). The low computational effort allows a flexible application of the model and a detailed investigation of the influences of the general settings. In the default version the model is driven by the NCEP/NCAR-reanalysis (Kalnay et al. 1996).

3 Verification of simulated wind statistics

The wind power industry has grown steadily during the recent years and constantly requires more reliable and detailed information on the wind climate on local and regional scales. As modeling improves it increasingly becomes the chosen alternative to near surface observations (e.g. Larsén et al. 2008). In this chapter it is investigated, if limited area models are able to reliably simulate boundary layer wind statistics over different land cover and terrain structures. In contrary to common approaches, i.e. using surface observations, measurements from tall towers are used.

The influence of the grid resolution, of the roughness lengths, and of the synoptic climatological forcing is investigated. Simulated wind statistics from two models with different downscaling procedures are compared. The differences in terrain height and land cover structure between the sites allow a closer analysis of the influence of the model grid environment. The simulations chosen for this investigation are CCLM-SNN50 (dynamical downscaling) and the Canadian Wind Energy Toolkit WEST (statistical-dynamical downscaling). State of the art wind mapping systems as WEST are a common tool for the prediction of the wind energy potential due to their less expensive application. They are often used for the design of wind resource maps. A Canadian Wind Atlas with a resolution of 5 km was generated with WEST and its validation shows reasonable results for different regions of Canada (Benoit and Yu 2003). A similar approach, based on

the mesoscale model KAMM, was used for modeling the climate of Ireland (Frank and Landberg 1997).

Wind atlases for Denmark, Ireland, Portugal were generated by means of a combination of KAMM and the wind atlas analysis and application program WAsP (Frank et al. 2001).

One major issue in the use of mesoscale models for the wind field simulation is the selection of an adequate grid resolution. It is assumed that with higher resolutions smaller scales can be reproduced. Thus, an added value for increasing grid resolution is expected. This is most important over more complex areas.

The statistical-dynamical downscaling approach is more computationally efficient than the dynamical downscaling approach. Therefore, WEST enables an investigation of an added value for increased grid resolution. Furthermore, the influence of the synoptic forcing and the land use on wind statistics (in particular mean wind profiles, wind speed distributions and wind direction distributions) is investigated.

WEST model simulations for Western Europe with typical mesoscale resolutions of 50, 20 and 10 km are conducted and are compared to the observational data and calculated mean fields of CCLM-SNN50 (~50 km resolution) for 50 and 100 m AGL. To consider the complex terrain and land structures of the southern stations, also high resolution (1km) WEST simulations are generated. Two reanalysis data sets (NCEP/NCAR Reanalysis (NCEP) (Kalnay et al. 1996) and the Japanese 25-year Reanalysis Project JRA-25 (JRA) (Onigi et al. 2007) are used as forcing data for WEST. Distortions due to differences of Canadian and European land use definitions are investigated by means of the USGS land use data, the CCLM-SNN50 roughness field and the European land use database CORINE.

3.1 Methods

Wind statistics for the period 2001-2005 are calculated for all towers using the output time interval from the CCLM-SNN50 model (three hours). The CCLM-SNN50 output represents instantaneous wind speeds averaged over the model time step of four minutes. Comparisons between mean wind fields from three-hourly values (averaged over five, ten or twenty minutes) and from values with the original measuring frequency, every five or ten minutes, reveal that adjusting the time step has such a small effect on the mean wind fields of the observations that deviations to the time steps of the WEST simulations can be neglected (not shown).

The measured wind statistics for the period 2001 - 2005 are assumed to be representatives for the true mean condition of the wind fields in the lowest 100 meter of the boundary layer. Simulated wind statistics over the same time period are taken from the output of the CCLM-SNN50 simulation and from WEST. A bilinear interpolation of the four tower surrounding grid points is used. For Cabauw only the three surrounding land boxes of the CCLM-SNN50 data are considered and an Inverse Distance Weighting is applied.

Mean wind speeds at 50 and 100 m height and their standard deviations are used for the analysis. In addition, wind speed frequency distributions at both heights are investigated after calculating the probability density functions (PDF). According to WEST the wind speed is therefore classified into 27 wind speed classes, each of them in the range of 1 m/s except of the first two and the last class. The first class represents the calm situations between 0 and 0.2 m/s, the second class the low wind speeds between 0.2 and 1 m/s. Wind speeds higher than 25 m/s are assigned to the last class (CHC 2006). The deviations between measured and simulated wind speed distributions are expressed by statistical skill scores as indicators for their similarity. A modification of the Perkins Score (Perkins et al. 2007), which is also known as histogram intersection index HI, is calculated for all simulations.

It is defined as

$$HI = 1 - \sum_{i=1}^n \min(h_{obs}, h_{simu}) \quad (3.1)$$

with n equals the number of bins and h_{obs} and h_{simu} as observed and simulated smoothed frequencies of the bins of the PDFs. The HI score subtracts the overlap of the simulated and observed PDF from One, so that the HI score equals zero for a perfect simulation of the observed PDF. This score is biased to the median wind speed classes. This means, it is more focused on deviations in the more frequent median wind speeds. In addition, another, unbiased skill score is calculated, which is more sensitive to deviations in the less frequent wind speed classes. The Chi² score

$$\chi^2 = \sum_{i=1}^n \frac{(h_{simu} - h_{obs})^2}{h_{obs}} \quad (3.2)$$

(with the same notation) weights the squared difference of two bins by the frequency of the bin in the observations. It is also equal to zero for a perfect simulated PDF.

The observations are partly logarithmically interpolated to the model level heights of 50 and 100 m. The limited validity of the logarithmic wind speed law to near-neutral cases is therefore ignored in agreement with WEST.

According to WEST the mean wind direction distributions are obtained by classifying the wind directions into twelve sectors each representing an angle of 30° (CHC 2006).

3.2 Results and Discussion

3.2.1 Comparison CCLM-SNN50 and WEST

Initially, the general performance of both models is tested by choosing the standard parameterization and default initial conditions of WEST and a spatial resolution of 50 km.

Northern stations:

The low resolution simulations (~50 km) of CCLM-SNN50 and WEST generate a reasonable simulation of the mean wind profile for Cabauw (with deviations < 0.4 m/s), but show a systematic overestimation of the mean wind profile in Hamburg (> 0.5 m/s). For Lindenberg a good simulation can be reached with CCLM-SNN50 instead of the large overestimation (of more than 0.8 m/s) simulated by WEST (Figure 3.1). The WEST simulation shows, in contrary to CCLM-SNN50, an overestimated variability, indicated by higher standard deviations.

For the three northern stations the HI score of the CCLM-SNN50 simulation is below 0.1 (Figure 3.2 a), describing an overlapping area between measured and simulated PDF of more than 90 %. The best simulation is obtained for Cabauw with an overlap of 93.3 and 96.8 %. The size of the overlap for the WEST simulation ranges between 84.9 and 90 % for these stations (Table 3.1). The Chi² score is close to Zero (< 0.041) for the CCLM-SNN50 simulation for the northern stations and comparatively higher (between 0.047 and 0.359) for the WEST simulation, indicating a worse simulation of the less frequent wind speed classes by WEST (Figure 3.2 b).

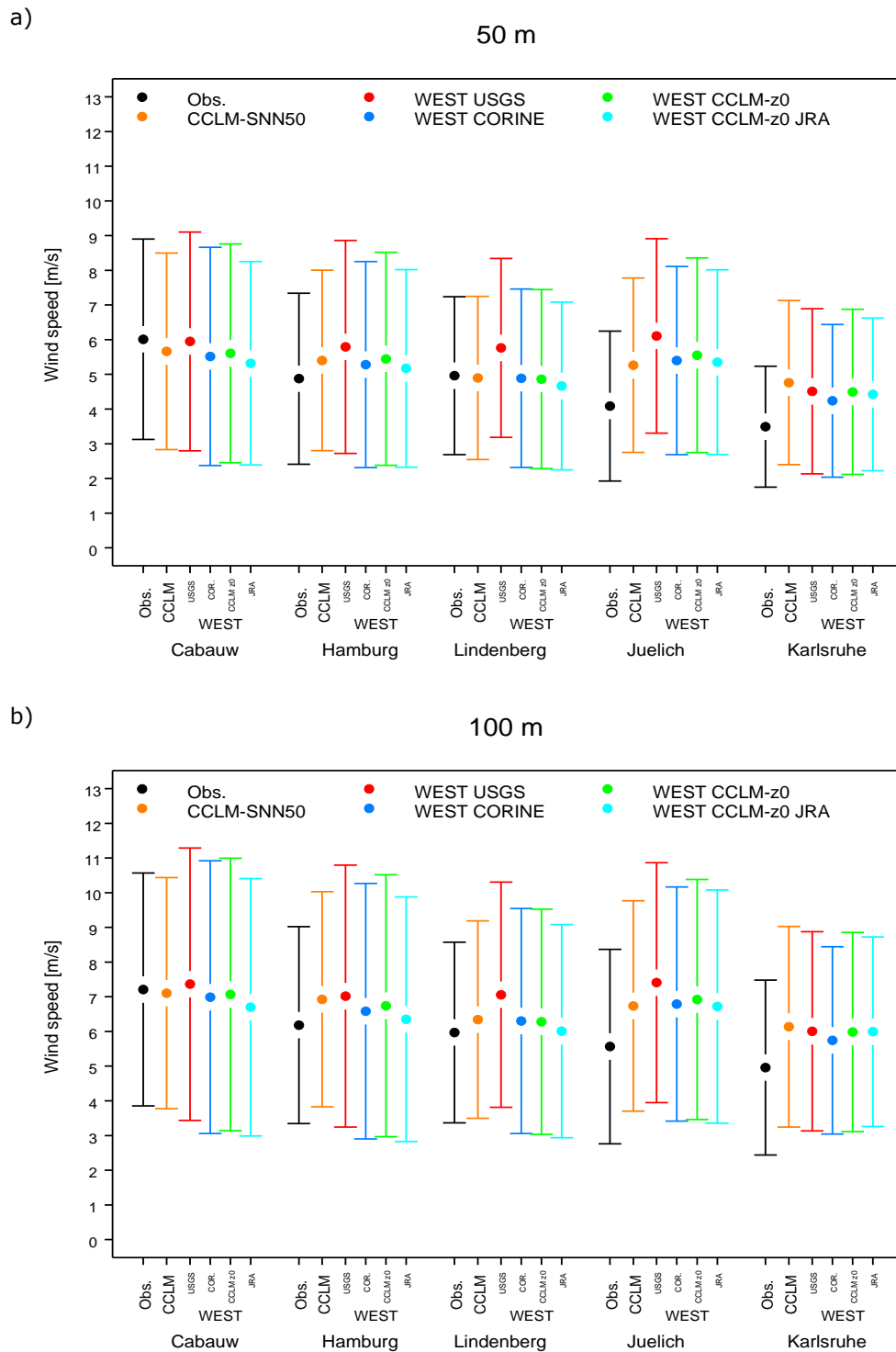


Figure 3.1: Observed and simulated mean wind speeds and their standard deviation (2001 - 2005) a) at 50 m and b) at 100 m, simulated with a spatial grid resolution of 50 km. Per station from left to right: CCLM-SNN50, WEST simulations: with USGS land use, with CORINE land use, with the CCLM roughness field and forced by NCEP and with the CCLM roughness field and forced by JRA.

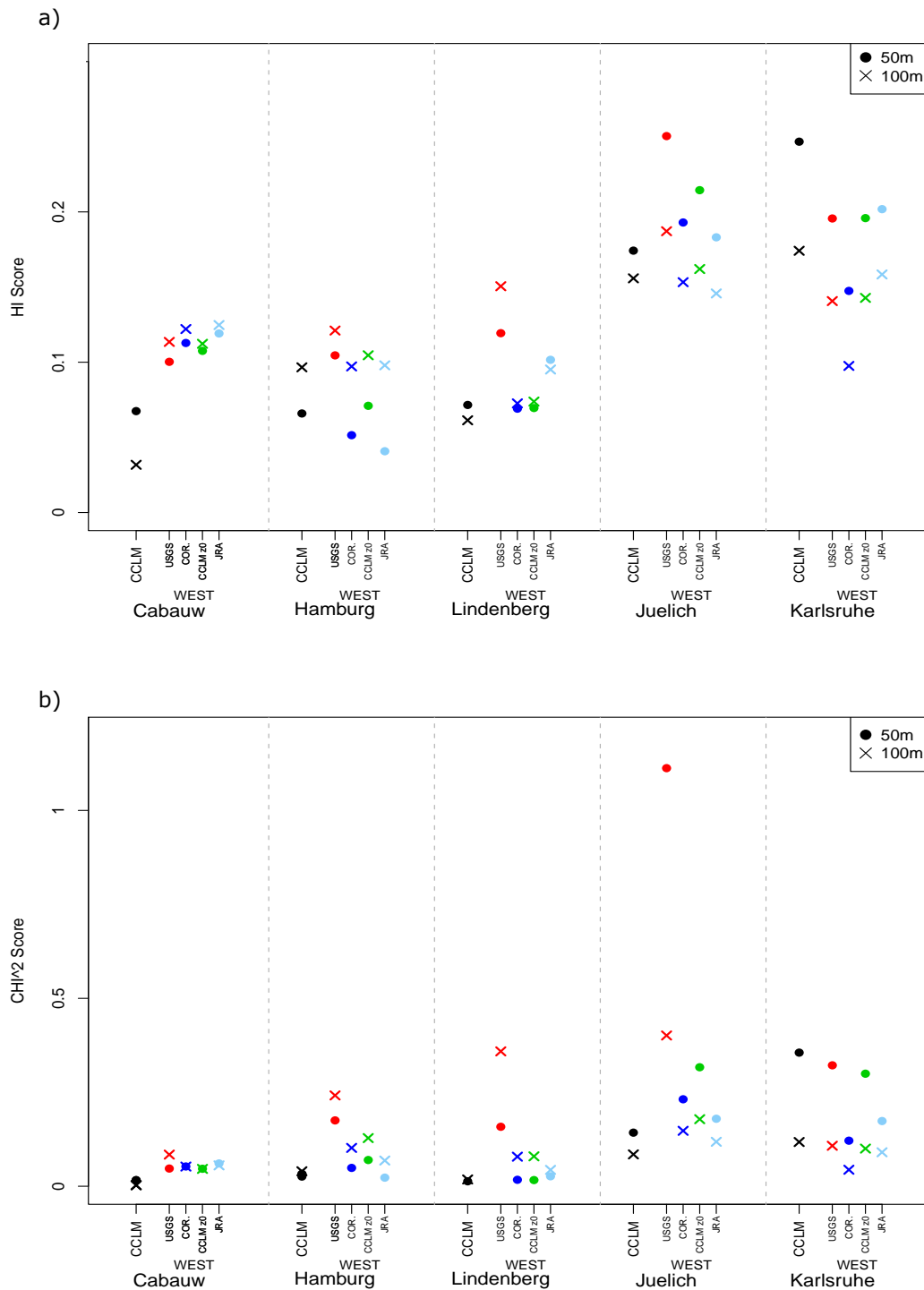


Figure 3.2: a) HI Scores and b) Chi² Scores for the simulated PDFs with a spatial grid resolution of 50 km. Per station from left to right: CCLM-SNN50 (CCLM), WEST simulations: with USGS land use, with CORINE land use, with the CCLM roughness field and forced by NCEP and with the CCLM roughness field and forced by JRA at 50 m (Point) and at 100 m (x).

Table 3.1.: Size of the overlap of observed and simulated wind speed PDFs in percent.

		Cabauw		Hamburg		Lindenberg		Juelich		Karlsruhe	
		50m	100m	50m	100m	50m	100m	50m	100m	50m	100m
CCLM-SNN50											
WEST											
50		93.3	96.8	93.4	90.3	92.8	93.9	82.6	84.5	75.3	82.6
50	USGS	90.0	88.6	89.5	87.9	88.1	84.9	75.0	81.3	80.4	85.9
	CORINE	88.7	87.8	94.9	90.3	93.1	92.7	80.7	84.7	85.3	90.2
	COSMO-CLM z0	89.2	88.8	92.9	89.5	93.0	92.6	78.6	83.8	80.4	85.7
	COSMO-CLM z0 JRA	88.1	87.5	95.9	90.2	89.8	90.5	81.7	85.4	79.8	84.2
20	USGS	89.8	89.2	90.2	88.4	86.6	84.6	77.2	80.8	74.8	78.3
	CORINE	89.7	90.3	93.4	88.7	91.7	89.7	84.1	85.0	80.9	84.9
10	USGS	89.8	90.7	84.9	88.3	84.2	82.4	82.7	82.8	74.3	77.4
	CORINE	88.7	92.3	94.7	91.4	92.7	91.1	85.5	82.1	80.6	84.7
1	CORINE	90.8	91.1	93.3	91.5	92.1	92.1	93.2	93.0	92.1	94.9

Both models reasonably simulate the wind direction distribution for Cabauw and Lindenberg with a slight underestimation of the frequency of easterly winds for WEST. This effect is shown for Cabauw in Figure 3.3.

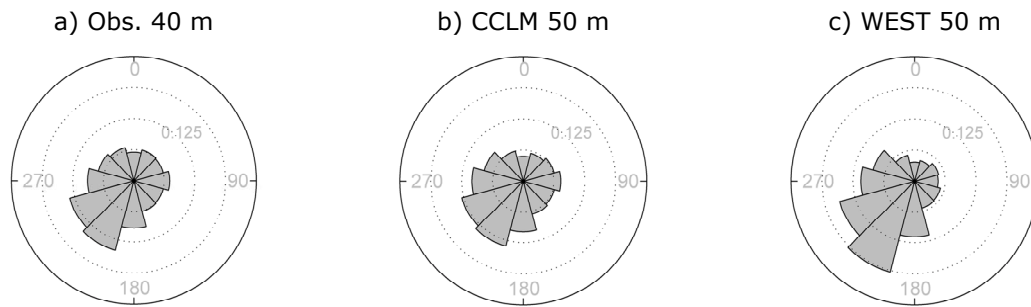


Figure 3.3: a) Observed wind direction distribution in Cabauw (2001-2005). Simulated wind direction distributions b) by CCLM-SNN50 and c) by WEST (50 km resolution).

The frequency of the main wind direction (W) in Hamburg is well simulated by WEST but underestimated by CCLM-SNN50 and both models simulate more south-westerly winds. A second peak in the wind direction distribution of Hamburg, in south easterly winds, is simulated but underestimated (Figure 3.4).

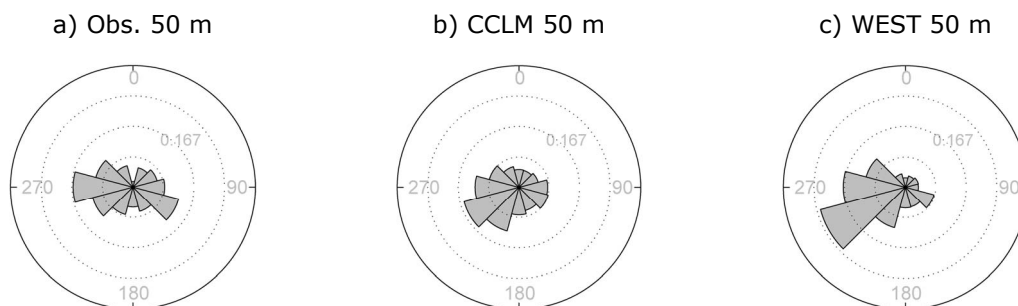


Figure 3.4: a) Observed wind direction distribution in Hamburg (2001 - 2005). Simulated wind direction distributions b) by CCLM-SNN50 and c) by WEST (50 km resolution).

Southern stations:

Both models show a systematic overestimation of the mean wind speed for the forest stations (> 1 m/s) with an extreme overestimation of more than 2 m/s for

Juelich at 50 m height by WEST (Figure 3.1). The lower variability of the wind speed at Karlsruhe is seen but overestimated by both models. The overlapping areas for the forest stations are comparatively small in a range of 75.3 - 84.5 % by CCLM-SNN50 and 75 - 85.9 % by WEST (Figure 3.2 a and Table 3.1). Also the Chi^2 score for CCLM-SNN50 is larger (with values between 0.085 and 0.356) for the forest stations in comparison to the results for the northern stations (Figure 3.2 b). With WEST the values for the Chi^2 score are, in comparison to the northern stations Hamburg and Lindenberg, not remarkably higher for the forest station Karlsruhe with values of 0.108 and 0.322. At the other forest station, Juelich, the Chi^2 score reaches a size of 0.401 and 1.113.

The wind direction distribution of Karlsruhe is strongly influenced by the orography. The wind is channelled due to the Upper Rhine valley with the main directions between 195° and 225° and between 45° and 75° (Figure 3.5). The complex orography is not resolved by the averaged fields in the models. CCLM-SNN50 simulates the correct main wind direction of south westerly winds, but with lower frequency, and underestimates the frequencies of east-north-easterly winds. The frequency of all other wind directions is overestimated.

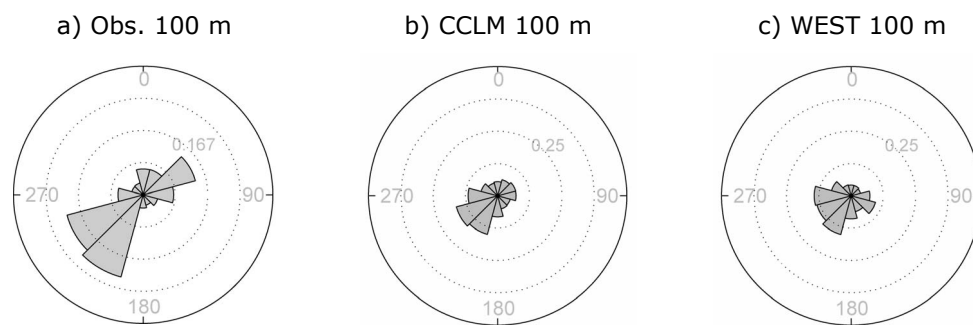


Figure 3.5: a) Observed wind direction distribution in Karlsruhe (2001 - 2005). Simulated wind direction distributions b) by CCLM-SNN50 and c) by WEST (50 km resolution).

The mean wind direction distribution of WEST shows more frequent westerly winds and also an underestimation of the observed main wind directions (Figure 3.5).

Summary

Both models show a systematic overestimation of the mean wind speed for the forest stations and for the urban station Hamburg. For the two other northern stations over rather homogenous terrain CCLM-SNN50 reasonably simulates the mean wind speed profiles, while WEST shows an overestimation at the station Lindenberg. As detected for the simulation of the wind speed profile, the deviations between observed and simulated PDF are mostly larger for the forest stations.

The simulated profiles by WEST show a higher agreement with the observations in three cases (at Karlsruhe at both heights and at Cabauw at 50 m). In the other cases the simulated profile by CCLM-SNN50 is closer to the observations. Comparing the performance for the simulation of the wind speed distributions by both models shows smaller scores and therewith smaller deviations to the observed PDFs with the CCLM-SNN50 simulation for four of the stations. Only for the station Karlsruhe the simulated PDF by WEST is, as the wind speed profile, closer to the observed PDF. The orography of both simulations is taken from the GTOPO30 data set (USGS 2009). The CCLM-SNN50 roughness fields show higher values for the grid boxes at Karlsruhe. Thus, differences are a result of different model dynamics or downscaling methods.

Summarizing for all stations, the wind direction distributions for the northern stations over comparably homogenous terrain can be reasonably simulated by both models with an overestimation of southwesterly winds for one station. A tendency towards an underestimation of the frequency of easterly winds is generally found for both models, but is stronger in the WEST simulation. The

channelisation effect due to the Upper Rhine valley for the station Karlsruhe is, however, not simulated by the models with the low spatial resolution.

3.2.2 Influence of the roughness field

The largest deviations between simulated and measured profiles for the stations with more complex land cover possibly indicate an inadequate representation of the roughness structures in the models (Note that in this study the terms roughness and roughness length (z_0) refer to the land use based roughness).

Within the preprocessing the model roughness lengths are generated by averaging predefined roughness fields with different resolutions over the grid box areas. The predefined fields are a result of land use definition routines. By means of satellite images the land cover data are classified into land use classes. These land use classes and the spatial resolutions of the map vary between different land use data sets. In order to assimilate the land cover data to the model, the land use classes are assigned to fixed land use classes of the respective model each with a specific roughness length.

Beside the uncertainty of satellite measurements and deviations in the spatial resolutions of different land cover data sets, major uncertainties occur within the classification process. This includes the land use detection and classification process, with uncertainties due to temporal variations or in the choice of training data (Castilla and Hay 2007). But also the assignment to the model land use classes is a critical point. Especially for the two latter points the consideration of regional differences is important. Conceivably a European forest does not necessarily match the definition of larger North American forests. Also roughness lengths of similar vegetation forms can be regionally different.

In order to have identical roughness descriptions in both models, the roughness fields are adjusted by interpolating the roughness lengths used by CCLM-SNN50

(based on ECOCLIMAP (Champeaux et al. 2005)) to the WEST 50 km grid. The 50 km simulation of WEST is repeated with the adjusted z_0 . To be able to investigate the influence of the roughness fields also for higher resolutions, we use the CORINE Land Cover 2000 (CORINE) (Bossard et al. 2000) data set with a spatial resolution of 100 m instead of the original data USGS (with a spatial resolution of 1 km) (Loveland et al. 2000). The CORINE data set consists of 44 different land use classes and covers Europe. These land use classes are assigned to the 26 land use classes of WEST considering assignments from Silva et al. (2007) and own considerations based on Stull (1988) and the specification of the WEST land use classes (CHC 2006) and the tower environments. After this classification, WEST simulations with a spatial resolution of 50, 20 and 10 km are conducted with new roughness fields based on CORINE.

Since the wind direction simulation is mainly influenced by the orography no effect of the replaced land use data set on the wind direction distributions is found.

The development of the model roughness lengths of WEST with increasing spatial resolution is shown in Figure 3.6. The roughness length based on USGS is smaller than the one based on CORINE in all cases for all resolutions. The roughness lengths from the interpolated CCLM-SNN50 roughness fields are mostly in between. Only for Lindenberg the roughness length based on ECOCLIMAP is slightly higher than the one based on CORINE.

The CORINE Land Cover data base should be advantageous to USGS due to a higher spatial resolution and the European origin. This also holds for the CCLM-SNN50 roughness field based on ECOCLIMAP. The effects of the differences on the mean wind speed profile and on the wind speed distribution and the reliability of the different roughness fields are evaluated in the following.

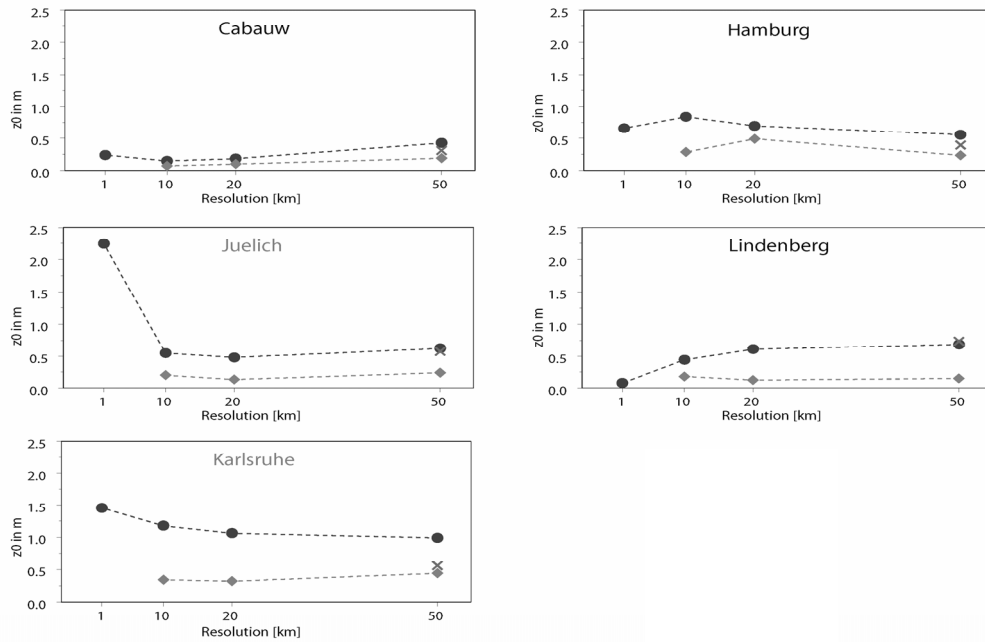


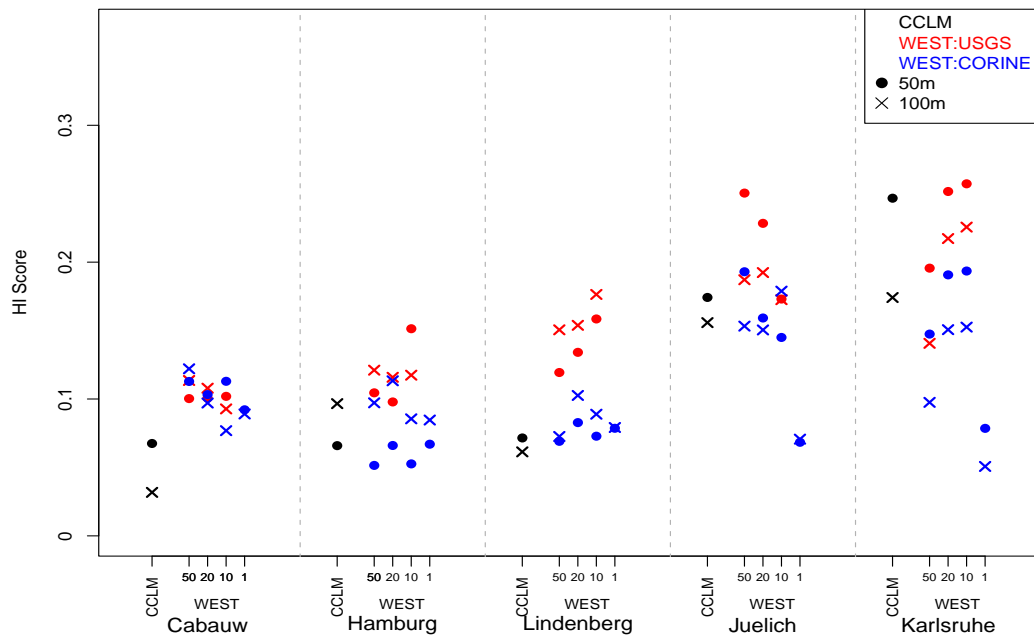
Figure 3.6: WEST roughness lengths in m based on CORINE (black) and USGS (grey) for different resolutions. WEST roughness length based on the CCLM-SNN50 roughness field ECOCLIMAP (X). Forest stations are marked with grey names.

Northern stations

Adjusting the roughness fields of WEST with the CCLM-SNN50 roughness field lead to quite similar simulations of the mean wind profile by both models. This results partly in a decrease in the simulation skill for Cabauw, with an underestimation of the mean wind speed (Figure 3.1) and a decrease in the wind speed PDF overlapping area at 50 m (Figure 3.2 a).

For Hamburg and Lindenberg the new roughness field reduces the mean wind speed by up to 0.35 m/s and up to 0.9 m/s, respectively, and it increases the overlap up to 3.9 and 7.7 % (Table 3.1). The overestimation of high wind speeds can be reduced for all northern stations, as indicated by lower Chi^2 scores (Figure 3.2 b). However, the overestimated wind speed variability of WEST is not reduced.

a)



b)

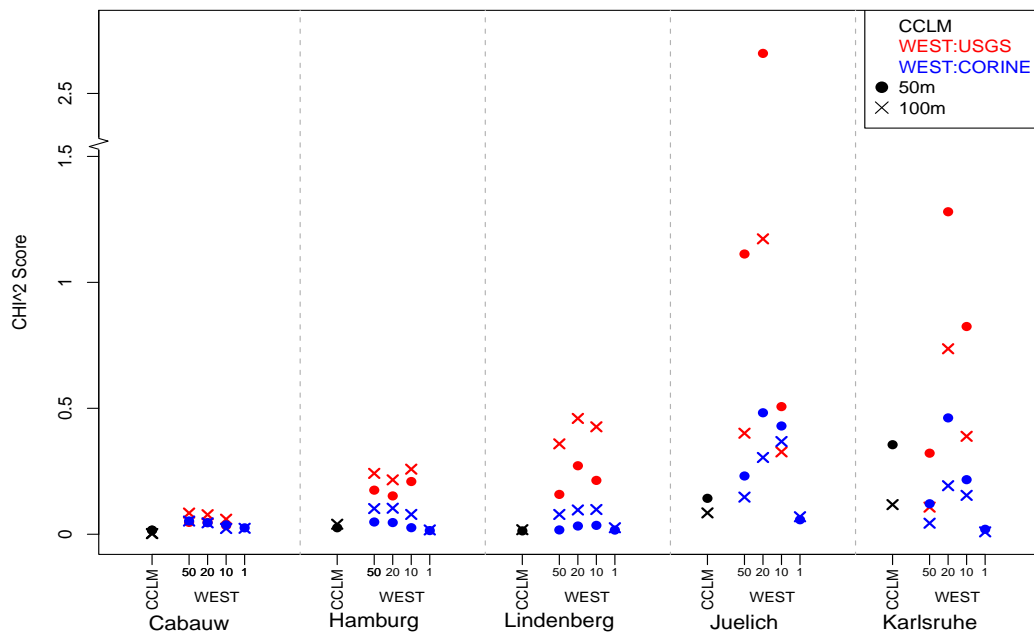


Figure 3.7: a) HI Scores and b) χ^2 Scores for the simulated PDFs with increasing grid resolution from 50 to 20 to 10 and to 1 km. Per station with CCLM-SNN50 (CCLM) (black), WEST simulations: with USGS land use (red), with CORINE land use (blue), at 50 m (Point) and at 100 m (x).

Replacing USGS by CORINE land use data leads to quite similar effects. Due to higher values of the roughness lengths the effect is stronger for Cabauw and Hamburg. This has again partly negative effects for Cabauw, especially at 50 m. For Hamburg and Lindenberg it results in decreased scores in comparison to the USGS land use for all resolutions. Increases in the overlapping PDF area up to 9.9 and 8.7 % respectively (Figure 3.7 a and Table 3.1) and lower Chi^2 scores are found for both stations (Figure 3.7 b). Opposite to the CCLM-SNN50 roughness field, the simulation skill for the wind speed variability partly increases with CORINE (Figure 3.8).

Southern stations

For Karlsruhe the effect of the CCLM-SNN50 roughness field is comparably small due to the small difference in the roughness lengths (Figure 3.6): For Juelich it helps to reduce the overestimation in the mean wind speeds up to 0.56 m/s and increases the PDF overlap of 3.6 and 2.5 % (Table 3.1), respectively, and strongly decreases the Chi^2 scores (Figure 3.7).

With the 50 km resolution the higher roughness of CORINE results in a stronger decrease of the overestimation of the mean wind speed for both stations and in increases in the overlapping areas of the wind speed PDFs (up to 5.7 % (Juelich) and 7.6 % (Karlsruhe), respectively (Table 3.1)). Also the effect on the Chi^2 scores is stronger as with the CCLM-SNN50 roughness lengths.

Similar effects can be observed for the higher resolutions (Figure 3.7 and Figure 3.8), where the higher roughness of CORINE reduces the wind speeds and improves the simulations of the wind speed distributions. Only the 10 km simulation constitutes an exception for the 100 m height at Juelich, where the simulation with CORINE leads to higher wind speeds and therewith to a reduced simulation skill.

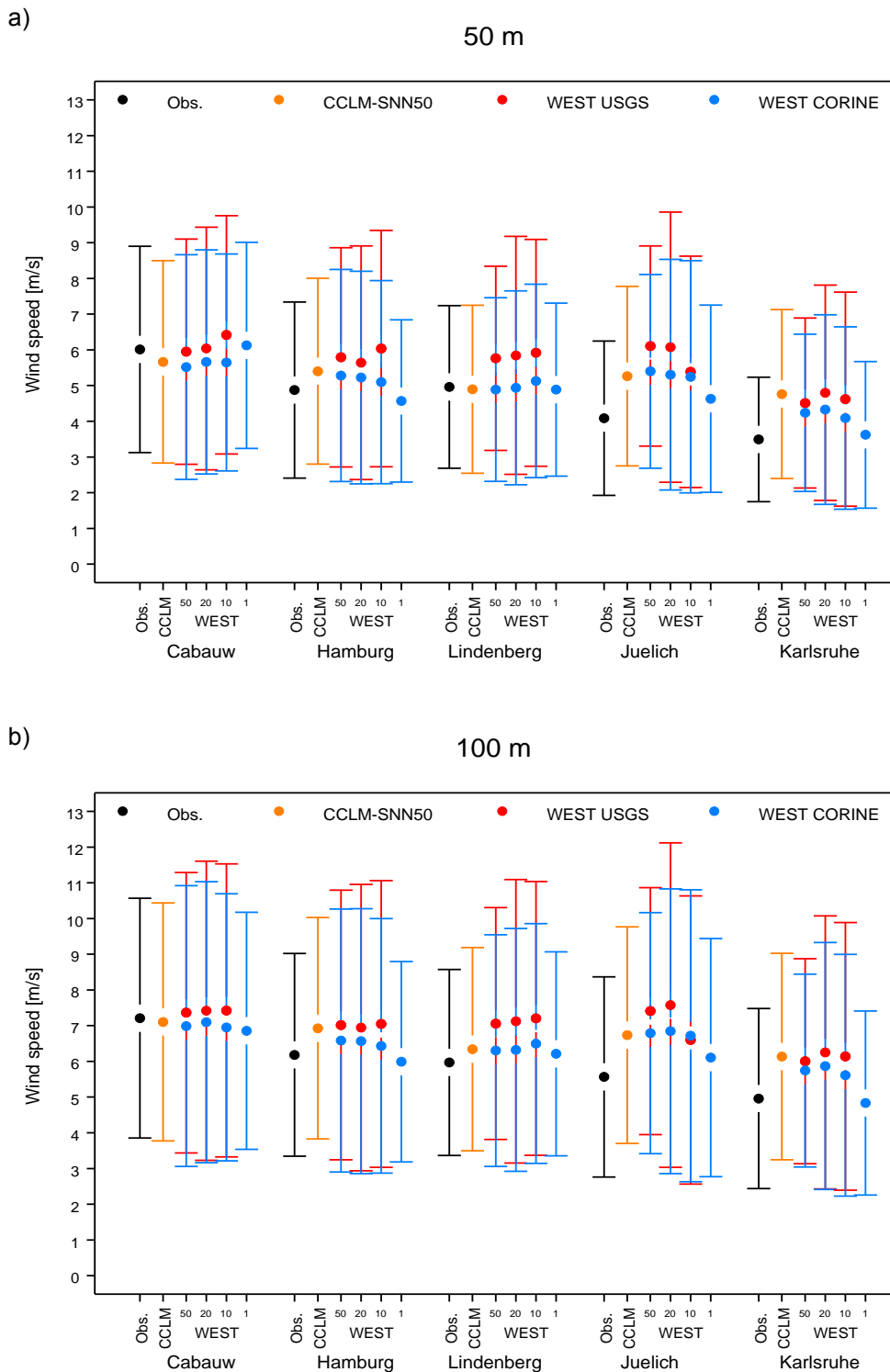


Figure 3.8: Observed and simulated mean wind speeds and their standard deviation (2001 - 2005) a) at 50 m and b) at 100 m with increasing grid resolution from 50 to 20 to 10 and to 1 km. Per station with CCLM-SNN50 (CCLM) (black), WEST simulations: with USGS land use (red), with CORINE land use (blue).

Summary

Adjusting the WEST roughness length to the CCLM-SNN50 roughness field leads to quite similar simulated profiles in both WEST and CCLM-SNN50. In addition, it generally improves the simulation for all stations except for Cabauw, where the USGS land use provides better results for the 50 m height and seems to be more conform to the roughness of the environment. The differences between the profiles with the old and the new roughness fields range from minimal 0.02 m/s (at 50 m height in Karlsruhe) to maximal 0.9 m/s (at 50 m height in Lindenberg).

Analogous improvements can be detected for the wind speed distributions. Except for Cabauw at 50 m, where the new roughness provides a larger HI score, and for Karlsruhe, where the deviations between the two versions of the model roughness fields are small, a better simulation can be reached with the new roughness field. The differences in the HI Score range between 0.000 and 0.076, indicating differences in the overlapping PDF areas from 0.0 to 7.7 %.

Comparing the results of the new WEST simulation with the results of CCLM-SNN50 shows also a large similarity for the simulation of the wind speed distributions. The sizes of the overlapping area are quite similar and not obviously better for one model. The occurrence of less frequent high wind speeds is, however, still better simulated by CCLM-SNN50 for four of the stations, indicated by smaller values of the Chi^2 score. Also the simulation skill regarding the wind speed variability is higher for CCLM-SNN50.

With CORINE, the overestimation of the mean wind speed could be reduced in most of the cases. In 25 of 30 cases (for all towers in both heights with all resolutions) the new roughness fields provide a better approximation of the mean wind profile. Four of the other five cases are found for Cabauw, as already seen for the CCLM-SNN50 roughness field. The differences between old and new profiles for the 50 km resolution have a range of 0.27 (Karlsruhe, 100 m) to 0.87 m/s (Lindenberg, 50 m). Additionally, the new land use data base provides a

better simulation of the wind speed distribution in the same 25 of 30 cases (83.33 %) indicated by a decrease in both scores. The differences in the HI Score range between 0.002 and 0.098, indicating differences in the overlapping PDF areas from 0.2 to 9.8 %.

In comparison to the CCLM-SNN50 roughness field CORINE provides better results for the simulation of the mean wind profile in 8 of 10 cases and of the wind speed PDF in 7 of 10 cases for the 50 km resolution, especially for the stations over more complex land structures.

In the case of the Cabauw tower, located over flat terrain, the default land use data base USGS seems to be more representative for the low roughness of the environment. In the other cases, the USGS data seem to underestimate the roughness. This especially holds for the forest stations, located in densely populated areas. Note, that the limited sample size only allows conclusions for these five stations and should not be simply generalized. But the differences obtained after replacing the land use data base show that not only the resolution of the land use data set but also the suitability for the simulation area is a decisive factor.

3.2.3 Influence of the spatial resolution

Because of the low computational effort, simulations of WEST with different spatial resolutions can be conducted for both land use databases. An added value due to higher spatial resolution and therefore a higher reproduction of complex structures is expected. However, the differences between simulated wind profiles obtained by the different resolutions 50, 20 and 10 km are relatively small and the wind speed over more complex land structures is strongly overestimated even with the 10 km resolution. To consider this complexity, high resolution simulations of WEST with a resolution of 1 km based on CORINE are conducted additionally. Each WEST simulation is driven by a climate table generated within

the classification process of the forcing data. It contains statistical information about the geostrophic wind distribution over the forcing period (here: 2001 - 2005) at one grid point close to the grid center. While the simulations with 50, 20 and 10 km spatial resolution are conducted on one large grid for all towers, five small grids are used for the simulations with 1 km resolution. Influences of different climate tables for the five model regions of the 1 km simulation and therefore a positive effect due to a higher representativity of the forcing data tables on the smaller simulation areas cannot be clearly separated from the improvements obtained by higher resolved model orography and land use. They are, however, assumed to be comparatively small considering the small spatial deviations of the geostrophic wind and regarding the results of Chapter 4.4.

Northern stations

Comparing the simulation skill for the northern stations no consistent improvement can be detected for an increasing resolution. The only cases, in which the deviation between simulated and observed mean wind speed decreases continuously with increasing resolution from 50 to 20 and to 10 km can be observed for the wind speed profile for Hamburg and for the median wind speed classes of the wind speed PDF for Cabauw at 100 m, both with CORINE land use. Additionally, the differences resulting from an increasing resolution are comparatively small with a maximum difference of 0.39 m/s and 5.3 % for USGS and 0.19 m/s and 2.7 % for CORINE, respectively (Figure 3.7 a, Figure 3.8 and Table 3.1). The influence on the simulation of less frequent wind speed classes, illustrated by means of the Chi² score, is very small, with maximum effects of 0.114 for USGS and 0.024 for CORINE (Figure 3.7 b). Also the wind speed variability changes only slightly (Figure 3.8).

Even a high spatial resolution of 1 km does not generally improve the simulation skill. For Cabauw at 100 m and for Hamburg and Lindenberg at 50 m the high resolution simulation shows larger deviations to the observed mean wind speed (Figure 3.1) and wind speed distribution than the best of the low resolution

simulations (Figure 3.7 and Figure 3.8). This also holds for the wind speed variability, which is partly too low.

The effect on the wind direction distributions is small for the low resolutions with only slight deviations in particular sectors. The high resolution simulations result in reduced westerly winds and an overestimation of south westerly winds for these stations, as shown for Cabauw (Figure 3.9).

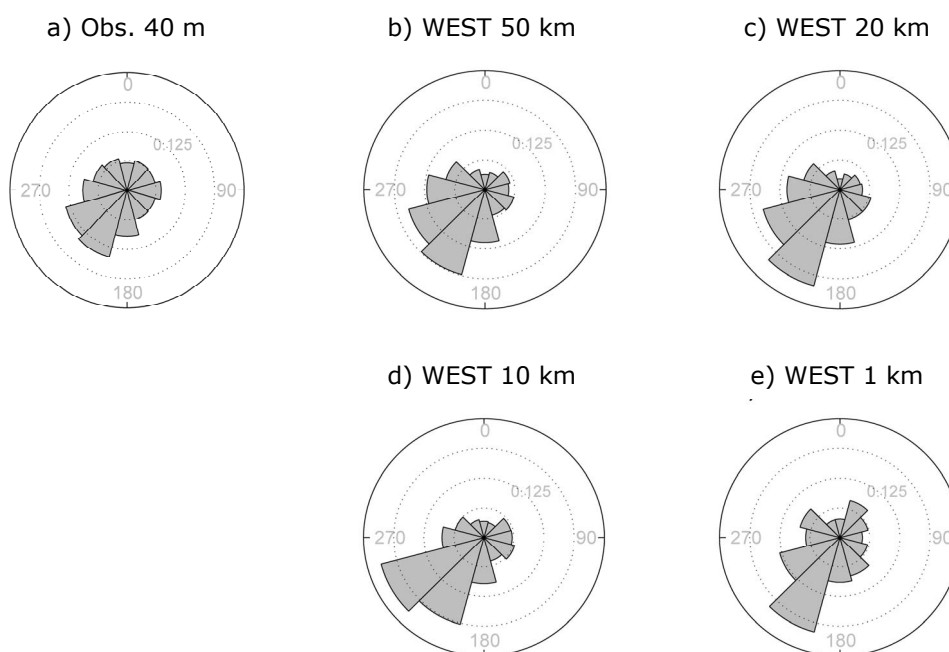


Figure 3.9: a) Observed and b) simulated WEST wind direction distributions at Cabauw (2001 - 2005) with a spatial resolution of 50, c) of 20, d) of 10 and e) of 1 km. Land use: CORINE, forcing: NCEP.

Southern stations

The simulations of the mean wind speed show continuous improvements for Juelich at 50 m with increasing resolution for both land use data sets. At 100 m the simulation skill partly decreases (Figure 3.1). This is also seen for Karlsruhe at both heights. This is quite similar to the results for the wind speed PDF, where the HI Score is consistently increasing for Karlsruhe and only partly decreasing for Juelich (Figure 3.7 a). The variability increases remarkably from 50 to 20 km

(Figure 3.8). Also higher Chi^2 scores are detected for both stations and heights for the 20 km resolution. That means, a decrease in the simulation skill of less frequent wind speed classes can be found for both stations. This is mostly followed by a higher simulation skill due to an increased resolution of 10 km. The Chi^2 score is, however, only in one case smaller for the 10 km resolution than for the 50 km resolution. In comparison to the effects on the northern stations, the effect on the southern stations is much stronger with a maximum effect of 2.152 (USGS) and 0.311 (CORINE) (Figure 3.7 b).

In contrary, increasing the resolution to 1 km leads to highest simulation skills for the mean wind speed and wind speed PDF for both stations: with a resisting overestimation in Juelich of more than 0.5 m/s (Figure 3.1) and an overlapping PDF area of 93 and 93.2 % (In comparison: 80.7 - 85.5 % for the low resolutions with CORINE). In Karlsruhe a deviation of only 0.13 m/s and an overlapping area of 92.1 and 94.9 % are found (In comparison: 80.6 - 90.2 % for the low resolutions with CORINE) (Figure 3.7, Figure 3.8 and Table 3.1). Also the overestimation in the wind speed variability is significantly reduced for both stations.

Increasing the resolution has a positive effect on the mean wind direction distribution at Karlsruhe (Figure 3.10). The channelisation of the wind due to the Upper Rhine valley is much more distinctive for the higher resolutions. While the 20 km resolution already gives a good representation of the prevailing SWW and SSW wind directions, the best approximation of the wind direction distribution is obtained with a 1 km resolution.

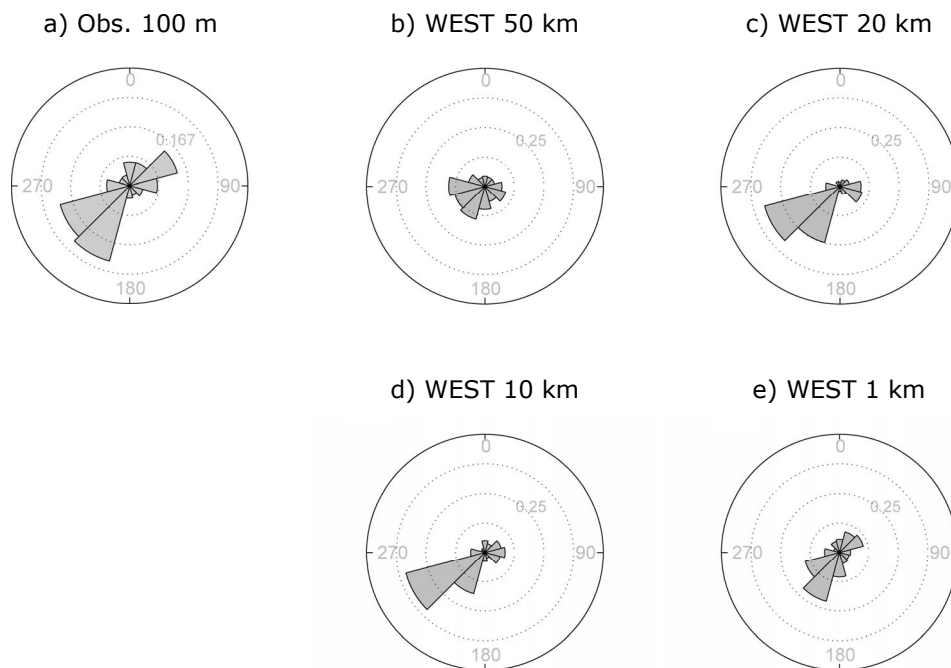


Figure 3.10: a) Observed and b) simulated WEST wind direction distributions at Karlsruhe (2001 - 2005) with a spatial resolution of 50, c) of 20, d) of 10 and e) of 1 km. Land use: CORINE, forcing: NCEP.

Summary

An increase of the resolution of WEST from 50 to 20 and 10 km does not necessarily improve the simulation of the mean wind speed profile. It only provides improvements in 10 of 20 cases for both roughness fields. Thus, a general added value is not detected. After replacing the roughness fields, the increasing spatial resolution improves the simulated wind profile in more cases (12 of 20 (CORINE) vs. 8 of 20 (USGS)). The magnitude of the effects of increasing the resolution from 50 to 20 to 10 km is, however, small. The differences in the wind speed profiles obtained with the new land use data are below 0.15 m/s for the increase to 20 km and below 0.26 m/s for the increase from 20 to 10 km. Comparing the differences between the 50 km and the 10 km simulation, a maximal difference of 0.24 m/s can be detected. With the old land use database the differences in the resulting wind profiles are comparably larger, for Juelich almost reaching 1 m/s.

Increasing the spatial resolution to 1 km leads to a reasonable agreement between modelled and measured wind profiles for four of the stations. The systematic overestimation of the wind profile for Juelich could be reduced but still remains. Although a higher roughness over the forests is used (Figure 3.6), it does not seem strong enough for this station. One possible explanation for the overestimation is that the trees act like a displaced surface. Establishing a displacement height (Stull 1988) would be a possible solution but is not realizable due to the low height of the first model level.

Comparing these observations for the wind profiles to the results for the wind speed distribution gives similar results. Increasing the resolution from 50 to 20 and from 20 to 10 km improves the wind speed distribution simulations in only 21 of 40 (52.5 %) cases for the Chi^2 score and in 17 of 40 (42.5 %) cases for the HI score. Split into an increasing resolution from 50 to 20 and an increasing from 20 to 10 km, it provides improvements in only 6 of 20 or 15 of 20 cases in the Chi^2 score and in 8 of 20 and in 9 of 20 cases in the HI score.

Increasing resolutions from 10 to 1 km produces clear and large improvements in the wind speed distributions for the southern stations. This is additionally indicated by improved wind speed variabilities for these stations. For the other stations both skill scores are not consistently smaller for the 1 km resolution vs. the best simulation of the low resolutions (50, 20 and 10 km). For these stations no consistent positive effect can be related to increasing the resolution to 1 km

As seen for the mean wind profiles, good simulations of the wind speed distributions for the northern stations can be reached with the low resolution simulations. The increased resolution does not necessarily result in smaller scores and therewith in more realistic simulations. Additionally, the deviations between observed and simulated wind speed distributions for these stations are small compared to the deviations for the forest stations especially with the low

resolutions. Only the very high resolution of 1 km can provide a reasonable approximation of the wind speed distributions over complex land structures.

A similar effect can be detected for the simulation of wind direction distributions. The low resolution simulations of WEST provide a reasonable simulation of the wind direction distribution over even and flat areas by reflecting the main wind directions and only slightly underestimating the frequency of easterly winds. Increasing the resolution to 20 and 10 km has only a small effect on the wind direction distributions. Effects of more complex structures (here shown for the channelisation effect of the Upper Rhine valley on the measurement tower in Karlsruhe) are not detected by the low resolution simulations of 50 km of WEST. But an increase of the spatial resolution continuously improves the simulation of this effect. So the high resolution simulation yields a reasonable performance of the mean wind direction distribution for this station.

3.2.4 Influence of the external forcing

The model performance strongly depends on the reliability of the driving fields in reproducing the true large scale conditions. This holds for both downscaling approaches. Due to differences in their assimilation scheme and assimilated data, regional differences between global reanalysis data sets occur (Reichler and Kim 2008).

The sensitivity of the Canadian model WEST to changes in forcing data is investigated by replacing the classification of wind speed data from NCEP-NCAR Reanalysis with a classification of the Japanese Reanalysis data set JRA (Japanese 25-year Reanalysis Project JRA-25, (Onogi et al. 2007)). Within the classification a new climate table is generated. The climate table represents the geostrophic wind speeds at one grid point close to the grid center. The 50 km simulation with the CCLM-SNN50 roughness field is repeated with the new climate table based on JRA.

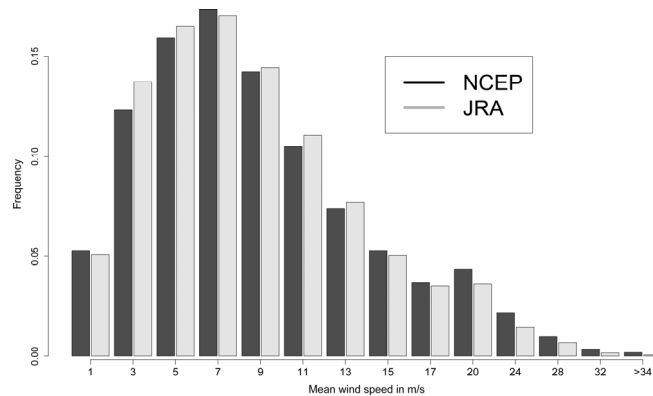


Figure 3.11: Occurrence frequency of the surface geostrophic wind speed classes in the climate tables of the forcing data sets NCEP/NCAR Reanalysis (left) and JRA Reanalysis (right).

Differences in the climate table from both forcing data sets are small (Figure 3.11 and Figure 3.12). Apparently, the frequency of high wind speed classes is higher in NCEP than in JRA at this grid point. The mean surface geostrophic wind speed is larger for NCEP. The mean wind direction distributions of both climate tables show prevailing winds from the south to west (180° - 270°) sectors. The frequency of easterly winds is slightly higher in the JRA classification table than in the NCEP classification table. This is also the case for the northerly winds. In compensation, the frequency of southerly and south westerly winds is slightly higher in the NCEP classification table.

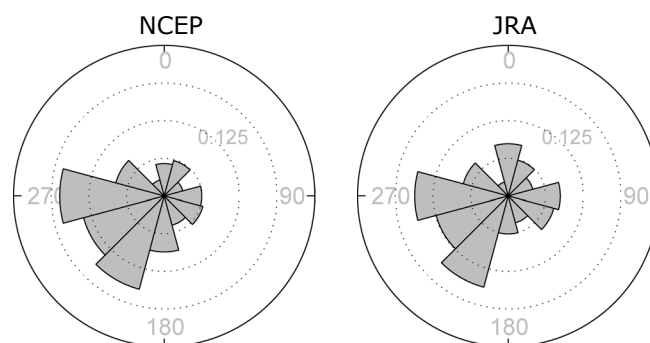


Figure 3.12: Occurrence frequency of the surface geostrophic wind direction classes in the climate tables of the forcing data sets NCEP/NCAR Reanalysis (left) and JRA Reanalysis (right).

The smaller mean wind speed of the JRA climate table conforms to the behavior of the simulated wind profiles (Figure 3.1). The model simulates a smaller wind speed when forced by JRA than for the NCEP forcing.

Northern stations

The JRA forcing reduces the mean wind speeds in a range of 0.2 – 0.39 m/s for the northern stations and therewith reduces the overestimation in Hamburg (at both heights) and at Lindenberg (at 100 m). Existing underestimations of mean winds speeds, as in Cabauw or Lindenberg at 50 m, are intensified (Figure 3.1). Also the value of the Chi^2 score increases for the latter cases (Figure 3.2 b). The differences in the overlapping areas of the wind speed PDFs are in a range of -3.2 to +3 % with positive effects only for Hamburg (Figure 3.2 a and Table 3.1). The general shape of the wind direction distributions remains unchanged. Only the frequency of easterly winds is better represented by the JRA forcing.

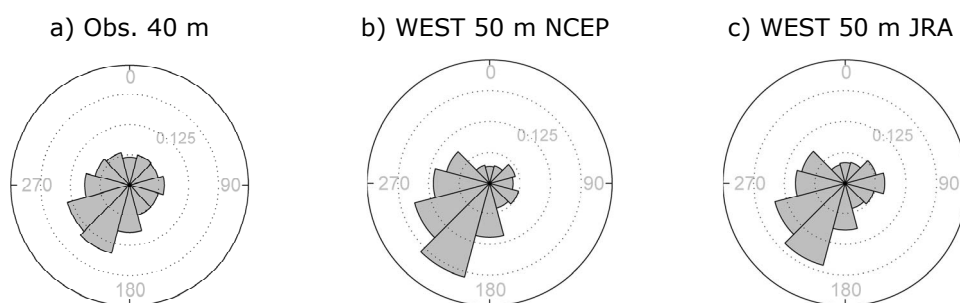


Figure 3.13: a) Observed and b) simulated wind direction distribution at Cabauw (2001 - 2005) by WEST with NCEP forcing and c) with JRA forcing. Both: CCLM-SNN50 roughness fields and 50 km resolution.

Southern stations

The effect on the mean wind speeds is comparatively smaller for the forest stations with a reduction of the overestimation at Juelich of 0.2 m/s and 0.0 m/s (100 m) and 0.07 m/s (50 m) for Karlsruhe (Figure 3.1). While the values of the Chi^2 score decrease for both, the values of the HI score increase for Karlsruhe (Figure 3.2). The differences in the overlapping areas of the wind speed PDFs are

in a range of -1.5 to +3.1 % with positive effects only for Juelich (Table 3.1). The effect on the wind direction distribution at Karlsruhe is, again, very small with a small decrease in the frequency of westerly winds and a small increase in ESE winds.

Summary

Summarizing the results for all stations, the JRA forcing improves the simulation of the mean wind speed due to a reduction of the wind speed in six of ten cases. For the wind speed distributions the new climatological forcing improved the simulation, represented by a decrease in both scores, in only four of ten cases. The effect on the wind direction distributions is mostly positive but small. The shapes of the wind roses are similar. Only very small differences occur between the frequencies, especially in the easterly winds. These are more frequent after the replacement conforming to the direction distribution of the climate table.

In comparison to the effects of changing the roughness lengths (maximal difference 0.9 m/s) the effect of the differences in the climate table on the mean wind profile is small. The magnitude of the deviations between the simulated profiles varies between a maximum difference of 0.39 m/s for the 100 m height in Hamburg and no difference at 100 m height for Karlsruhe. The effects are more distinctive for the northern stations over more homogeneous terrain. The effects on the simulation of the wind speed distributions are in a range of 0.6 to maximal 3.2 % in the overlapping area of the PDFs.

3.3 Conclusions

A sensitivity analysis is conducted focusing on the influence of model roughness, grid resolution, and forcing data on simulated wind statistics in the atmospheric boundary layer. Two models with different downscaling procedures are compared and the simulated wind statistics are verified by means of five year observation data from five meteorological masts using the measured wind speed and wind

directions at 50 and 100 m height. One simulation is generated by the regional climate model CCLM-SNN50 with a spatial resolution of ~50 km. The Wind Energy Simulation Toolkit WEST is used for simulating mean wind fields over the same period starting with the spatial resolution of the RCM and increasing the resolution to 20, 10 and finally 1 km. To evaluate the influence of the model roughness field, the roughness lengths of these WEST simulations are generated by means of two different land use data sets (with different spatial resolution) and the roughness field of the CCLM-SNN50 simulation additionally. Replacing the forcing NCEP data by the Japanese Reanalysis JRA shows only small changes.

The low resolution simulations (~50 km) of both models show a similar behavior after assimilating the CCLM-SNN50 roughness length to WEST. The mean vertical wind speed profiles and the frequency of median wind speed classes in the wind speed distributions differ only slightly. The stations in flat terrain and relatively simple land cover are better simulated than the results for the stations over more complex terrain, where the mean wind speeds are systematically overestimated by both models. The frequency of less frequent wind speed classes is better simulated by CCLM-SNN50 for four of the stations.

The most important findings of the sensitivity analysis are listed briefly below:

Land use:

The improvement in the wind speed simulation obtained due to the replacement of the roughness lengths shows the strong influence of the roughness field on the simulation of the mean wind speed profile and the wind speed distribution independently from the resolution. Using the highly resolved (100 m) land use database CORINE provides an improvement versus the land use database USGS with a resolution of 1 km in 25 of 30 cases (for five towers, two heights and three resolutions) for the mean wind profile and for the wind speed distribution. At one station over homogeneous terrain the higher roughness based on CORINE partly decreases the simulation skill. It is shown that a correct land cover data set is very

important for modeling of near surface wind fields. In this study not only the higher resolution of the CORINE (Corine Land Cover 2000) database should guarantee a higher accuracy than fields from the lower resolved data USGS. But also the suitability for the simulation area is a decisive factor. Therefore, not only the suitability of the land use data itself but also the assignment to the model land use classes and their roughness definition should be verified. Due to differences between international land cover definitions a correct assignment of land use classes is necessary and a verification of the suitability of the roughness data is strongly recommended.

Forcing data:

Restricted to this case and the grid point chosen in this study, the differences between the two Reanalysis databases NCEP and JRA are small and have therefore only small effects on the simulated wind statistics. The simulation skill undoubtedly depends on the validity and representativity of the forcing data. Small uncertainties in the climate table have a comparably low effect on the simulated wind speeds and wind directions.

Resolution:

Wind fields over flat terrain and rather uniform land cover can reasonably be simulated with a low resolution. The wind fields over complex terrain show strong deviations for all “low”⁴ grid resolutions. In 50 % of all investigated cases, increasing the resolution from 50 km to 20 km and 10 km does not lead to an added value in the simulation of the mean wind speed profile.

Additionally, the increased resolution did not improve the simulation of the wind speed distribution in 47.5 % or 57.5 % of the cases for the simulation of the wind speed distribution, according to two skill scores. Furthermore, the changes are

⁴ 50, 20 and 10 km

comparably small with a maximum of 0.26 m/s in the mean wind speeds with the CORINE land use data base.

A simulation with a 1 km resolution provides large improvements for the mean wind profiles especially over complex terrain. The high spatial resolution leads to a reasonable agreement of modelled and measured wind profiles for four of the stations. For one forest station the overestimation of the mean wind speeds can be reduced with the high resolution but still remains. Similar arguments hold for the wind speed PDF. A high resolution clearly improves the simulated wind speed distribution over complex land cover and complex terrain structure. For the stations over rather uniform terrain no added value for the simulation of the wind speed PDF with the high resolution is detected.

Effects of complex orographic structures like the channelisation in the Upper Rhine Valley are not detected in the 50 km simulation. The higher the resolution the stronger the effect of the channelisation is reflected in the simulated wind direction distribution. Over even and flat areas the low resolution simulations of both models suffice for a reasonable simulation of the mean wind direction distribution.

For very complex land cover structures like suburbs, forests or densely populated areas or complex orographic structures an appropriate high resolution is necessary. The resolution should be aligned to the complexity of the environment otherwise an added value is not assured for additional computational effort.

4 Verification of simulated wind time series

The sensitivity analysis in Chapter 3 shows that an adequate representation of surface terrain and land cover is crucial for a reasonable simulation of mean wind statistics. In addition to reasonably simulated mean wind conditions a realistic simulation of temporal wind variability is required e.g. for wind energy purposes. Time series of wind speed are used in several areas: Not only in the wind energy industry but also as input forcing for the simulation of other atmospheric or ecologic processes (e.g. for storm surge models (e.g. Grossmann et al. 2007) or for marine pollution models (e.g. Chrastansky et al. 2008)). Thus, a more detailed investigation of the wind speed distribution and its mean temporal variation is conducted and the skill of simulating extreme events is analyzed.

Because of its dynamic-statistical downscaling approach, WEST is not suitable for the simulation of time series. Here, two COSMO-CLM simulations are compared to the met mast's wind measurements: the CCLM-SNN50 simulation has a spatial resolution of 50 km, the CCLM-LC20 simulation of 20 km. Both simulations use different nudging schemes and provide different simulation periods (see Section 2.2.2).

4.1 General time series analysis

4.1.1 Methods

The approach for comparing wind fields of both COSMO-CLM simulations with met mast data is mostly similar to that described in Chapter 3.1. Again, wind speed and wind direction time series are extracted from the tower data and from the simulations using the output time step from both COSMO-CLM simulations (3 h).

Two alterations to the former approach are made:

1. In order to eliminate uncertainties due to model interpolation routines, the data are now taken directly at the model level heights at ca. 34 m, ca. 110 m and ca. 203 m. The observational data are partly logarithmically interpolated between the two neighbouring heights. The uncertainty induced by a simple logarithmic interpolation is assumed very small because of the small vertical distance between the measuring heights. In cases where the highest met masts measurement is at 200 m, the wind speed is extrapolated to ca. 203 m using measurements from the to highest observation levels.
2. Due to some large gaps in the observations before 2000 and due to different starting times (Table 4.1), gaps in measurements and simulations were adjusted. Hence, resulting wind statistics are not representative over the whole reference period.

The wind fields of the COSMO-CLM simulations are to be considered as values at a model grid box averaged over the model time step of a few minutes. Observational data are twenty, ten or five minute averages at one specific point. In order to investigate the influence of different averaging periods, observations at Lindenberg with different averaging times (of ten minutes, of one hour, of three hours) at the output time of the model (every three hours) are compared to the simulated values of CCLM-SNN50. The difference between the three

observational time series is much smaller than their deviation to the simulation. This is supported by only small differences in the statistical scores between observations and simulation: The correlation coefficient between observation and simulation does not change for different averaging times. Differences of 0.01 m/s are found between the Bias and RMSE of the ten minute and hourly means. In the case of three-hourly means the RMSE between observation and simulation is reduced (by 0.1 m/s) due to the smoothing, but significant deviations in the Bias are not detected. So a major influence of the averaging time can be neglected. Since one scope of this study is the investigation of extreme events, the original observational averaging time is used.

Table 4.1: Availability of the observational data over the reference periods

	Observational data availability	
	CCLM-SNN50	CCLM-LC20
	2001 - 2005	1991 - 2000
Cabauw	2001 - 2005	05/2000 - 12/2000
Hamburg	2001 - 2005	-
Lindenberg	2001 - 2005	06/1998 - 2000
Juelich	2001 - 2005	1995 - 2000
Karlsruhe	2001 - 2005	1991 - 2000

After the data preparation the model performance is illustrated by scatter plots and investigated by means of common statistical scores: The Bias, the difference between observation and model mean and the Root Mean Square Error (RMSE) are measures for the deviations between the time series.

The RMSE is given by

$$RMSE = \sqrt{\frac{1}{n} \sum_{i=1}^n (x_i - y_i)^2} \quad (4.1)$$

with x and y as observed and simulated wind speed and n as sample size.

The Pearson correlation coefficient

$$\text{Corr}_p(x, y) = \frac{\frac{1}{n-1} \sum_{i=1}^n (x_i - \bar{x})(y_i - \bar{y})}{s_x s_y} \quad (4.2)$$

reflects the degree of the linear relationship between two normal distributed data sets. It is defined in a range of -1 to +1. The normal distribution assumption does not necessarily hold for the investigated time series. Wind speeds are generally assumed to be Weibull or Gamma distributed (Kiss and Jánosi 2008). But to allow a comparison with results of other studies, the Pearson correlation coefficient is calculated. The Spearman rang correlation coefficient, which is independent from the data distributions, is also determined for a more statistically profound analysis. Therefore, the measurements are replaced by their ranks. In contrary to the Pearson correlation the relationship between the time series is not necessarily linear but monotone.

4.1.2 Results and Discussion

CCLM-SNN50

The direct comparison with observations by means of scatter plots of the time series from the CCLM-SNN50 simulation at model level height (here at ca. 110 m) shows similar results for the five stations as for the verification of the wind statistics basing on interpolated values between two model level heights in Chapter 3. The distribution of wind speed is comparably well simulated for Cabauw and Lindenberg. For both forest stations and the urban station Hamburg it is shifted to higher wind speeds (Figure 4.1). This is mostly visible for the predominant median wind speeds in red. Similar characteristics can be found for the 34 m and 204 m data (not shown). Due to the higher influences of the forest on the measurements at the lowest level, the largest deviations between the distributions for the *Southern stations* are found at 34 m.

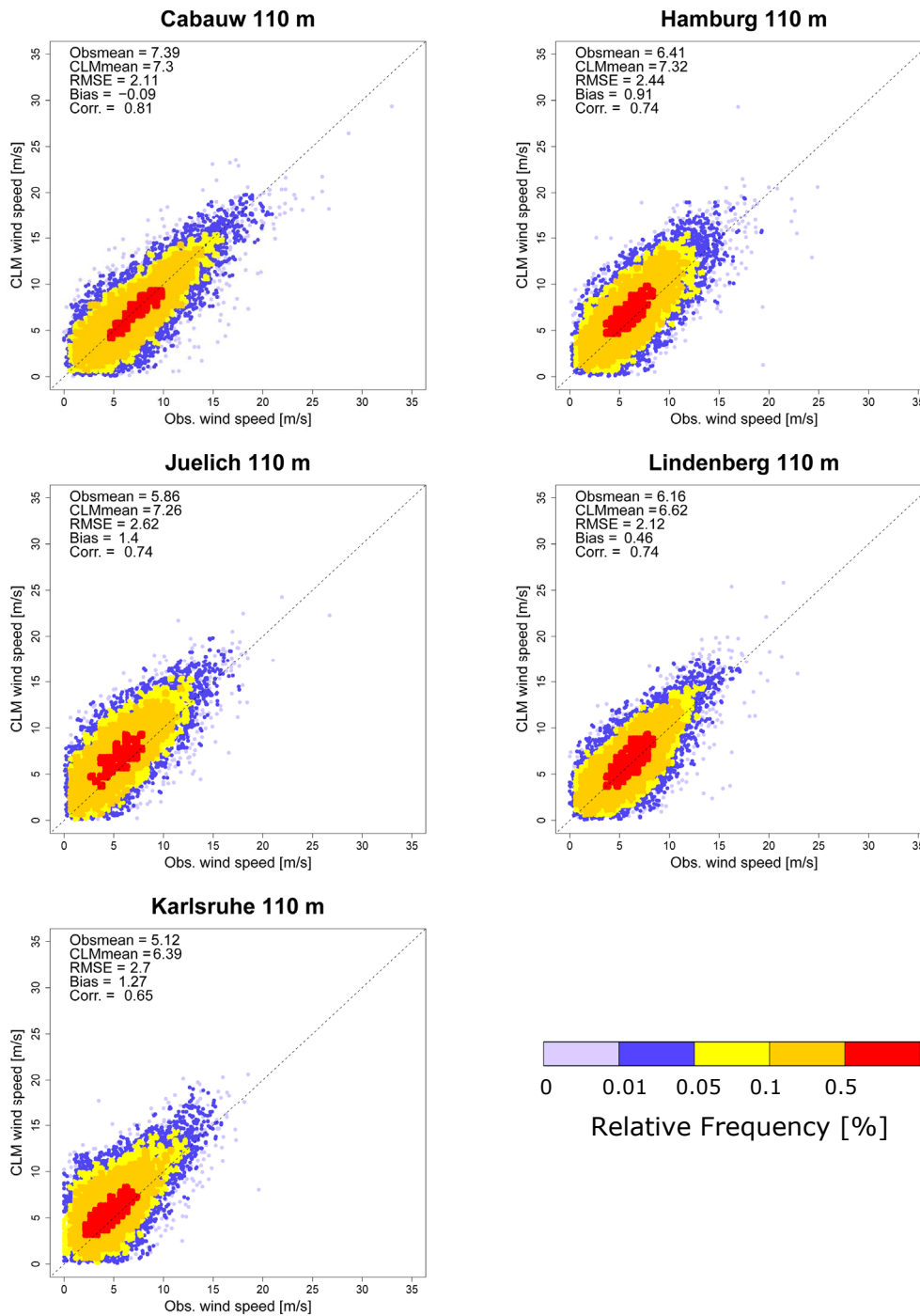


Figure 4.1: Scatterplots of observed and simulated wind speed time series of CCLM-SNN50 at ca. 110 m over the reference period 2001 - 2005. The Mean of observations (Obsmean) and simulation (CLMmean). The Root Mean Square Error (RMSE), the Bias and the Pearson Correlation coefficient.

This is confirmed by higher values of the Root Mean Square Error (RMSE) as well as of the Bias between the wind speed time series. The smallest values are found for Cabauw and Lindenberg for all heights (Table 4.2). The high wind speed variability at Cabauw is simulated by the model. The lower variability for the other stations is slightly overestimated.

The highest Spearman correlation coefficients can be found for Cabauw with values of 0.78 and 0.80. The correlation coefficients are in a similar range of 0.69 to 0.76 for Hamburg, Lindenberg and Juelich. The station Karlsruhe, in the most complex terrain, shows the lowest correlations around 0.60. The values of the Pearson correlations (0.64 - 0.82) are comparable to results in the literature for offshore stations. Winterfeldt and Weisse (2009) found correlations in a range of 0.7 - 0.81, Weisse and Guenther (2007) in a range of 0.66 - 0.82 both for coastal or offshore stations and spectrally nudged simulations.

The RMSE and the standard deviation increase consistently with the height of the model level in most of the cases. The correlation coefficients show, except at the forest stations, only slight modifications with increasing model level heights.

CCLM-LC20

Unfortunately, the Hindcast Period of the CCLM-LC20 simulation ends in the year 2000. Therefore, no direct comparison with CCLM-SNN50 is possible. Also almost all observation periods do not cover the whole simulation period (Table 4.1). In comparison to CCLM-SNN50, observed and simulated wind speeds by CCLM-LC20 over the available data periods show quite opposite results. The differences between observed and simulated wind speed distributions are now smaller for the forest stations (Figure 4.2). The Bias for the *Forest stations* is comparably small with differences in the means of less than 0.3 m/s at 110 m. For the *Northern stations*, over rather uniform terrain, the Bias shows an underestimation of the wind speeds of ca. 0.7 m/s.

Table 4.2: RMSE (in m/s), Bias (in m/s) and Correlation Coefficients (Spearman and Pearson) between observed and simulated (CCLM-SNN50) time series and their standard deviations (in m/s) over the reference period 2001 - 2005

CCLM-SNN50															
	Cabauw			Hamburg			Lindenberg			Juelich			Karlsruhe		
	34	110	204	34	110	204	34	110	204	34	110	204	34	110	204
RMSE	1.67	2.11	2.58	1.95	2.44	3.00	1.70	2.12	-	2.60	2.62	-	2.69	2.7	3.36
Bias	-0.11	-0.09	0.35	0.79	0.91	1.10	0.70	0.46	-	1.91	1.40	-	2.02	1.27	1.25
S_{obs}	2.74	3.45	4.20	2.25	2.92	3.61	2.12	2.70	-	1.79	2.91	-	1.45	2.61	3.64
S_{clim}	2.71	3.40	4.28	2.60	3.25	4.19	2.31	2.98	-	2.52	3.22	-	2.32	3.01	3.89
Corrs	0.78	0.80	0.80	0.72	0.72	0.76	0.71	0.71	-	0.69	0.72	-	0.55	0.59	0.62
CorrP	0.81	0.81	0.82	0.74	0.74	0.75	0.76	0.74	-	0.72	0.74	-	0.64	0.65	0.66

Table 4.3: RMSE (in m/s), Bias (in m/s) and Correlation Coefficient (Spearman and Pearson) between observed and simulated (CCLM-LC20) time series and their standard deviations (in m/s) over the available periods to 2000

CCLM-LC20												
	Cabauw			Lindenberg			Juelich			Karlsruhe		
	34	110	204	34	110	204	34	110	204	34	110	204
RMSE	2.63	3.34	3.93	2.27	2.65	-	2.06	2.73	-	1.72	2.44	3.20
Bias	-0.70	-0.77	-0.33	-1.10	-0.79	-	0.95	0.17	-	0.68	-0.28	-0.27
S_{obs}	2.75	3.52	4.37	2.29	2.77	-	1.87	3.11	-	1.58	2.80	3.67
S_{clim}	2.29	2.88	3.60	1.58	2.27	-	2.03	2.73	-	1.73	2.46	3.27
Corrs	0.50	0.50	0.53	0.47	0.49	-	0.53	0.55	-	0.46	0.51	0.53
CorrP	0.51	0.50	0.53	0.52	0.51	-	0.57	0.57	-	0.55	0.58	0.58

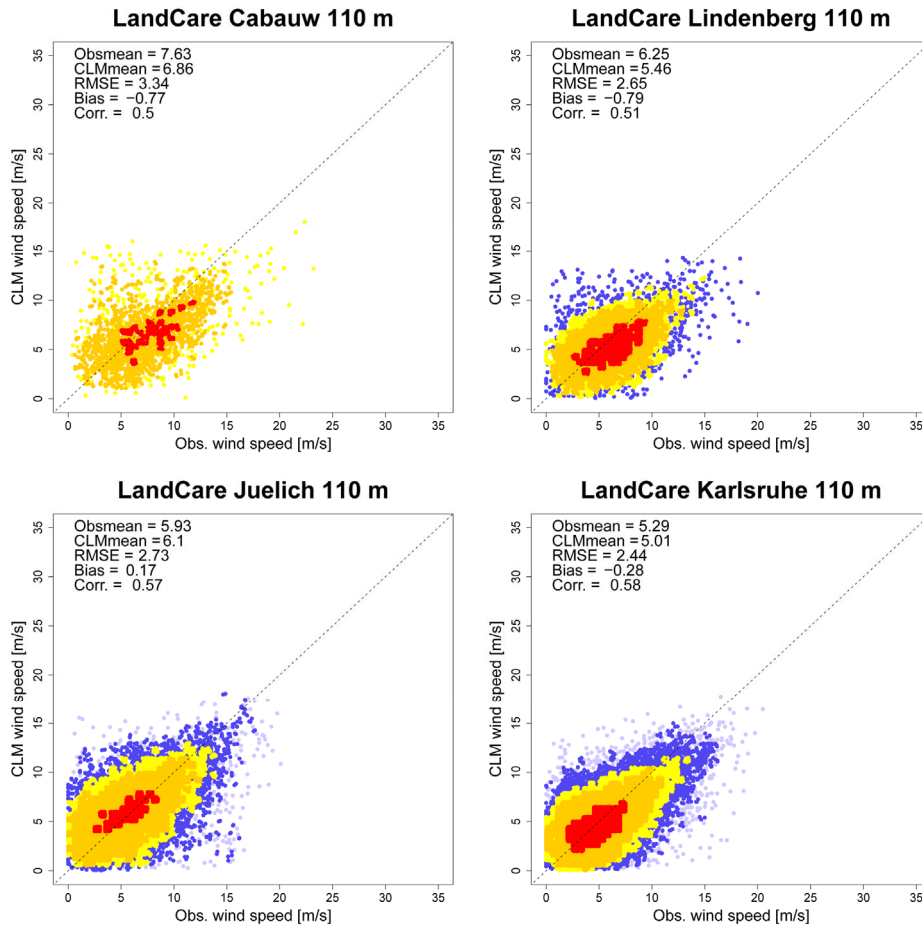


Figure 4.2: Scatterplots of observed and simulated wind speed time series of CCLM-LC20 at ca. 110 m over the accessible data periods. The Mean of observations (Obsmean) and simulation (CLMmean). The Root Mean Square Error (RMSE), the Bias and the Correlation coefficient.

The simulated wind speeds are generally too low for Cabauw and Lindenberg. The CCLM-LC20 simulation shows as well a strongly underestimated wind speed variability reflected by smaller standard deviations (Table 4.3). This holds for all stations but is most obvious for the *Northern stations*. This is contrary to the results found for CCLM-SNN50 with a reasonably simulated variability for Cabauw and only slight overestimations for the further stations. Regarding results from Chapter 3 an increase of the wind speed variability due to the higher resolution was expected. The Spearman correlation coefficients are in comparison to CCLM-SNN50 small between 0.46 and 0.55 for all stations. This indicates in addition a lower simulation skill of CCLM-LC20 for the simulation of the temporal variability. In order to investigate if the low wind speeds at the *Northern*

stations are an artefact of the reduced observation period (Table 4.1), mean and maximal wind speeds over the period 1991 - 1995 are calculated from the model output. These are compared to CCLM-SNN50 wind speeds over 2001 - 2005: While mean wind speeds are in a range of 0.8 to 1.4 m/s lower, maximum wind speeds are up to 10 m/s lower in CCLM-LC20. Available observations as well as the NCEP/NCAR Reanalysis do not show such a significant deviation between the wind speeds of both periods.

The observed wind directions show similar conditions as over the CCLM-SNN50 period 2001 - 2005. The simulation for the *Northern stations* shows no added value versus the CCLM-SNN50 wind directions due to higher spatial resolution, as it was already seen for WEST. The higher resolved orography field, however, improves the simulation of the complex terrain at Karlsruhe, as seen in Chapter 3. The channelisation of the Upper Rhine valley is already notable but not fully resolved (Figure 4.3).

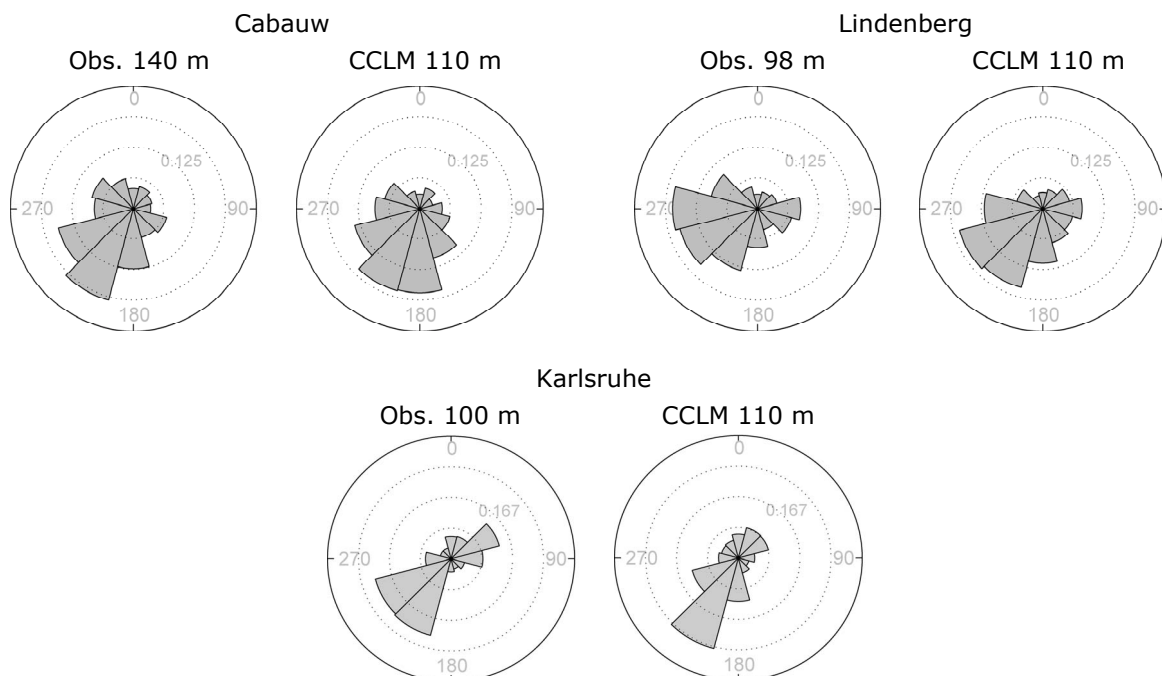


Figure 4.3: Observed and simulated (CCLM-LC20) wind direction distributions at Cabauw, Lindenberg and Karlsruhe as available from 1991 - 2000.

Overall, an added value due to the higher spatial resolution of the CCLM-LC20 simulation is only found for the wind direction distribution over complex terrain. The mean wind speed and its standard deviation is distinctively lower as of CCLM-SNN50 and thereby underestimated for the stations over relatively homogeneous terrain.

High values of Bias, HI-Score and RMSE can be directly connected to an inadequate representation of station roughness or orography, which influence the absolute wind speed. Low correlation coefficients, however, indicate a discrepancy between the temporal variability of model wind and observations. The temporal variation of wind speed in the lower atmosphere is dominated by a number of factors: seasonal variation of cyclonic and acyclonic conditions, diurnal variation due to heat transport processes, variability due to the large scale circulation and synoptic conditions, regional effects like land-sea interactions, and small scale turbulences. Spectral analysis by van der Hoven (1957) shows that the latter are found in the high frequency ranges with a peak at one minute. They are therefore neglected in the investigation of the averaged fields of the models and observations. In order to analyse the simulation skill for the remaining factors a detailed investigation is performed.

4.1.2.1 Annual cycle

The annual cycle of wind speed is strongly connected to the atmospheric state. In winter the European wind climate is dominated by passing cyclones, whereas more frequent anticyclonic conditions shape the wind climate of the summer months. This leads to high wind speeds from November to February due to increased storm intensity and reduced wind speeds from May to October (Christoffer and Ulbricht-Eissing 1989).

CCLM-SNN50

For all observations reduced wind speeds from May to September and higher wind speeds from October to March are evident in the period 2001 - 2005.

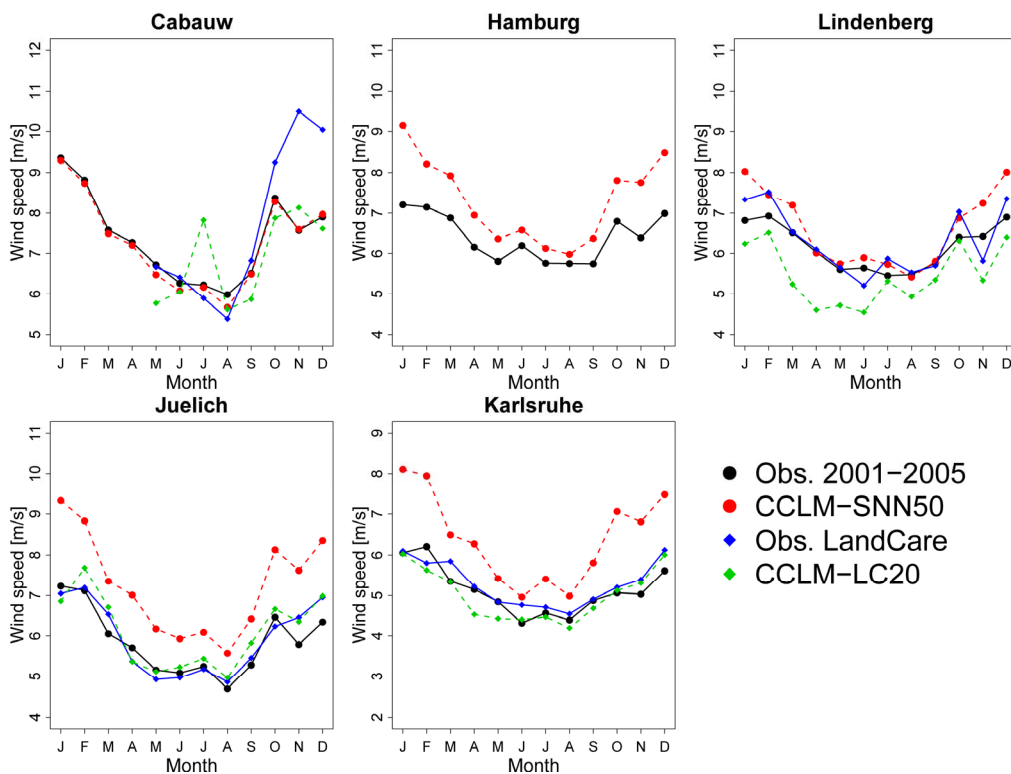


Figure 4.4: Averaged annual cycle of wind speed at ca. 110 m height. Black: Observations 2001 - 2005, Blue: Observations CCLM-LC20 periods, Red: CCLM-SNN50 and Green: CCLM-LC20.

While the behaviour is quite similar for all stations, the annual cycle is strongest for Cabauw and comparable flat for the other stations (Figure 4.4). The wind speeds of the CCLM-SNN50 simulation generally show a strong annual cycle – thus too strong for the latter cases. The overall correlation with the observations is good, mostly reasonably simulating monthly variations with only small deviations.

CCLM-LC20

For Cabauw observations for the CCLM-LC20 period were only available from May to December 2000 (Table 4.1). The observed wind speed in 2000 shows a pronounced annual cycle with a strong increase in October and a maximum wind speed in November (Figure 4.4). These stormy winter months are not simulated by the model. Instead, a very strong July with wind speeds as high as the simulated winter months can be found. This stormy July 2000 can also be found

in the grid boxes of the other stations. But due to the averaging over more than one year (Table 4.1) it is not so visible in the averaged annual cycle of the other stations (Figure 4.4). A similar pattern is not found in the observations. Thus, the strong wind speeds in July 2000 may be a product of an incorrect reproduction in the forcing reanalysis or in the RCM.

The mean annual cycle of wind speed from 1998 to 2000 in Lindenberg is quite similar to that over the period 2001 - 2005 with weaker winds in November. This is simulated by the model. In general, the observations and the CCLM-LC20 simulation show a high correlation with a consistent overestimation, which is in particular visible in spring. Compared to CCLM-SNN50 the annual cycle for the southern stations simulated by CCLM-LC20 is weaker and fits reasonably to the observations.

4.1.2.2 Diurnal Cycle

The diurnal cycle is strongest on clear summer days. Therefore, only averages over the summer months are shown in this section. Figure 4.5 shows a high similarity of the observed diurnal cycles over the summer months of both periods. The observations show a similar strong diurnal cycle with a daily maximum around noon or the afternoon followed by a decrease of the wind speed in the evening. This conforms to the thermal circulation with strong mixing of the near surface boundary layer during daytime and stable stratification at night. Regional patterns due to land sea breeze (e.g. at Cabauw) or mountain valley flow are not detectable.

The diurnal cycle of the CCLM-SNN50 simulation shows a good temporal agreement with the observations but with a smaller amplitude. The diurnal cycle of the CCLM-LC20 simulation is slightly too strong for Cabauw and too smooth for the other stations (Figure 4.6).

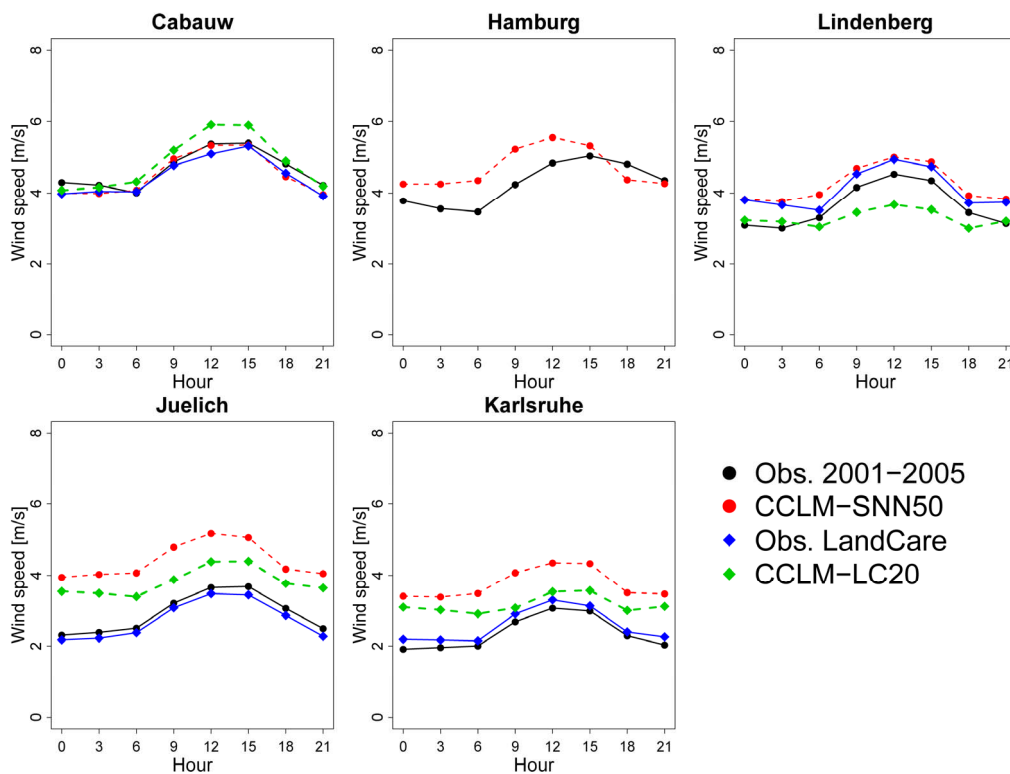


Figure 4.5: Average diurnal cycle in summer (JJA) at ca. 33 m height. Black: Observations 2001 - 2005, Blue: Observations CCLM-LC20 periods, Red: CCLM-SNN50 and Green: CCLM-LC20.

Above a specific height, the so called reversal height, the diurnal cycle changes phase, especially at clear days in summer. Above the stable layer at night the wind speed or flow increases due to a reduced downward transfer of momentum to lower layers (Wieringa 1989). The reversal height is typically found between 60 and 80 m AGL over land. High nocturnal wind speed and a morning minima can be found in the observations (Figure 4.6). Only at Juelich the nightly wind speeds are relatively weak in both periods probably due to the rougher surface. In general, the observed diurnal cycles over both time periods show again a high agreement for all stations. Both simulations generate a correct diurnal variation with strong wind speeds at night and a minimum in the morning, but weaker as observed. Brockhaus et al. (2008) found that COSMO-CLM simulates a too low temperature range in summer, resulting from an underestimation of incoming short wave radiation (Jaeger et al. 2008). Regarding the strong dependence of

wind speed on the thermal circulation and stratification, this gives a reasonable explanation for the underestimated diurnal wind speed cycle at both heights.

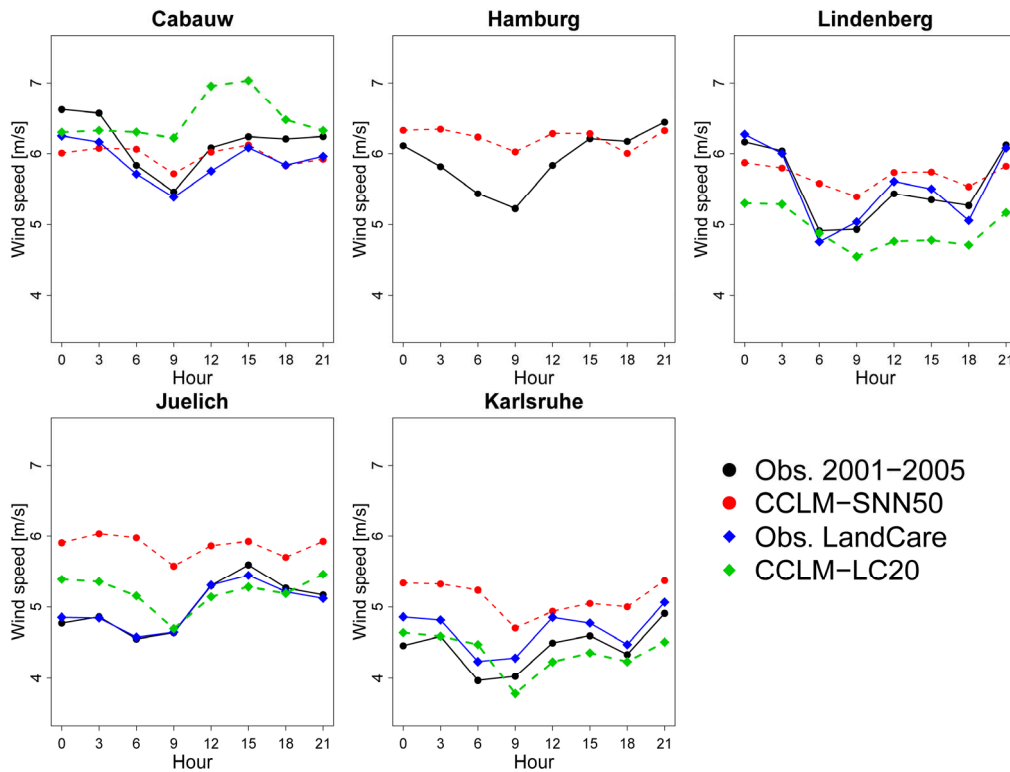


Figure 4.6: Average diurnal cycle in summer (JJA) at ca. 110 m height. Black: Observations 2001 - 2005, Blue: Observations CCLM-LC20 periods, Red: CCLM-SNN50 and Green: CCLM-LC20.

Only for the 110 m height at Cabauw the diurnal cycle is overestimated by CCLM-LC20 and does not show a phase reversal. This is probably due to extreme strong winds in July 2000 and is no indication of an inappropriate simulation of thermal processes.

4.1.2.3 Interannual variability

Both simulations show a reasonable agreement with the observed interannual variability of the annual means and 99th percentiles. This conforms to results found in the literature (e.g. Weisse et al. 2009) and is not explicitly shown here.

The natural variability due to large scale circulation patterns plays a major role in the temporal behaviour of wind speed. The European wind climate and its year to year variability is strongly dominated by large scale circulations. The dominant large scale pattern for the European winter season is the North Atlantic Oscillation (NAO). The NAO is defined as the variability of the pressure gradient between the Azores High and the Iceland Low. Thus, the NAO index (NAOI) is an indicator for the strength of westerly flow over the North Atlantic and Western Europe (Wanner et al. 2001). By means of the ERA40-Reanalysis Donat et al. 2009 found that most of the Central European storm days (ca. 80 %) occurred within positive NAO phases.

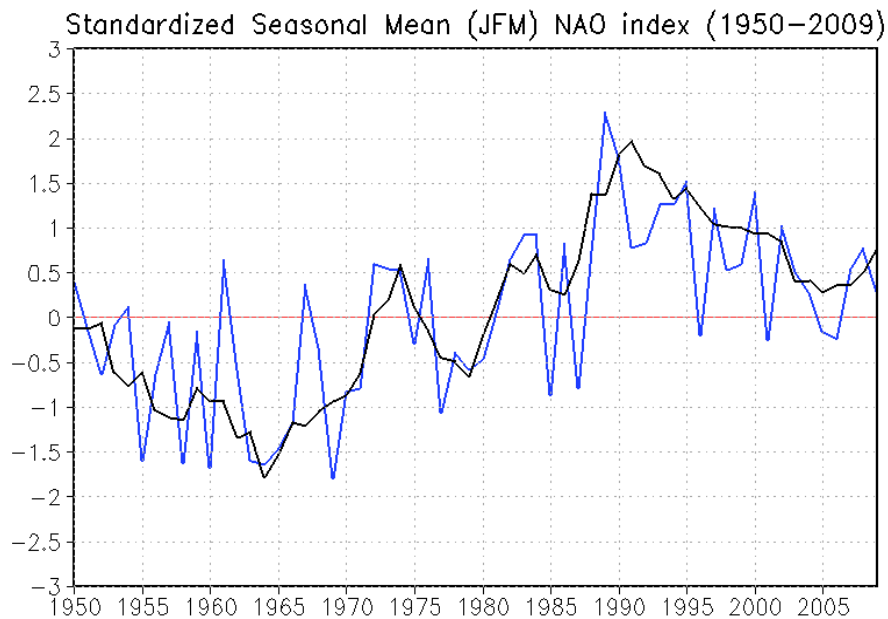


Figure 4.7: NAOI index 1950 - 2009. The standardized seasonal mean NAO index (blue) and the standardized five-year running mean of the index (black).⁵

Figure 4.7 shows the standardized NAOI, based on daily averages provided by the Climate Prediction Center of the US National Weather Service. Except for the years 1996, 2001 and 2005 the NAOI shows positive values over the investigated period. Strongly positive indices can be found for 1995, 1997, 2000 and 2002.

⁵ http://www.cpc.noaa.gov/products/precip/CWlink/pna/JFM_season_ao_index.shtml

In order to investigate if the NAO variability is found in the observations and simulated by the models, means and 99th percentiles of the same months are compared in Figure 4.8.

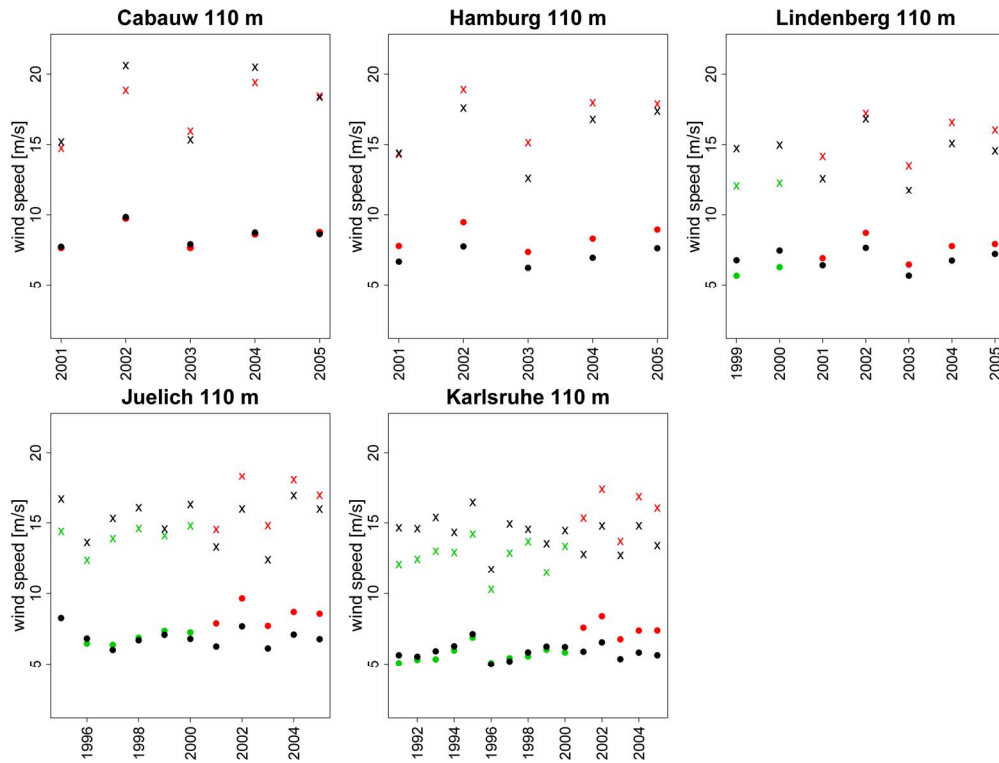


Figure 4.8: Mean wind speed (Dot) and 99th percentiles (x) of the NAO month (JFM); observations (black), CCLM-SNN50 (red) and CCLM-LC20 (green).

The (averaged) positive and negative NAO phases are reflected in the results of both, models and observations. E.g. the positive phase in 2002 results in a local peak for each station mean and 99th percentile, while the low winds in 1996 result in a minimum for Juelich and Karlsruhe. Overall a reasonable correlation between the simulated winter variability and differences in the NAO can be seen. This is indicative of a correct simulation of the variation in the North Atlantic storm track, strongly linked to the NAO. A more detailed investigation is conducted in Chapter 5.

4.2 Storm detection

In order to validate the model performance regarding the simulation of extreme events, storms statistics by means of the tower measurements and both simulations are calculated. The objective is to see if the RCM is able to simulate extreme high wind speeds leading to storm damage or storm surges. Previous studies report that RCMs tend to underestimate strong wind speeds. Räsänen et al. (2004) found maximum wind speeds too low over Europe using the regional model RCAO with highest wind speeds of 25 m/s over a 30 year period. In comparison with coastal and offshore stations Weisse et al. (2005) and Rockel and Woth (2007) detected an underestimation of storm events. These results were found for near-surface measurements and extrapolated model wind speeds down to 10 m heights. Such investigations shall now be repeated by means of the tower measurements and without vertical extrapolation of the model wind speeds. Due to the higher disturbances on the lower measurements and the reduced sample size above 200 m, the analysis is only conducted for results at ca. 110 m.

4.2.1 Methods

For the general data preparation see Chapter 4.1.1. A first investigation is conducted by means of QQ-Plots in Figure 4.9. The wind speed time series are separated into twelve wind direction sectors. Note that in contrary to the common practice, not only the ninety-nine values of the quantiles but the full distributions are plotted against each other. This cares for a better survey of the high wind speeds. The red lines represent the thresholds for eight and nine Beaufort. This differs from approaches of other studies, where the threshold for severe storms is set at ten Beaufort. However, due to the reduced wind speeds over land, compared in this study, a lower threshold is used. Values exceeding the red line indicate that either a measurement or a simulation (or both) exceeds the threshold. In case of a perfect simulation, the points would be on the dotted lines midway through the sectors. On the right hand side underestimated wind speeds are below these lines. This occurs vice versa on the left hand side. For a better understanding underestimated wind speeds are red coloured and an example is illustrated.

The number of storms is determined using the value over threshold technique. Following the approach of Weisse et al. (2005), two individual storm events must be separated by at least 24 h. The threshold for a storm event is 17.2 m/s (8 Beaufort). The individuality definition allows a time shift between simulated and observed events of seven time steps of 3 hours in both directions. The number of storms found in observations and model (YY), only in observations (YN) and only in model (NY) is calculated for each station. Using these numbers the probability of detection, also known as Hit Rate

$$POD = \frac{YY}{YY + YN} \quad (4.3)$$

and the False Alarm Ratio

$$FAR = \frac{NY}{NY + YY} \quad (4.4)$$

are determined. In other words, the POD explains how many observed events are correctly detected by the model. The FAR gives the ratio of simulated events, that are not observed. POD equals One and FAR equals Zero for a perfect simulation of the number of storm events (Nurmi 2003).

4.2.2 Results

QQ-Plots

CCLM-SNN50

The separation into wind direction classes allows an investigation for the overestimated wind speeds found for the forest stations and Hamburg in CCLM-SNN50. While the overestimation of wind speed can be seen for the forest stations in all sectors, the overestimation at Hamburg is mostly seen at southerly sectors and not, as expected, from the city direction NW (Figure 4.9).

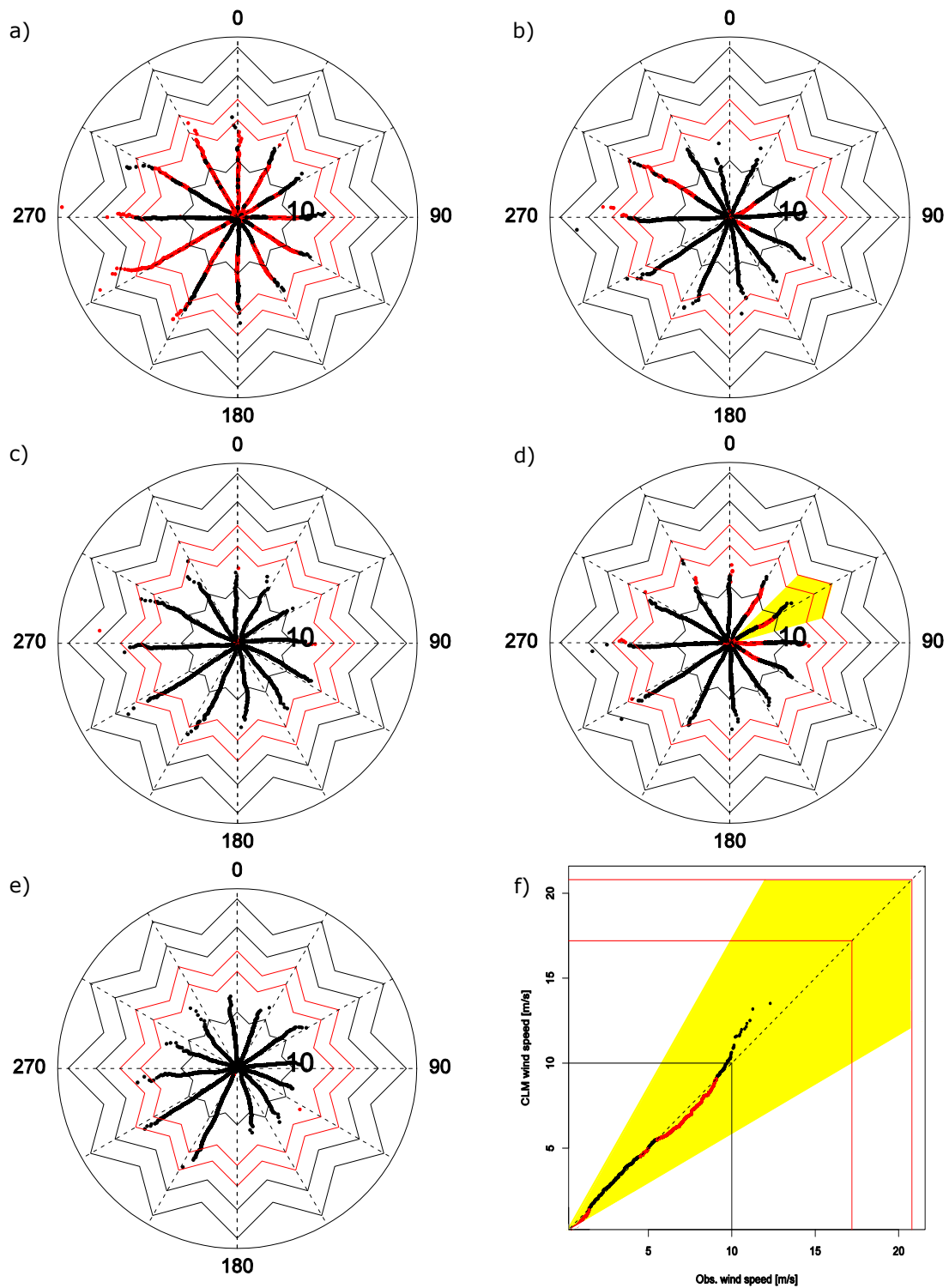


Figure 4.9: QQ-plots of measured and simulated (CCLM-SNN50) wind speed at ca. 110 m. separated into observed wind direction sectors. a) Cabauw b) Hamburg c) Juelich d) Lindenberg and e) Karlsruhe. Black points are overestimated, red points underestimated by the model. The red stars indicate the thresholds 17.2 or 20.8 m/s. For a perfect simulation the points would be on the dotted grey lines. f) Example for one wind direction sector from d).

The overestimation of northerly wind speeds may be an effect of the mast disturbances, which could not be fully removed. Also the wind speed at Lindenberg shows a small overestimation from southerly directions. Wind speeds above 17.2 m/s are only found from westerly directions. Strong wind speeds > 20.8 m/s are rare and single events. They are mostly from westerly and WSW direction. This is in agreement with literature (e.g. Donat et al. (2009) found that most of the storms, that affect central Europe, are westerly). The strong wind speeds are partly over- and partly underestimated. At the forest stations the overestimation decreases for higher wind speeds.

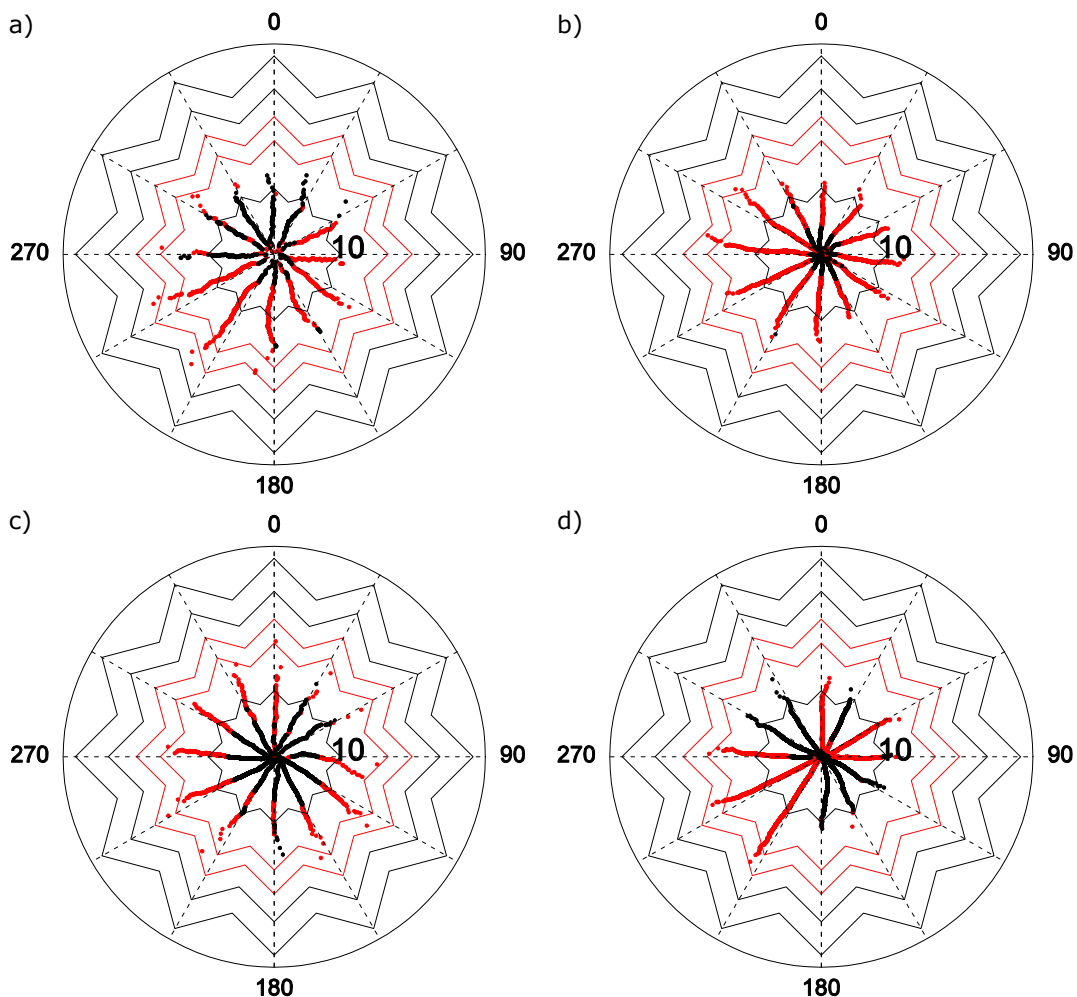


Figure 4.10: QQ-plots of measured and simulated (CCLM-LC20) wind speed at ca. 110 m. separated into observed wind direction sectors. a) Cabauw b) Lindenberg c) Juelich and d) Karlsruhe. Black points are overestimated, red points underestimated by the model. The red stars indicate the thresholds 17.2 or 20.8 m/s. For a perfect simulation the points would be on the dotted grey lines.

CCLM-LC20

For Cabauw the distribution simulated by CCLM-LC20 is divided into a strongly underestimated onshore wind flow and a slightly overestimated and less frequent offshore flow, resulting in an overall overestimation of the mean wind speed (Figure 4.10). The wind speeds at Lindenberg are generally underestimated. In Juelich the model overestimates the low wind speeds over the forest but shows underestimated high wind speeds from almost all directions. Due to the Upper Rhine Valley, which is not fully resolved, wind speeds from SE are overestimated at Karlsruhe, while the winds from South West to West are underestimated. Wind speeds higher 17.2 m/s are rare during the CCLM-LC20 periods and underestimated for all stations. Strong wind speeds > 20.8 m/s are therefore scarce, single events.

Whether the simulations correctly reproduce the temporal and spatial occurrence of the observed storm events is investigated by means of a Hit Rate/False Alarm ratio analysis (See Chapter 4.2.1 for method description).

Hit Rate /False Alarm ratio analysis*CCLM-SNN50*

Table 4.4 shows the results of the Hit Rate analysis of storms > 17.8 m/s for CCLM-SNN50. Due to its geographical position the station Cabauw is most frequently hit by a storm event. The frequency of storms during 2001 - 2005 decreases with increasing terrain complexity and land use, resulting in only five storm events at Karlsruhe over the five year period. Around two-thirds of the storm events measured at the northern stations are simulated by the model, as indicated by POD values above 0.67. At the southern stations the number of correctly simulated events is smaller with PODs of 0.5 and 0.6. This supports the hypothesis that strong wind speeds are underestimated by the model. The model also simulates storm events, which are not seen in the observations, so called False Alarms. This number increases with complexity of the terrain. Events between the 3 h model time step can be seen in the observations but obviously not

in the model. Therefore, these data are not considered in the analysis. But some of the False Alarm events are neither found in the observations at the model time step nor in between the model time steps.

Table 4.4: Number of observed and simulated (CCLM-SNN50) events > 17.2 m/s. YY: Observed and simulated; YN: Observed and not simulated NY: Not Observed but simulated; POD and False Alarm Ratio (FAR)

	Obs. – CCLM-SNN50 (2001 - 2005)				
	Cabauw	Hamburg	Lindenberg	Juelich	Karlsruhe
YY	29	15	6	6	3
YN	12	6	3	6	2
NY	9	10	10	14	11
POD	0.71	0.71	0.67	0.5	0.6
FAR	0.24	0.40	0.63	0.70	0.79

CCLM-LC20

Due to the partly shorter observation period, the northern stations show much less storm events during the CCLM-LC20 period (Table 4.5). Only one of the overall storm events of eleven is simulated by the model. At the southern stations more events are observed but the number of the correctly simulated events is clearly reduced (Juelich 33 % and Karlsruhe one of twenty). Due to the reduced variability and generally low simulated wind speed (Chapter 4.1.2), only two False Alarms are simulated.

Table 4.5: Number of observed and simulated (CCLM-LC20) events > 17.2 m/s. YY: Observed and simulated; YN: Observed and not simulated NY: Not Observed but simulated; POD and False Alarm Ratio (FAR)

	Obs. – CCLM-LC20 (until 2000)			
	Cabauw	Lindenberg	Juelich	Karlsruhe
YY	1	0	4	1
YN	4	6	17	19
NY	0	0	2	0
POD	0.20	0	0.19	0.05
FAR	0	0	0.33	0

For a more detailed investigation the observed and simulated wind speeds for more severe events > 20.8 m/s are directly compared. Observed and simulated wind speeds exceeding the threshold of 20.8 m/s are listed in Table 4.6 and Table 4.7. To allow for a time shift the maximum wind speed of the counterpart at the particular output time and seven time steps before and after the detected event is selected. If available, the name of the connected low pressure system is specified as provided in the storm documentation of the prospective year by the “Deutsche Rück” (Axer et al. 2005; Axer et al. 2006). The storm fronts at the northern stations are detected but mostly underestimated in their intensity by CCLM-SNN50. Some exceptions exist. For instance low pressure system Jeanett is underestimated at Cabauw and Juelich, while overestimated at Hamburg and Lindenberg. Some wind speeds at Juelich are overestimated during strong storm events probably because the roughness is not described appropriately. No event is found for Karlsruhe within both periods.

During the CCLM-LC20 periods strong wind events are infrequent, as already found within the Hit Rate analysis. So, only two events are detected at Cabauw with a highest measured wind speed of 23.2 m/s and a simulated one of 18 m/s.

Table 4.7: Maximum of observed and simulated wind speed during extreme storm events (> 20.8 m/s) in the CCLM-LC20 period - 2000.

		Cabauw	
		Obs.	CCLM
1993	09.12.	-	-
1995	23.01.	-	-
1996	29.08.	-	-
2000	30.10. Nicole	23.2	15.6
	13.12.	22.4	18.1

The most interesting cases are investigated by comparing the observed pressure fields with the pressure field of the forcing, the NCEP/NCAR Reanalysis 1.

In comparison to the documented position and intensity of the low pressure system Jeanett in the “Berliner Wetterkarte”⁶ of the 28th of October 2000, its track is found to be shifted more southerly in the reanalysis with a stronger as observed central pressure. This conforms to the higher simulated wind speeds found at Hamburg and Lindenberg. Also the observations between the model output interval of three hours are below the simulated high wind speed.

The lowest simulated wind speed during a storm event is found for Lindenberg during “Pia”. A comparison with the “Berliner Wetterkarte” shows that the position of the pressure system is correctly reproduced in the reanalysis, while its intensity is found even slightly higher than observed. The maximum wind speed of 22.9 m/s is measured at six am. Unfortunately, no pressure field from that time is available for comparison. Around that time step the simulated wind speeds are higher than the observations.

So the discrepancies between model and observation in both cases are probably induced by a flawed forcing pressure field.

The low pressure system “Nicole” is correctly reproduced by the reanalysis in both, position and intensity of the central pressure. So, the underestimated wind speed in the model is not a result of an incorrect forcing. Surveying the pressure field of the CCLM-LC20 simulation shows that the center of Nicole is clearly shifted to the North West, even though the forcing induces the correct pressure distribution. Similar cases, in which patterns in the RCM fields (without spectral nudging) occur dissimilar to the forcing data, were already reported by von Storch et al. (2000). In the reported cases simulations using spectral nudging improved the reproduction of the pressure pattern. The results of this study confirms that the spectral nudging approach, used in CCLM-SNN50 but not in CCLM-LC20, improves the simulation of storm tracks by forcing the pressure systems on their

⁶<http://wkserv.met.fu-berlin.de/>

tracks. However, due to the very limited sample size, the different model versions and observation periods, this should be investigated in more detail.

4.3 Summary and conclusions

In spite of deviant observation periods, conclusions about the simulation skill of CCLM-SNN50 and CCLM-LC20 regarding temporal scales can be drawn. The CCLM-SNN50 simulation shows a sufficient reproduction of the large scale circulations. The correlation coefficients are comparable to values based on coastal and offshore stations found in the literature. The interannual variability is reasonably simulated. While the amplitude of the annual cycle is overestimated for all stations except Cabauw, the diurnal cycle of wind speed especially in summer is underestimated. That can be attributed to an underestimated diurnal temperature range in summer reported by Brockhaus et al. (2008) due to an underestimation of the incoming short wave radiation in COSMO-CLM (Jaeger et al. 2008). Also the strength of the inversion at night is underestimated. Correlations of daily means, around 10 % higher as of 3 hourly values, indicate a deficit in the simulation of local fluctuations on smaller temporal scales (< 24 h). This is supported by results of a spectral analysis of the simulations from the RCM REMO, which showed a smoothed variation at smaller scales than half a day (Larsén et al. 2008).

This also holds for the CCLM-LC20 simulation, which generally simulates unrealistic lower wind speed with strongly underestimated variability. Hence, the lower simulation of the annual cycle agrees better with the observations, but cannot be assessed as added value due to the higher spatial resolution. Also the lower correlation coefficients show no improvement versus the CCLM-SNN50 simulation. An added value is only found for the wind direction distribution over complex terrain due to the higher resolved orography.

No definite explanation for the low simulation skill of the higher resolved CCLM-LC20 simulation for the wind speed simulation is found. The good simulation of the wind direction distribution by CCLM-LC20 indicates a reasonable representativity of the model orography. The differences in the roughness fields of both models are small. The interpolation of observations to model level height is identical for both models. Adjusting the gaps ensures a comparison of similar conditions. Remaining possible explanations for the discrepancies are the higher temporal discretisation of CCLM-LC20, the different model versions and the spectral nudging approach. An evaluation of the nudging approach by Weisse and Feser (2003) shows that spectral nudging indeed improves the simulation of near surface wind speeds. Von Storch et al. (2000) studied the reproduction of pressure fields in REMO with and without the spectral nudging approach. It was found that with the nudging approach the pressure distribution of the forcing was reasonably reproduced in the model. Without the spectral nudging significantly deviating patterns were generated. Such deviations between model and reanalysis pressure field are also found in this study for a severe storm event in the CCLM-LC20 simulation without spectral nudging. A shift in the storm track results in underestimated wind speeds. Results from investigations of severe events in the CCLM-SNN50 simulation suggest that the differences between model and observations rather result from an incorrect pressure reproduction in the driving field but not in the model. However, this is only investigated for a small number of cases and should be repeated by means of two simulations only differing in the use of a nudging approach.

A storm detection by means of measurements and model output confirms the previous assumptions that regional climate models underestimate the occurrence of strong wind speeds over land. Over homogenous terrain and with spectral nudging one third of the storm events larger than 17.2 m/s are not detected by the 50 km simulation. A direct comparison of wind speeds during severe storm events > 20.8 m/s confirms that the model tends to underestimate the measured wind speeds. However, despite the averaging over the grid box, the model is able to

simulate strong wind speeds (e.g. 29.4 m/s). In some cases high wind speeds are even overestimated. A Hit Rate-False Alarm analysis with wind events > 17.2 m/s reveals that the model simulates high wind speed events, which are not observed. Assuming a high reliability of the tower measurements, these false alarms must be produced by the model and/or the forcing. The existence of such false alarms implies a risk for the validation of the model only by the frequency of observed and simulated events per time range. Hence, a Hit Rate - False Alarm study, as presented in this study, should be preferred. With a higher temporal resolution, for instance hourly output, the number of False Alarms should be strongly reduced. False alarms, e.g. due to overestimations in the forcing reanalysis would remain.

5 Trend analysis of simulated wind fields

The wind and even more the storm climates are an important issue in the climate change discussions. Since the occurrence of severe storms like Kyrill and the associated damages not only the public is concerned. Insurance companies as well as wind energy turbine operators also require more information about possible changes in global and local wind climates. There is need for more information. As a result the number of publications about trends in mean wind speed and storminess increased rapidly during recent years. As is shown exemplary for the German Bight stations in the introduction, near surface measurements are hardly usable for such studies due to their inhomogeneity. To receive information about changes in the wind climate, different approaches basing on different kinds of data are obtained.

Simulated wind fields provide a frequently chosen alternative. They are either taken from reanalysis or by reanalysis-driven Hindcasts. Smits et al. (2005) made out contrary trends for reanalysis and measurement data in the Netherlands. Siegismund and Schrum (2001) detected an increase of the annual mean wind speed of about 10 % over the North Sea based on the NCEP reanalysis over the period 1958 - 1997. Also based on NCEP, Pryor and Barthelmie (2003) found increased wind speeds at 850 hPa over the Baltic Sea during the latter half of the 20th century in both mean and extreme wind speeds.

Alexander et al. (2005) used pressure values to show a similar increase in the number of storms over the UK since 1950. However, updated time series show that an increase until 1990 was followed by a decrease since the 1990s (e. g. Matulla et al. 2007; Alexandersson et al. 2000).

Several other studies were conducted using pressure readings over very long time scales from different stations over Europe (e.g. Barring and Fortuniak (2009) starting 1780; Schmith et al. (1997) starting 1875; Schmidt (2001) starting 1879) with similar results. The longer time series indicate an increase in storminess from 1970 to 1990 but in a range of decadal variability (e.g. Kaas et al. 1996). Schmidt and von Storch (1993) calculated geostrophic wind speed on basis of pressure data, which were stationary over 1870 to 1990 without an increase in the last decades.

Beside the investigation of existing trends in reanalysis or hindcast data, climate scenarios are tested for the occurrence of future trends. Several indications about future trends in wind speed can be found in the literature. Most of them are connected to changes in the North-Atlantic storm track. Rockel and Woth (2007) identified increases in the storm climate with most significant trends for regions, influenced by the North Atlantic extra-tropical storms. Carnell et al (1996) show more storm activity in the North-East Atlantic. This is linked to a northern shift of the North Atlantic storm track (Bengtsson et al. 2006; Knippertz et al. 2000) and is therefore connected with a weakening in Mediterranean regions (Walter et al. 2006; Knippertz et al. 2000; Lionello et al. 2008). Räisänen et al. (2004) showed that the trends in the scenarios of RCAO strongly depend on the selected driving GCM.

To consider changes in the trends of storminess and to be able to distinguish between natural variability and large scale trends Weisse et al. (2005) used a piecewise trend statistic to detect changes in storminess over the Northeast Atlantic and the North Sea in a Hindcast simulation with the regional simulation

model REMO. As a result they showed that the trend pattern derived by a simple linear model does not remain constant over the whole reference period.

After proofing that RCMs are indeed able to reasonably simulating the yearly variability, as shown in Chapter 4, such an approach shall now be applied to two regional climate model simulations and to the two forcing reanalysis data sets. The scope is to see, if both reanalyses show similar trend patterns of the mean and extreme wind speed and how far their behavior is reproduced in the RCMs. The influence of a higher spatial resolution on the trend patterns is also investigated.

5.1 Methods

Annual means and annual 99th percentiles are derived for all data sets over the reference period 1961 - 2000. To avoid conversion from pressure levels to constant levels heights, extrapolated 10 m winds are compared in the following. Uncertainties due to the extrapolation or different temporal resolution are not considered, focusing rather on the sign and the pattern of trends and not on absolute values.

As a first step, linear trends over the whole time period are fitted to the time series. Following Weisse et al. (2005) the piecewise trend approach is applied afterwards. Within this progress two trend lines are fitted into the time series, allowing the trend to change strength or even sign at year T without losing continuity. This is done by a least square method. The Brier skill score (BSS) gives indication if the piecewise trend shows more skill than the single trend approach.

The BSS is given as

$$BSS = 1 - \frac{\sigma_{PW}^2}{\sigma_L^2} \quad (5.1)$$

where σ_{PW} and σ_L represent the standard deviation of the error of the piecewise trend and the simple linear model. The BSS ranges from 0 to 1. For increasing BSS the piecewise linear trend model gives improvements versus the simple linear model. To assess the significance of the linear trends a Mann-Kendall-Test is applied (Weisse et al. 2005). To consider the temporal correlation of the time series, a “prewhitening” approach, introduced by von Storch (1995) is used.

5.2 Results for Europe 1961 - 2000

Figure 5.1 shows the linear trends in the 99th percentiles of the four models over the time period 1961 - 2000. The trend patterns and significance patterns are quite similar for the simulations and the forcing reanalysis. The strongest positive trends are found for the North East Atlantic.

As reported by Weisse et al. (2005) for the number of storms, an increase of the wind speed can be found for all four data sets and for both mean annual wind speed and 99th percentiles north of approximately 45°. A decrease is found in some southern areas and south of the European continent. This confirms the hypotheses of a northward shift of storm tracks, detected in the frequencies of cyclones in NCEP and ERA (Trigo 2006; Schmith et al. 1998; Ulbrich and Christoph 1999; Sickmüller et al. 2000).

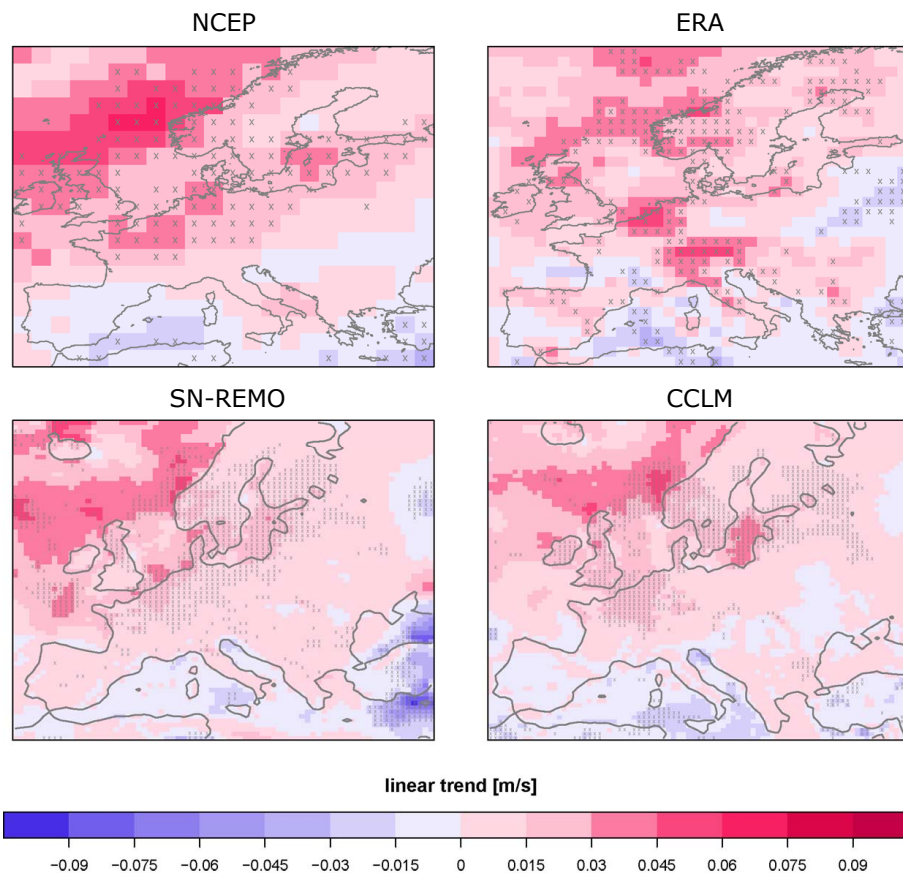


Figure 5.1: Linear trend in the 99th percentiles 1961 - 2000; First row: NCEP/NCAR Reanalysis (left) and ERA40 Reanalysis (right); Second row: SN-REMO (left), CCLM-SNE50 (right), Grid boxes with significant trends are labeled by grey x.

ERA40 and CCLM-SNE50 generally show less significant trends. Though patterns of trend and significance of all data are relatively similar, regional differences occur. Significant positive trend for the North Sea and the German Bight are detected in NCEP and SN-REMO. They are not significant in ERA40 and CCLM-SNE50. This also holds for parts of Germany. A strong increase in the Alpine area and in northern Italy can only be found in ERA40. Significant negative trends can be found for Mediterranean areas: In NCEP and SN-REMO mainly off the Turkish coast and in ERA40 and CCLM-SNE50 more in the western part. The trend pattern of ERA40 shows a strong decrease in Eastern Europe, which is not as strong and broad detected in NCEP. Similar discrepancies were already detected for the frequency of cyclones over parts of Asia (Trigo 2006) and suggest a cautious interpretation for these areas.

Generally, both Reanalyses show similar large scale patterns with differences in regional scales. This is probably induced by differences in the spatial resolution, assimilation schemes and assimilated observations. The RCMs reproduce the trend patterns of the driving reanalyses. Influences of the higher spatial resolution can only be found on regional scales, e.g. the stronger transition between land and sea grid boxes of the RCMs, which is most visible in the Mediterranean Sea (e.g. at the coast of Italy).

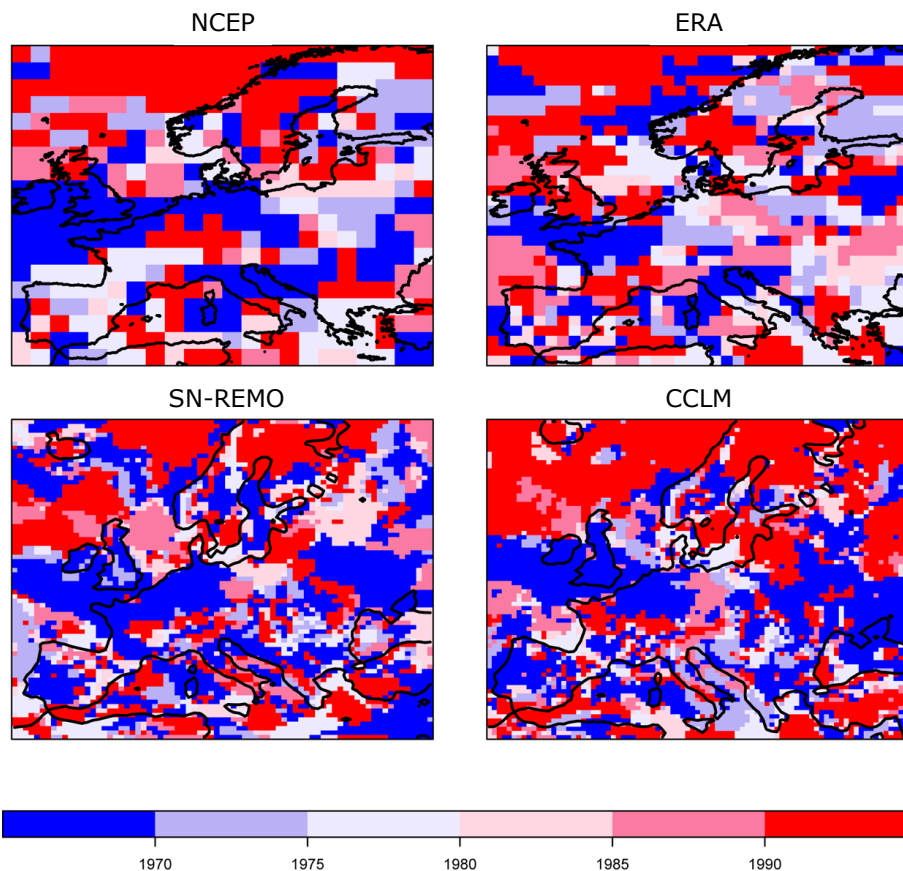


Figure 5.2: Year T at which the piecewise linear model shows a shift in the 99th percentiles; First row: NCEP/NCAR Reanalysis (left) and ERA40 Reanalysis (right); Second row: SN-REMO (left), CCLM-SNE50 (right).

Based on these results, the existence of significant increasing trends in the northern European climate, as reported in some of the studies, was indeed confirmed, also if regional discrepancies between the reanalyses can be found.

However, the regions with non-significant trend signals prevail, indicating a rather stationary wind and storm behavior.

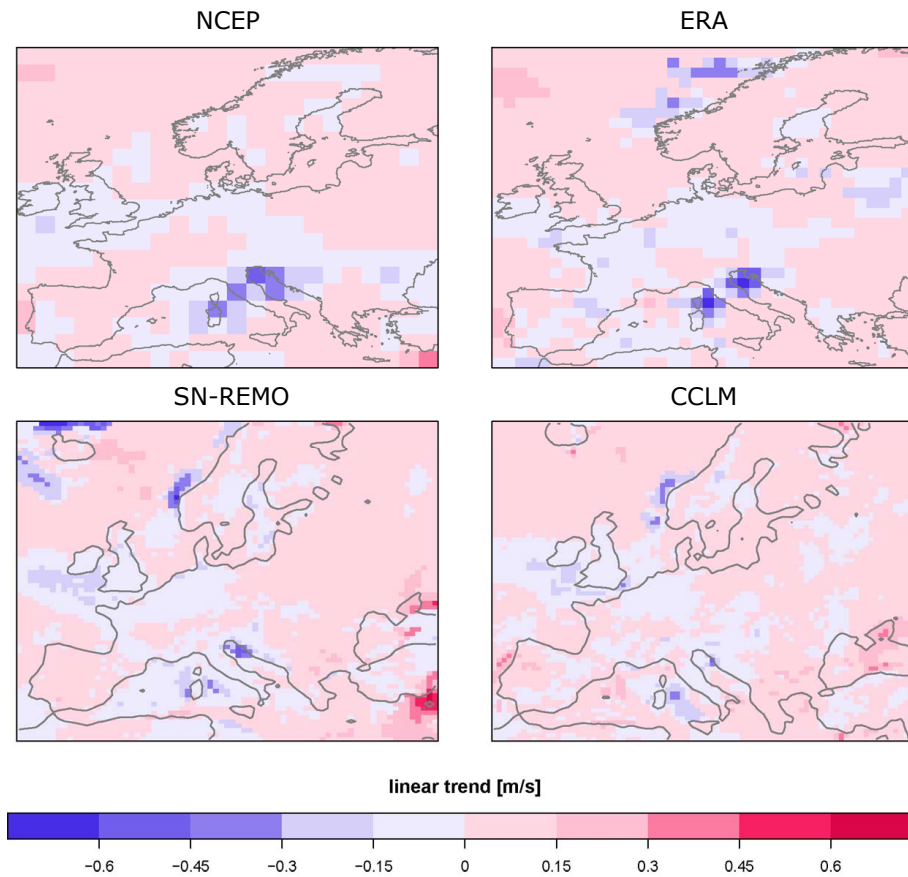


Figure 5.3: Linear Trend in the 99th percentiles in the 1961 - T period; First row: NCEP/NCAR Reanalysis (left) and ERA40 Reanalysis (right); Second row: SN-REMO (left), CCLM-SNE50 (right).

To investigate the representativity for the whole observation period, the piecewise linear model is applied. The year T, at which the piecewise linear trend model detects a switch for the 99th percentiles, is shown in Figure 5.2. The general distribution of T appears quite noisy. This makes a physical interpretation difficult. However, two dominant patterns are emphasized. The first one ranges from the western boundary over Great Britain to the northern half of Germany, indicating a phase change before 1970. This pattern is found in the 99th percentiles starting with a decreasing trend (Figure 5.3), changing into an increase

afterwards (Figure 5.4). In comparison to the other data, this pattern seems to be shifted southerly, not covering Great Britain in the ERA Reanalysis.

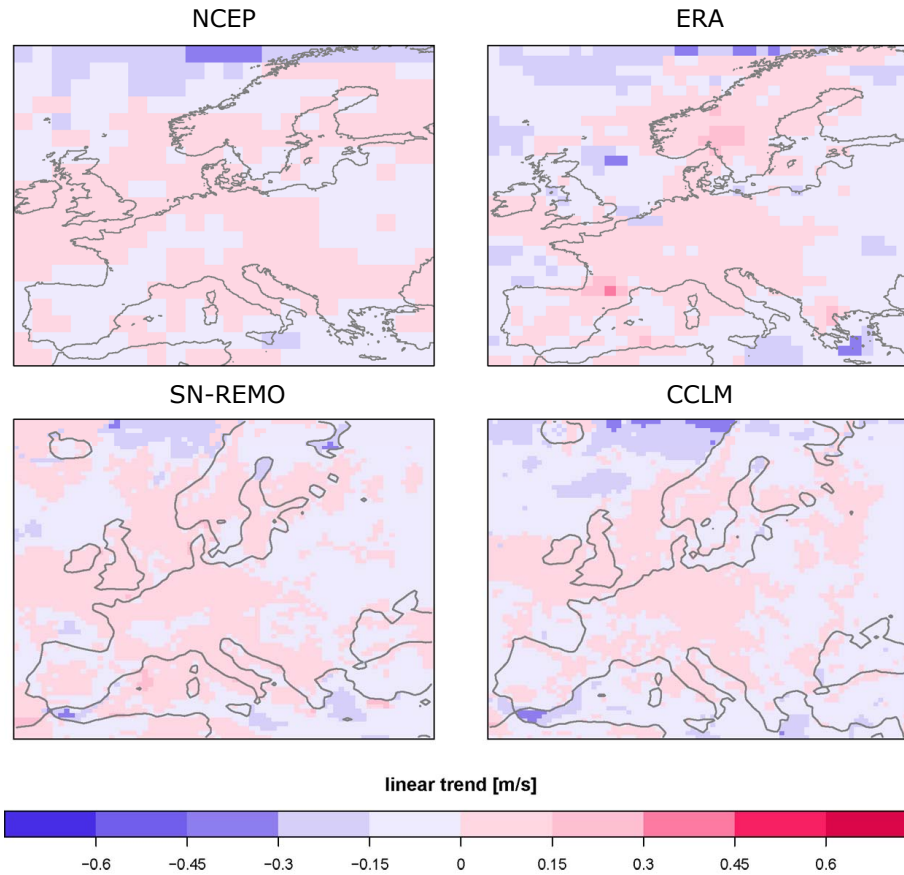


Figure 5.4: Linear Trend in the 99th percentiles in the $T - 2000$ period. First row: NCEP/NCAR Reanalysis (left) and ERA40 Reanalysis (right); Second row: SN-REMO (left), CCLM-SNE50 (right)

The second dominant pattern, north of the first pattern, indicates a change from positive to negative in the 1990s for the North East Atlantic. The increase in the northerly pattern until 1990s (Figure 5.3) can be related to an increase of the NAO-index (Figure 4.7) and therewith to a northerly shifted North Atlantic storm track (Trigo 2006). The shift in the trend pattern confirms that the storm track is shifted southerly afterwards (Figure 5.4). This agrees with more dominant negative NAO phases after 1990 (Figure 4.7).

The existence of these shifts in the trends is confirmed by the BSS, which indicates an improvement versus the linear model for this pattern in all data sets (Figure 5.5).

The trend over the Baltic Sea, described by Pryor and Barthelmie (2003), cannot be clearly verified. The time T , at which a shift is indicated, is very noisy and shows no consistent behaviour between the data sets (Figure 5.2). While NCEP and CCLM-SNE50 show an increasing trend in a wider area around Gotland until the 90s, followed by a decrease afterwards, the patterns in ERA and SN-REMO indicate a shift at the beginning of the reference period (Figure 5.3 and Figure 5.4). For a convincing conclusion, a more detailed investigation of the time series should be applied.

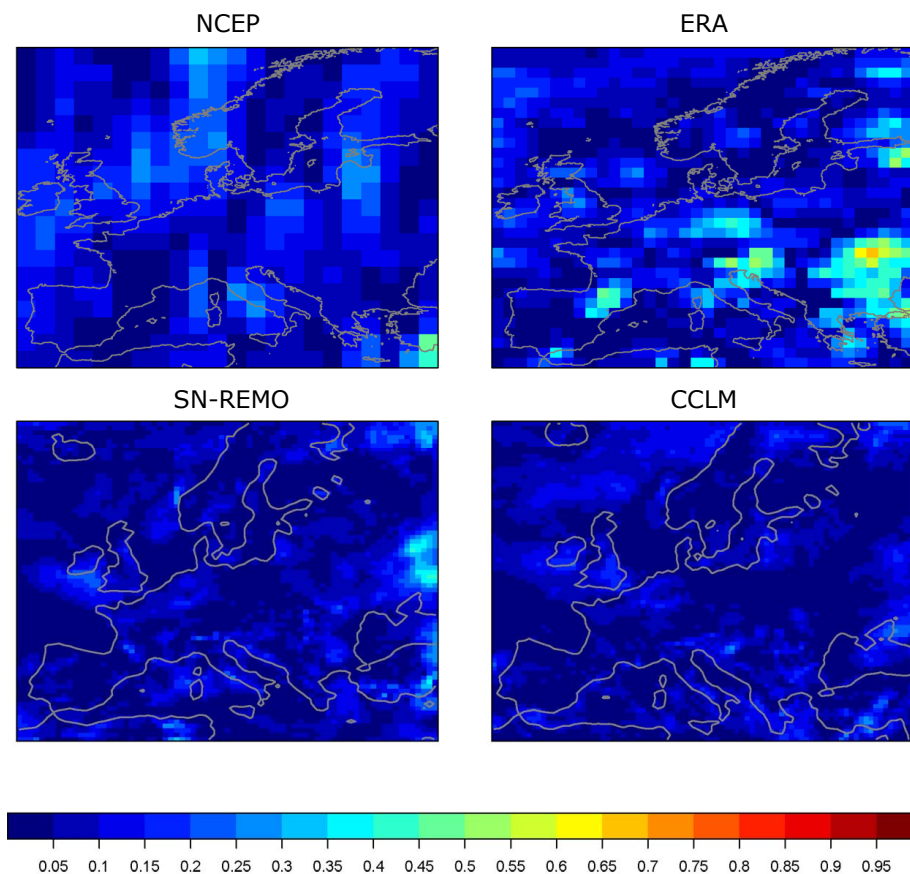


Figure 5.5: BSS of the 99th percentiles. First row: NCEP/NCAR Reanalysis (left) and ERA40 Reanalysis (right); Second row: SN-REMO (left), CCLM-SNE50 (right).

Results for the yearly mean are not explicitly illustrated, but shortly described. The patterns of linear trends as well as the significance show a strong similarity to those of the 99th percentiles. Furthermore, similar times of trend shift can be found, which are less noisy, showing more regional correlations. The two dominant patterns are also found, again with a southerly shift in ERA. Regional discrepancies, as found in the 99th percentiles of the reanalyses, also occur. E.g. a negative trend in north-westerly parts of the Mediterranean Sea is detected in ERA and CCLM-SNE50, while no significant signal is seen in NCEP and SN-REMO.

5.3 Summary and conclusions

A trend analysis of annual mean wind speed and the 99th percentiles shows a high agreement between the temporal variation of the two reanalysis data sets NCEP and ERA. The patterns of significant trends are mostly similar with regional discrepancies between both Reanalyses data sets. These are mainly detected for the Mediterranean regions as well as in parts of Eastern Europe/Western Asia. These discrepancies can be related to the higher spatial resolution of ERA or by differences in the assimilation scheme and data.

Trends in wind and storm climate are mostly linked to changes in large scale circulations, for instance in the North Atlantic storm track due to the NAO. Because the large scales of the reanalysis data sets are forced into the RCMs, they basically reproduce the trend pattern with differences in regional scales due to their higher spatial and temporal resolution. This mostly affects regions of higher terrain complexity and the land sea transition at complex coasts, where RCMs show added value versus the reanalysis data (Winterfeldt et al. 2009).

The wind trends for annual wind speed and 99th percentiles over the period 1961 - 2000 show two contrary trend patterns with an increase in the North East Atlantic and Northern Central Europe and a decrease in the Mediterranean regions. This

confirms the hypotheses of a northerly shift of the North Atlantic Storm track. A piecewise trend analysis reveals that these patterns change during the considered time period. After 1990 the increase in mean and strong wind speeds over the North East Atlantic is followed by a decrease. This suggests a southerly shift of the North Atlantic storm track after 1990 and agrees with the temporal variation of the NAO (Figure 4.7).

6 Summary and outlook

Within this study data from measurement towers are shown to be a better alternative to near surface observations and, over homogeneous terrain, an appropriate basis for the verification of mesoscale wind speed simulations.

By means of data from five measurement towers it is verified that low spatial resolution regional climate models are able to reasonably simulate mean wind statistics as well as instantaneous wind speeds over relatively homogeneous terrain such as found in Northern Germany. This holds for dynamical as well as for statistical-dynamical downscaling approaches. Mean statistics, distributions and the annual and diurnal cycle and interannual variability can be simulated with a reasonable accuracy. Deficits are found for sites over complex terrain and land use. The simulation skill is linked to the reproduction of thermally induced circulation patterns. Fluctuations on small scales are not captured with a coarse resolution. An added value for increasing resolution is only verified for the simulation of wind directions, strongly linked to the regional orography, or for a high resolution of 1 km. Only a high resolution (as of 1 km in this study) suffices for a reasonable simulation of wind statistics over complex terrain. Increasing the resolution from mesoscales of 50 to 20 km with the dynamical downscaling and of 50 to 20 to 10 km with the statistical-dynamical downscaling approach does not show the expected improvement for the wind speed simulation.

It is shown that an appropriate representation of the orography and land use is vitally important. Furthermore, differences in international land use definitions are found.

A tendency towards an underestimation of strong wind speeds is detected and confirms previous studies. Using a spectral nudging approach, only two-thirds of the storms are detected by the simulation and are mostly underestimated in their intensity. However, the RCM is able to simulate high wind speeds of almost 30 m/s. The simulations contain storm events, which cannot be found in the observations. These storm events are likely induced by an inappropriate pressure perturbation in the synoptic forcing. The conducted comparisons support previous findings that the tracks of cyclones are better reproduced with the use of spectral nudging. A more detailed investigation based on the tower measurements with two simulations only differing in the use of spectral nudging could give more evidence.

In order to circumvent inconsistencies in near surface measurements and uncertainties due to model extrapolation down to 10 m height, the verification process is based on measurements from tall towers. Therefore, an interpolation between two measurement heights is sometimes necessary. A logarithmic interpolation routine is used, neglecting the limited validity of the logarithmic law. An interpolation based on the Monin Obukhov length could probably give slightly higher accuracy. However, test analysis with interpolated values for available measuring heights show much smaller uncertainties as reported in the literature for an extrapolation approach from lower heights to wind turbine hub height with consideration of the stratification (Strack and Albers 1996). Differences between the chosen approach and the also commonly used simple power law approach are negligible.

A trend analysis of two RCM simulations and their forcing data sets supports the existence of a northward shift of the North Atlantic storm track until 1990,

reported in several studies. A piecewise linear trend model shows that this northward shift and the correlated increase in the frequency of cyclones is followed by a decrease in 1990. This is linked to the observed variation of the NAO.

Deviations in the trend patterns of RCMs and lower resolved reanalyses are only shown at regional scales, where the higher resolution of the RCM should give more detail, e. g. at land sea transitions.

Regional discrepancies of the reanalyses are detected. These are results of different resolutions, different assimilation schemes and - data. Because major deviations appear over Eastern Europe/Asia, a comparison with the Japanese JRA reanalysis, assuming a higher accuracy for this region, could give more information about the reliability of the reanalysis.

List of Abbreviations

AGL	Above ground level
ASL	Above sea level
CCLM	COSMO-CLM
CLM	COSMO-CLM
CORINE	CORINE Landcover 2000
DWD	German Weather Service
ECMWF	European Center for Medium-Range Forecast
EM	Europa Modell
ERA	ERA 40 Reanalysis of the ECMWF
GCM	General circulation model
JRA	Japanese 25-year Reanalysis Project
LM	Lokal Modell
NAO(I)	North Atlantic Oscillation (Index)
NCEP	NCEP/NCAR Reanalysis 1
NCEP/NCAR	National Centers for Environmental Prediction/National Center for Atmospheric Research
PDF	Probability Density Function
RCM	Regional Climate Model
SYNOP	Synoptic Measuring net (DWD)
WEST	Wind Energy Simulation Toolkit

List of Figures

Figure 1.1: Positions of the chosen stations along the coasts of the German Bight.	4
Figure 1.2: Yearly means of wind speed measurements from five synoptic near coastal stations	5
Figure 1.3: Yearly 99th percentiles of wind speed measurements from five synoptic near coastal stations.....	6
Figure 1.4: Position of the wind masts on the island of Helgoland since 1964.....	8
Figure 3.1: Observed and simulated mean wind speeds and their standard deviation (2001 - 2005) a) at 50 m and b) at 100 m, simulated with a spatial grid resolution of 50 km.....	22
Figure 3.2: a) HI Scores and b) Chi ² Scores for the simulated PDFs with a spatial grid resolution of 50 km.....	23
Figure 3.3: a) Observed wind direction distribution in Cabauw (2001 - 2005). Simulated wind direction distributions b) by CCLM-SNN50 and c) by WEST (50 km resolution).....	25
Figure 3.4: a) Observed wind direction distribution in Hamburg (2001 - 2005). Simulated wind direction distributions b) by CCLM-SNN50 and c) by WEST (50 km resolution).....	25
Figure 3.5: a) Observed wind direction distribution in Karlsruhe (2001 - 2005). Simulated wind direction distributions b) by CCLM-SNN50 and c) by WEST (50 km resolution).....	26
Figure 3.6: WEST roughness lengths	30

Figure 3.7: a) HI Scores and b) χ^2 Scores for the simulated PDFs with increasing grid resolution from 50 to 20 to 10 and to 1 km.....	31
Figure 3.8: Observed and simulated mean wind speeds and their standard deviation (2001 - 2005) a) at 50 m and b) at 100 m with increasing grid resolution from 50 to 20 to 10 and to 1 km	33
Figure 3.9: a) Observed and b) simulated WEST wind direction distributions at Cabauw (2001 - 2005) with a spatial resolution of 50, c) of 20, d) of 10 and e) of 1 km. Land use: CORINE, forcing: NCEP	37
Figure 3.10: a)Observed and b) simulated WEST wind direction distributions at Karlsruhe (2001 - 2005) with a spatial resolution of 50, c) of 20, d) of 10 and e) of 1 km. Land use: CORINE, forcing: NCEP	39
Figure 3.11: Occurrence frequency of the surface geostrophic wind speed classes in the climate table of the forcing data sets NCEP/NCAR Reanalysis (left) and JRA Reanalysis (right).....	42
Figure 3.12: Occurrence frequency of the surface geostrophic wind direction in the climate table of the forcing data sets NCEP/NCAR Reanalysis (left) and JRA Reanalysis (right).....	42
Figure 3.13: a) Observed and b) simulated wind direction distribution at Cabauw (2001 - 2005) by WEST with NCEP forcing and c) with JRA forcing. Both: CCLM-SNN50 roughness fields and 50 km resolution.....	43
Figure 4.1: Scatterplots of observed and simulated wind speed time series of CCLM-SNN50 at ca. 110 m over the reference period 2001 - 2005.....	53
Figure 4.2: Scatterplots of observed and simulated wind speed time series of CCLM-LC20 at ca. 110 m over the accessible data periods	56
Figure 4.3: Observed and simulated (CCLM-LC20) wind direction distributions at Cabauw, Lindenberg and Karlsruhe as available from 1991 - 2000	57
Figure 4.4: Averaged annual cycle of wind speed at ca. 110 m height	59
Figure 4.5: Average diurnal cycle in summer (JJA) at ca. 33 m height	61
Figure 4.6: Average diurnal cycle in summer (JJA) at ca. 110 m height	62
Figure 4.7: NAOI index 1950 - 2009.....	63

Figure 4.8: Mean wind speed (Dot) and 99th percentiles (x) of the NAO month (JFM); observations (black), CCLM-SNN50 (red) and CCLM-LC20 (green).	64
Figure 4.9: QQ-plots of measured and simulated (CCLM-SNN50) wind speed at ca. 110 m. separated into observed wind direction sectors.....	67
Figure 4.10: QQ-plots of measured and simulated (CCLM-LC20) wind speed at ca. 110 m. separated into observed wind direction sectors.....	68
Figure 5.1: Linear trend in the 99th percentiles 1961 - 2000	81
Figure 5.2: Year T at which the piecewise linear model shows a shift in the 99th percentiles	82
Figure 5.3: Linear Trend in the 99th percentiles in the 1961 - T period	83
Figure 5.4: Linear Trend in the 99th percentiles in the T - 2000.....	84
Figure 5.5: BSS of the 99th percentiles	85

List of Tables

Table 2.1: Description Tower Measurements.....	12
Table 3.1: Size of the overlap of observed and simulated wind speed PDFs in percent.....	24
Table 4.1: Availability of the observational data over the reference periods.....	51
Table 4.2: RMSE (in m/s), Bias (in m/s) and Correlation Coefficients (Spearman and Pearsson) between observed and simulated (CCLM-SNN50) time series and their standard deviations (in m/s) over the reference period 2001 - 2005	55
Table 4.3: RMSE (in m/s), Bias (in m/s) and Correlation Coefficient (Spearman and Pearsson) between observed and simulated (CCLM-LC20) time series and their standard deviations (in m/s) over the available periods to 2000	55
Table 4.4: Number of observed and simulated (CCLM-SNN50) events > 17.2 m/s. YY: Observed and simulated; YN: Observed and not simulated NY: Not Observed but simulated; POD and False Alarm Ratio (FAR).....	70
Table 4.5: Number of observed and simulated (CCLM-LC20) events > 17.2 m/s. YY: Observed and simulated; YN: Observed and not simulated NY: Not Observed but simulated; POD and False Alarm Ratio (FAR).....	70
Table 4.6: Maximum of observed and simulated wind speed during extreme storm events (> 20.8 m/s) in the CCLM-SNN50 period 2001 - 2005	71
Table 4.7: Maximum of observed and simulated wind speed during extreme storm events (> 20.8 m/s) in the CCLM-LC20 period - 2000.	72

References

- Alexander, L.V., Tett, S.F.B. and Jonsson, T. (2005): Recent observed changes in severe storms over the United Kingdom and Iceland. *Geophys. Res. Lett.*, **32**: L13704. doi: 10.1029/2005GL022371
- Alexandersson, H., Tuomenvirta, H., Schmith, T. and Iden, K. (2000): Trends of storms in NW Europe derived from an updated pressure data set. *Climate Res.* **14**: 71-73.
- Axer, T., Bistry, T. Faust, E., Fietze, S., Müller, M. and Prechtel, M. (2005): Sturmdokumentation Deutschland 1997-2004. Deutsche Rückversicherung AG, Düsseldorf. http://www.deutscherueck.de/uploads/tx_dbdownloads/Sturmdoku_1997-2004.pdf
- Axer, T., Bistry, T., Fietze, S., Müller, M. and Prechtel, M. (2006): Sturmdokumentation Deutschland 2005. Deutsche Rückversicherung AG, Düsseldorf. http://www.deutscherueck.de/uploads/tx_dbdownloads/Sturmdokumentation_2005.pdf
- Bärring, L. and Fortuniak, K. (2009): Multi-indices analysis of southern Scandinavian storminess 1780-2005 and links to interdecadal variations in the NW Europe-North Sea region. *Int. J. Climatol.*, **29** (3): 373-384. doi: 10.1002/joc

- Behrendt, J., Penda, E., Finkler, A. and Polte-Rudolf, C. (2009): Beschreibung der Datenbasis des NKDZ. Deutscher Wetterdienst, *Referat „Nationale Klimaüberwachung“* 2.7. http://www.dwd.de/bvbw/generator/Sites/DWDWWW/Content/Oeffentlichkeit/KU/KU2/KU21/datenbasis/german/kollektive_beschreibung,templateId=raw,property=publicationFile.pdf/kollektive_beschreibung.pdf
- Bengtsson, L., Hodges, K.I. and Roeckner, E. (2006): Storm Tracks and Climate Change. *J. Climate*, **19** (15): 3518-3543.
- Beniston, M., Stephenson, D.B., Christensen, O.B., Ferro, C.A.T., Frei, C., Goyette, S., Halsnaes, K., Holt, T., Jylhä, K., Koffi, B., Palutikof, J., Schöll, R., Semmler, T. and Woth, K. (2007): Future extreme events in European climate: an exploration of regional climate model projections. *Clim. Change*, **81**: 71-95. doi: 10.1007/s10584-006-9226-z
- Benoit, R., Yu, W. and Glazer, A. (2004): A wind energy atlas for Canada: solving the challenge of large-area wind resource mapping. Environment Canada, Dorval. http://www.2004ewec.info/files/23_1400_robertbenoit_01.pdf
- Benoit, R. and Yu, W. (2003): A Validated Highresolution Canadian Wind Atlas. Validation of selected preliminary results obtained in EOLE mode. Prepared to the request of NRCAN. Environment Canada/MRB, Dorval.
- Böhm, U., Kücken, M., Ahrens, W., Block, A., Hauffe, D., Keuler, K., Rockel, B. and Will, A. (2006): CCLM-SNN50 - the climate version of LM: Brief description and long-term applications. *COSMO Newsletter*, **6**.
- Bossard, M., Feranec, J. and Otahel, J. (2000): CORINE land cover technical guide – addendum 2000. Technical report 40. European Environment Agency, Copenhagen. http://www.epa.ie/downloads/data/corinedata/EPA_Corine_technical_guide_update_2000.pdf
- Brockhaus, P., Lüthi, D. and Schär, C. (2008): Aspects of the Diurnal Cycle in a Regional Climate Model. *Meteorol. Z.*, **17** (4): 433-443.

- Canadian Hydraulic Center (CHC) and Environment Canada (2006): AnemoScope Wind Energy Simulation and Mapping Reference Guide. http://www.anemoscope.ca/Documents/AnemoScope_ReferenceGuide.pdf
- Carnell, R.E., Senior, C.A. and Mitchell, J.F.B. (1996): An assessment of measures of storminess: simulated changes in northern hemisphere winter due to increasing CO₂. *Clim. Dyn.*, **12** (7): 467-476.
- Castilla, G. and Hay, G.J. (2007): Uncertainties in land use data. *Hydrol. Earth Syst. Sci.*, **11**: 1857-1868.
- Champeaux, J.L., Masson, V. and Chauvin, F. (2005): ECOCLIMAP: a global database of land surface parameters at 1km resolution. *Meteorol. Appl.*, **12** (1): 29-32. doi: 10.1017/S1350482705001519
- Chrastansky, A., Callies, U. and Fleet, D.M. (2008): Estimation of the impact of prevailing weather conditions on the occurrence of oilcontaminated dead birds on the German North Sea coast. *Environ. Pollution*, **157** (1): 194-198. doi: 10.1016/j.envpol.2008.07.004
- Christoffer, J. and Ulbricht-Eissing, M. (1989): Die bodennahen Windverhältnisse in der Bundesrepublik Deutschland. *Berichte des Deutschen Wetterdienstes*, **147**, 2., vollständig neu bearbeitete Auflage, Offenbach.
- Doms, G., Förstner, J., Heise, E., Herzog, H.-J., Raschendorfer, M., Schrodin, R., Reinhardt, T. and Vogel, B. (2005): A description of the nonhydrostatic regional model LM Part II: Physical parameterization. Deutscher Wetterdienst, Offenbach. <http://www.cosmo-model.org/content/model/documentation/core/default.htm>
- Doms, G. and Schättler, U. (2002): A description of the nonhydrostatic regional model LM Part I: Dynamics and Numerics. Deutscher Wetterdienst, Offenbach. <http://www.cosmo-model.org/content/model/documentation/core/default.htm#p1>

- Donat, N., Leckebusch, G.C., Pinto, J.G. and Ulbrich, U. (2009): Examination of wind storms over Central Europe with respect to circulation weather types and NAO phases. *Int. J. Climatol.*, doi: 10.1002/joc.1982
- Feser, F. and von Storch, H. (2005): A spatial two-dimensional discrete filter for limited-area-model evaluation purposes. *Mon. Wea. Rev.*, **133** (6): 1774-1786. doi: 10.1175/MWR2939.1
- Feser, F., Weisse, R. and von Storch, H. (2001): Multi-decadal Atmospheric Modeling for Europe Yields Multi-purpose Data. *EOS*, **82** (28): 305-310.
- Frank, H.P., Rathmann, O., Mortensen, N.G. and Landberg, L. (2001): The Numerical Wind Atlas – The KAMM/WASP Method. Risø National Laboratory, Denmark.
- Frank, H.P. and Landberg, L. (1997): Modelling the wind climate of Ireland. *Boundary-Layer Meteorol.*, **85** (3): 359-378.
- Frey-Buness, F., Heimann, D. and Sausen, R. (1995): A statistical-dynamical downscaling procedure for global climate simulations. *Theor. Appl. Climatol.*, **50** (3-4): 117-131. doi: 10.1007/BF00866111
- Grossmann, I., Woth, K. and von Storch, H. (2007): Localization of global climate change: Storm surge scenarios for Hamburg in 2030 and 2085. *Die Küste*, **71**: 169-182.
- Hewitt, C.D. and Griggs, D.J. (2004): Ensembles-Based Predictions of Climate Changes and Their Impacts. *Eos Trans. AGU*, **85** (52). doi: 10.1029/2004EO520005.
- Jacob, D. and Podzun, R. (1997): Sensitivity studies with the regional climate model REMO. *Meteor. Atmos. Phys.*, **63** (1-2): 119-129. doi: 10.1007/BF01025368
- Jaeger, E.B., Anders, I., Lüthi, D., Rockel, B., Schär, C. and Seneviratne, S.I. (2008): Analysis of ERA40-driven CLM simulations for Europe. *Meteorol. Z.*, **17** (4): 349-367. doi: 10.1127/0941-2948/2008/0301

- Kaas, E., Li, T. and Schmith, T. (1996): Statistical hindcast of wind climatology in the North Atlantic and northwestern European region. *Climate Res.*, **7** (2): 97-110.
- Kalnay, E., Kanamitsu, M., Kistler, R., Collins, W., Deaven, D., Gandin, L., Iredell, M., Saha, S., White, G., Woollen, J., Zhu, Y., Leetmaa, A., Reynolds, R., Chelliah, M., Ebisuzaki, W., Higgins, W., Janowiak, J., Mo, K.C., Ropelewski, C., Wang, J., Jenne, R. and Joseph, D. (1996): The NCEP/NCAR 40-year Reanalysis Project. *Bull. Am. Meteorol. Soc.*, **77** (3): 437-471.
- Kiss, P. and Jánosi, I. (2008): Comprehensive empirical analysis of ERA-40 surface wind speed distribution over Europe. *Energy Conversion and Management*, **49** (8): 2142-2151. doi: 10.1016/j.enconman.2008.02.003
- Kistler, R., Kalnay, E., Collins, W., Saha, S., White, G., Woollen, J., Chelliah, M., Ebisuzaki, W., Kanamitsu, M., Kousky, V., van den Dool, H., Jenne, R. and Fiorino, M. (2001): The NCEP-NCAR 50-Year Reanalysis: Monthly Means CD-ROM and Documentation. *Bull. Am. Meteorol. Soc.*, **82** (2): 247-267.
- Knippertz, P., Ulbrich, U. and Speth, P. (2000): Changing cyclones and surface wind speeds over North Atlantic and Europe in a transient GHG experiment. *Climate Res.*, **15**: 109-122.
- Köstner B., Bernhofer Ch., Anter, J., Gömann H, Kersebaum, K.C., Kreins P., Kuhnert, M., Lindau, R., Manderscheid R., Mengelkamp H.-T., Mirschel, W., Nendel, C., Nozinski, E., Richwien, M., Paetzold, A., Simmer C., Stonner, R., Weigel H.-J., Wenkel K.-O., Wieland R (2007): Anpassung ländlicher Räume an regionale Klimaänderungen – die Wissensplattform LandCaRe-DSS. *Klimaschutz und Anpassung an die Klimafolgen*: 295-302
- Larsén, X.G., Mann, J., Göttel, H. and Jacob, D. (2008): Wind climate and extreme winds from the regional climate model REMO. *Proc. of EWEC 2008*, Brussels.

- Lionello, P., Boldrin, U. and Giorgi, F. (2008): Future changes in cyclone climatology over Europe as inferred from a regional climate simulation. *Clim. Dynam.*, **30** (6): 657-671. doi: 10.1007/s00382-007-0315-0
- Loveland, T.R., Reed, B.C., Brown, J.F., Ohlen, D.O., Zhu, Y., Yang, L. and Merchant, J.W. (2000): Development of a global land cover characteristics database and IGBP DISCover from 1-km AVHRR data. *Int. J. Rem. Sens.*, **21** (6-7): 1303-1330. doi: 10.1080/014311600210191
- Matulla, C., Schöner, W., Alexandersson, H., von Storch, H. and Wang, X.L. (2007): European storminess: late nineteenth century to present. *Clim. Dyn.*, doi: 10.1007/s00382-007-0333-y
- Mengelkamp, H.-T. (1999): Wind climate simulation over complex terrain and wind turbine energy output estimation. *Theor. Appl. Climatol.*, **63** (3-4): 129-139. doi: 10.1007/s007040050098
- Niemeier, U. and Schlünzen, K.H. (1993): Modelling Steep Terrain Influences on Flow Patterns at the Isle of Helgoland. *Beitr. Phys. Atmos.*, **66** (1-2): 45-62.
- Nurmi, P. (2003): Recommendations on the verification of local weather forecasts. *ECMWF Technical Memorandum*, **430**: 19.
- Onogi, K., Tsutsui, J., Koide, H., Sakamoto, M., Kobayashi, S., Hatsushika, H., Matsumoto, T., Yamazaki, N., Kamahori, H., Takahashi, K., Kadokura, S., Wada, K., Kato, K., Oyama, R., Ose, T., Mannoji, N. and Taira, R. (2007): The JRA-25 Reanalysis. *JMSJ*, **85** (3): 369-432. doi: 10.2151/jmsj.85.369
- Perkins, S.E., Pitman, A.J., Holbrook, N.J. and McAneney, J. (2007): Evaluation of the AR4 Climate Models' Simulated Daily Maximum Temperature, Minimum Temperature, and Precipitation over Australia Using Probability Density Functions. *J. Climate*, **20**: 4356-4376. doi: 10.1175/JCLI4253.1
- Pinard, J.D.J.-P., Benoit, R. and Yu, W. (2005): A WEST Wind Climate Simulation of the Mountainous Yukon. *Atmos.-Ocean*, **43** (3): 259-282. doi: 10.3137/ao.430306

- Pryor, S.C. and Barthelmie, R.J. (2003): Long-term trends in near-surface flow over the Baltic. *Int. J. Climatol.*, **23**: 271-289. doi: 10.1002/joc.878
- Räisänen, J., Hansson, U., Ullerstig, A., Döscher, R., Graham, L.P., Jones, C., Meier, H.E.M., Samuelsson, P. and Willén, U. (2004) : European climate in the late twenty-first century: regional simulations with two driving global models and two forcing scenarios. *Clim. Dynam.*, **22** (1): 13-31. doi: 10.1007/s00382-003-0365-x
- Reichler, T. and Kim, J. (2008): Uncertainties in the climate mean state of global observations, reanalyses, and the GFDL climate model. *J. Geophys. Res.*, **113**: D05106. doi: 10.1029/2007JD009278.
- Rockel, B. and Woth, K. (2007): Extremes of near-surface wind speed over Europe and their future changes as estimated from an ensemble of RCM simulations. *Clim. Change*, **81**: 267-280. doi: 10.1007/s10584-006-9227-y
- Schmidt, H. (2001): Die Entwicklung der Sturmhäufigkeit in der Deutschen Bucht zwischen 1879 und 2000. DWD, *Klimastatusbericht 2001*: 199-205.
- Schmidt, H. and von Storch, H. (1993): German Bight Storms analysed. *Nature*, **365**: 791.
- Schmidt, H., Pätsch, J., Günther, H., Hennemuth-Oberle, B. (1993): Ein begleitendes Windmeßprogramm auf der Insel Helgoland für die dort zu errichtende Windkraftanlage. Deutscher Wetterdienst: Seewetteramt Hamburg.
- Schmidt, H., and Pätsch, J. (1992): Meteorologische Messungen auf Norderney und Modellrechnungen. Abschlussbericht zum KFKI-Forschungsvorhaben: Wechselwirkungen zwischen Küstenbauwerken und mariner Umwelt. Deutscher Wetterdienst: Seewetteramt Hamburg.
- Schmith, T., Kaas, E. and Li, T.S. (1998): Northeast Atlantic winter storminess 1875-1995 reanalyzed. *Clim. Dynam.*, **14** (7-8): 529-536.

- Schmith, T., Alexandersson, H., Iden, K. and Tuomenvirta, H. (1997): North Atlantic-European pressure observations 1868-1995 (WASA dataset version 1.0). *Technical Report*, **97-3**. DMI, Copenhagen.
- Sickmüller, M., Blender, R. and Fraedrich F. (2000): Observed winter cyclone tracks in the northern hemisphere in re-analysed ECMWF data. *Q.J.R.Meteorol. Soc.*, **126**: 591-620.
- Siegismund, F. and Schrum, C. (2001): Decadal changes in the wind forcing over the North Sea. *Climate Res.*, **18**: 39-45.
- Silva, J., Ribeiro, C. and Guedes, R. (2007): Roughness length classification of CORINE Land Cover classes. http://www.ewec2007proceedings.info/allfiles/2/545_Ewec2007_fullpaper.pdf
- Smits, A., Klein Tank, A.M.G. and Können, G.P. (2005): Trend in storminess over the Netherlands, 1962-2002. *Int. J. Climatol.*, **25**: 1331-1344. doi: 10.1002/joc.1195.
- Strack, M. and Albers, A. (1996): Analyse und Extrapolation des Windprofils am 130 meter-messmast des DWD. *DEWI-Magazin*, **8**: 65-75.
- Stull, R. (1988): An introduction to Boundary Layer Meteorology. Kluwer Academic Publishers: Dordrecht: 381-382.
- Tanguay, M., Robert, A. and Laprise, R. (1990): A semi-implicit semi-lagrangian fully compressible regional forecast model. *Mon. Wea. Rev.*, **118** (10): 1970-1980. doi: 10.1175/1520-0493(1990)118<1970:ASISLF>2.0.CO;2
- Thomas, S.J., Girard, C., Benoit, R., Desgagné, M. and Pellerin, P. (1998): A new adiabatic kernel for the MC2 model. *Atmos.-Ocean*, **36**: 241-270.
- Trigo, I.F. (2006): Climatology and interannual variability of storm-tracks in the Euro-Atlantic sector: a comparison between ERA-40 and NCEP/NCAR reanalyses. *Clim. Dynam.*, **26** (2-3): 127-143. doi: 10.1007/s00382-005-0065-9
- Troen, I. and Petersen, E.L. (1998): European Wind Atlas. Published for the EU Commission DGXII. Risø National Laboratory, Denmark.

- Ulbrich, U. and Christoph, M. (1999): A shift of the NAO and increasing storm track activity over Europe due to anthropogenic greenhouse gas forcing. *Clim. Dynam.*, **15** (7): 551-559. doi: 10.1007/s003820050299
- Uppala, S.M., Allberg, K., Simmons, P.W., Andreae, A.J., Da Costa, U., Bechtold, V., Fiorino, M., Gibson, J.K., Haseler, J., Hernandez, A., Kelly, G.A., Li, X., Onogi, K., Saarinen, S., Sokka, N., Allan, R.P., Andersson, E., Arpe, K., Balmaseda, M.A., Beljaars, A.C.M., Van De Berg, L., Bidlot, J., Bormann, N., Caires, S., Chevallier, F., Dethof, A., Dragosavac, M., Fisher, M., Fuentes, M., Hagemann, S., H'olm, E., Hoskins, B.J., Isaksen, L., Janssen, P.A.E.M., Jenne, R., McNally, A.P., Mahfouf, J.F., Morcrette, J.J., Rayner, N.A., Saunders, R.W., Simon, P., Sterl, A., Trennberth, K.E., Untch, A., Vasiljevic, D., Viterbo, P. and Woollen, J. (2005): The ERA-40 re-analysis. *Quart. J. R. Meteor. Soc.*, **131** (612): 2961-3012. doi: 10.1256/qj.04.176
- U.S. Geological Survey (USGS) (2009): GTOPO 30 Documentation. http://eros.usgs.gov/#/Find_Data/Products_and_Data_Available/gtopo30_info
- van der Hoven, I. (1957): Power Spectrum of horizontal wind speed in the frequency range from 0.0007 to 900 cycles per hour. *J. Atmos. Sci.*, **14** (2): 160-164.
- van der Meulen, J.P. (2000): Wind measurements: potential wind speed derived from wind speed fluctuations measurements, and the representativity of wind stations. *Instruments and Observing Methods Reports*, **74** (WMO/TD-No. 1028): 72-75.
- von Storch, H., Langenberg, H. and Feser, F. (2000): A Spectral Nudging Technique for Dynamical Downscaling Purposes. *Mon. Wea. Rev.*, **128**: 3664-3673.
- von Storch, H. (1995): Missuses of Statistical Analysis in Climate Research. In: von Storch, H. and Navarra, A. (eds.): *Analysis of Climate Variability Applications of Statistical Techniques*. Springer Verlag: 11-26.

- Walter A., Keuler, K., Jacob, D., Knoche, R., Block, A., Kotlarski, S., Müller-Westermeier, G., Rechid, D. and Ahrens, W. (2006): A high resolution reference data set of German wind velocity 1951-2001 and comparison with regional climate model results. *Meteorol. Z.*, **15** (6): 585-596.
- Wanner, H., Brönnimann, S., Casty, C., Gyalistras, D., Luterbacher, J., Schmutz, C., Stephenson, D.B. and Xoplaki, E. (2001): North Atlantic Oscillation – Concepts and studies. *Surveys in Geophysics*, **22**: 321-382.
- Weisse, R., von Storch, H., Callies, U., Chrastansky, A., Feser, F., Grabemann, I., Guenther, H., Pluess, A., Stoye, T., Tellkamp, J., Winterfeldt, J. and Woth, K. (2009): Regional meteo-marine reanalyses and climate change projections: Results for Northern Europe and potentials for coastal and offshore applications. *Bull.Amerc.Meteor. Soc.*, doi: 10.1175/2008BAMS2713.1
- Weisse, R. and Günther, H. (2007): Wave climate and long-term changes for the Southern North Sea obtained from a high-resolution hindcast 1958-2002. *Ocean Dynamics*, **57**: 161-172
- Weisse, R., von Storch, H. and Feser, F. (2005): Northeast Atlantic and North Sea storminess as simulated by a regional climate model during 1958-2001 and comparison with observations. *J. Climate*, **18** (3): 465-479.
- Weisse, R. and Feser, F. (2003): Evaluation of a method to reduce uncertainty in wind hindcasts performed with regional atmosphere models. *Coastal Engineering*, **48**: 211-255.
- Wieringa, J. (1996): Does representative wind information exist? *J. Wind Eng. Ind. Aerodyn.*, **65** (1-3): 1-12. doi: 10.1016/S0167-6105(97)00017-2
- Wieringa, J. (1989): Shapes of annual frequency distributions of wind speed observed on high meteorological masts. *Boundary-Layer Meteorology*, **47**, (1-4): 85-110.
- Wieringa, J. (1983): Description Requirements for assessment of non-ideal wind stations: for example Aachen. *J. Wind Eng. Ind. Aerodyn.*, **11** (1-3): 121-131.

- Wieringa, J. (1976): An objective exposure correction method for average wind speeds measured at sheltered location. *Quart. J. Roy. Meteor. Soc.*, **102** (431): 241-253. doi: 10.1002/qj.49710243119
- Winterfeldt, J. and Weisse, R. (2009): Assessment of value added for surface marine wind speed obtained from two Regional Climate Models. *Mon. Wea. Rev.*, **137** (9): 2955-2965. doi: 10.1175/2009MWR2704.1
- World Meteorological Organization (WMO) (2008): Guide to meteorological instruments and methods of observation. WMO-No. **8**: 1.5-1-1.5-14.
- Yu, W., Benoit, R., Girard, C., Glazer, A., Lemarquis, D., Salmon, J.R. and Pinard, J.-P. (2006): Wind Energy Simulation Toolkit (WEST): A wind mapping system for use by wind-energy industry. *Wind Engin.*, **30** (1): 15-33. doi: 10.1260/03095240677764145 0

Appendix

Table A1: Station meta data. Provided by Gudrun Rosenhagen (DWD)

Station	Station histories			
	Height [m]	Time period	Location	
	AGL/ASL		N	E
List	14/30	1948 - 23.11.1964	55°00'41" 08°24'57" Flakturm	
	12/38	24.11.1964 - today	55°00'48" 08°24'47" Möwengrund	
Helgoland	16/20	29.08.1952 - 28.02.1964	54°10'37" 07°53'31" Tonnenhof	
	15/19	29.02.1964 - 09.11.1989	54°10'35" 07°53'35" Tonnenhof	
	10/15	09.11.1989 - 07.12.1989	54°11'16" 07°54'46" Airport dune	
	10/15	07.12.1989 - today	54°10'20" 07°53'59" Mole	
Norderney	18/31	01.05.1947 - 02.04.1960	53°44'25" 07°10'12" Georgshoehe	
	20/33	02.04.1960 - 12.05.1966	53°44'25" 07°10'12" Georgshoehe	
	28/42	12.05.1966 - 11.12.1978	53°44'25" 07°10'12" Georgshoehe	
	21/34	11.12.1978 - 31.08.1981	53°44'25" 07°10'12" Georgshoehe	
	12/23	01.09.1981 - today	53°42'50" 07°09'09" Januskopf	
Bremerhaven	25/31	1949 - 15.04.1962	53°34'12" 08°32'55" Signalturm	
	12/18	16.04.1962 - 31.10.1997	53°32'04" 08°34'41"	
	10/16	01.11.1997 - 09.06.1998	53°32'04" 08°34'41"	
	12/19	10.06.1998 - today	53°32'05" 08°34'38"	
Cuxhaven	26/30	1951 - 06.04.1972	53°52'22" 08°42'29"	
	26/31	07.04.1972 - 19.02.2004	53°52'23" 08°42'25" Alte Liebe	
	10/13	20.02.2004 - today	53°52'29" 08°42'38" Alte Liebe	

Acknowledgements

My study strongly relied on the availability of the data. Therefore I am very grateful to the following institutions:

- The Meteorological Institute of the University Hamburg, the KNMI, the German Weather Service, the Research Center Juelich and the Research Center Karlsruhe for providing the tower data.
- The Japanese Meteorological Agency, the Central Research Institute of Electric Power Industry (CRIEPI), the Data Support Section of the Scientific Computing Division at the National Center for Atmospheric Research and the European Centre for Medium-Range Weather Forecasts for providing their reanalysis data sets.
- The European Environmental Agency for supplying the CORINE data set.
- The Numerical Weather Prediction Research Section of Environment Canada and especially Dr. Wei Yu for his support with WEST.
- The GKSS research Centre for the provision of the CCLM and SNREMO data (Dr. Beate Geyer and Dr. Frauke Feser)

- The German Weather Service and especially Gudrun Rosenhagen for providing data from weather stations.

I would like to thank Prof. Dr. Hans von Storch and Dr. Heinz-Theo Mengelkamp for their scientific support and for giving me the opportunity to accomplish this thesis at the Institute for Coastal Research at the GKSS Research Center.

Above all I would like to thank my friends, my family, the proof readers and all the others who supported me in any scientific or other way.

A special thanks goes to Ivonne for being such a good listener and to my boy friend for his patience, his optimism, his support and his love.

